

Transformer Model for Transient Recovery
Voltage at Transformer Limited Fault
Current Interruption

Myo Min Thein

July, 2012

Doctoral Dissertation

Transformer Model for Transient Recovery
Voltage at Transformer Limited Fault
Current Interruption

By
Myo Min Thein
(Student No: 09589501)

Supervisor: Prof. Masayuki Hikita

Department of Electrical and Electronic Engineering
Graduate School of Engineering
Kyushu Institute of Technology

6. 7. 2012

TABLE OF CONTENTS

Chapter 1 Introduction	1
1.1 Electricity in Our Modern World.....	1
1.2 Overview of Electric Power System.....	2
1.3 The Role of Power Transformer in the Power System.....	4
1.4 Research Background	4
1.5 Research Trend of Circuit Switching Phenomenon.....	5
1.6 Transient Recovery Voltage.....	6
1.7 Transformer Limited Fault.....	7
1.8 Transformer Models and Frequency Range.....	11
1.9 Dissertation Outline.....	13
References.....	16
Chapter 2 Frequency Response Analysis	18
2.1 Introduction.....	18
2.2 General Application of FRA in the Power System Transformer.....	19
2.3 Property of FRA Measurement.....	20
2.4 Detectability of Faults by FRA Device.....	20
2.5 Application of FRA Measurement in our Research.....	21
References.....	23
Chapter 3 Investigation of Transformer Model for Transient Recovery Voltage Calculation at Transformer Limited Fault Condition by EMTP	24
3.1 Introduction.....	24
3.2 Transformer Limited Fault in the Power System.....	25
3.3 Impedance Measurement.....	26
3.3.1 FRA Measurement.....	26
3.3.2 Impedance Calculation Procedure.....	30
3.3.3 Precise Calculation Analysis.....	31
3.4 Experiment.....	35
3.4.1 Transformer for Experiment.....	35
3.4.2 Current Injection Measurement.....	36

3.5	EMTP Model with CIJ Circuit.....	39
3.6	Discussion.....	41
3.7	Conclusion.....	42
	References.....	43

Chapter 4 Investigation of TRV under Transformer Limited Fault Condition by Frequency Dependent Equivalent Circuit.....45

4.1	Introduction.....	45
4.2	Example of Experiment Setup.....	46
4.3	Experiment Results.....	50
4.4	Examination of Frequency Dependency.....	55
4.4.1	Impedance Frequency Response.....	55
4.5	Frequency Dependent Equivalent Circuit.....	58
4.6	TRV Calculation Using Frequency-Dependent Equivalent Circuit	60
4.6.1	Discussion.....	64
4.7	Study of TRV Characteristics with Extra Capacitance Values at TLF Condition..	64
4.7.1	Experiment Setup.....	65
4.7.2	Experiment Results.....	65
4.7.3	EMTP Simulation Result.....	67
4.7.4	Discussion.....	69
4.8	Conclusion.....	70
	References.....	71

Chapter 5 Study of Transformer Iron Core Characteristics at a High Frequency.....72

5.1	Introduction.....	72
5.2	Current Ratio Measurement Experiment.....	73
5.2.1	Experiment Setup... ..	73
5.2.2	Experiment Results	79
5.2.3	Consideration.....	80
5.3	Current Injection Experiment with Charging Capacitor.....	82
5.3.1	Current Injection with Different Capacitors.....	82
5.3.2	Experiment Results.....	85
5.4	Current Injection Experiment with Power Amplifier.....	88

5.4.1 Experiment Setup.....	88
5.4.2 Experiment Results.....	91
5.5 Discussion.....	92
5.6 Conclusion.....	94
References.....	95
Chapter 6 Conclusion.....	96
Conclusion.....	96
Acknowledgment.....	99
List of Publication.....	101

Chapter 1

Introduction

1.1 Electricity in Our Modern World

Electricity, more convenient secondary energy, can be produced by using any source of energy as one of the primary energy source. Mechanical energy, heat, light, or chemical reactions are included in primary energy sources. Electricity was, at first, used primarily for lighting and gradually found more broadly-based applications as a power source. Electricity becomes the main source of energy that supports almost all of our daily life facilities and technologies because it is the most convenient and omnipresent energy available today. The astounding technological developments of our age are highly dependent upon a safe, reliable, and economic supply of electric power [1].

Electricity is mainly generated by using various kinds of electromechanical generators at an electric power station. Most of bulk electric power is commercially produced by hydroelectric power plant using potential of water, nuclear power plant using the nuclear reactors and thermal power plant by burning coal, oil, or natural gas. However, those types of electric power generation have consequence disadvantages. For instance, climate change exacerbates the hazards of huge dams, radioactive radiations from the accidentally damage of the reactors in the nuclear power plant, costly maintenance of radioactive waste, and getting lost of fossil fuel, natural gas and CO₂ emission.

In recent years, distributed power generation from renewable energy source such as photovoltaic generation (PV), micro-turbines, fuel cells, tidal power, geothermal energy and wind turbine generation has attracted great attention from the viewpoints of environmental considerations and energy security. Massive research and study of new energy generation method are being implemented with the encouragement of academic, industrial and government sectors, especially in developed countries. Consequently, construction of power farms are being increased based on the renewable energy sources. To protect the global environment and long-lasting of our dwelling world, distributed

generations (DGs) are expected to be increasingly introduced and taking parts in the front line of electricity generation in coming years.

1.2 Overview of Electric Power System

Electric power system is an interconnected and a complex one, which can be divided into power generation plants, transmission lines, substations, and distribution networks. It is a continuous network linking between the energy generated power plants and the end users. Power plant provides bulk amount of electricity to the load center and substation via transmission line. Electric power is delivered to the variety of end users via the distribution networks.

Power generation economics balance the operation costs of different energy forms (thermal, nuclear, natural gas, hydroelectric and etc.) with the cost of power delivery across the transmission network. Advantages of economics and market scales are used to select the maximum sized generator and available firm power that would retain the reliability policies for the load dispatch authorities in terms of loss and load probability.

Transmission systems are designed through extensive deterministic single and multiple steady-state contingency analysis and dynamic stability analysis for investigating the impact of generation and bulk transmission loss on system security. The transmission system concentrates on the efficient and secure delivery of bulk power and the selection of the appropriate sources of generation. The larger the customer, the higher level of voltage is used to deliver the electric power. A higher voltage will reduce the energy lost during the transmission process of the electricity.

Transformers are essential part of the electric power system because it has the ability to change voltage and current levels, which enables the electric power system to generate electric power, to transmit and distribute electric power and to utilize power at an economical and suitable level [2, 3]. As shown in figure 1.1, the voltage of electricity generated at the power plant is increased to a higher level with step-up transformers. This power is transmitted to bulk power substation via high voltage transmission (HV, EHV, and UHV). The electricity is delivered to the distributed end users and customers who required variety of voltage levels by using distribution networks and substations. When electricity is transmitted to various end points of the power grid, the voltage of the electricity will be reduced to a useable level with step-down transformers for industrial customers and residential customers. So, transformers are a vital component of the electric power system, and they are extensively used and help to meet the growing energy needs all of the electric power systems.

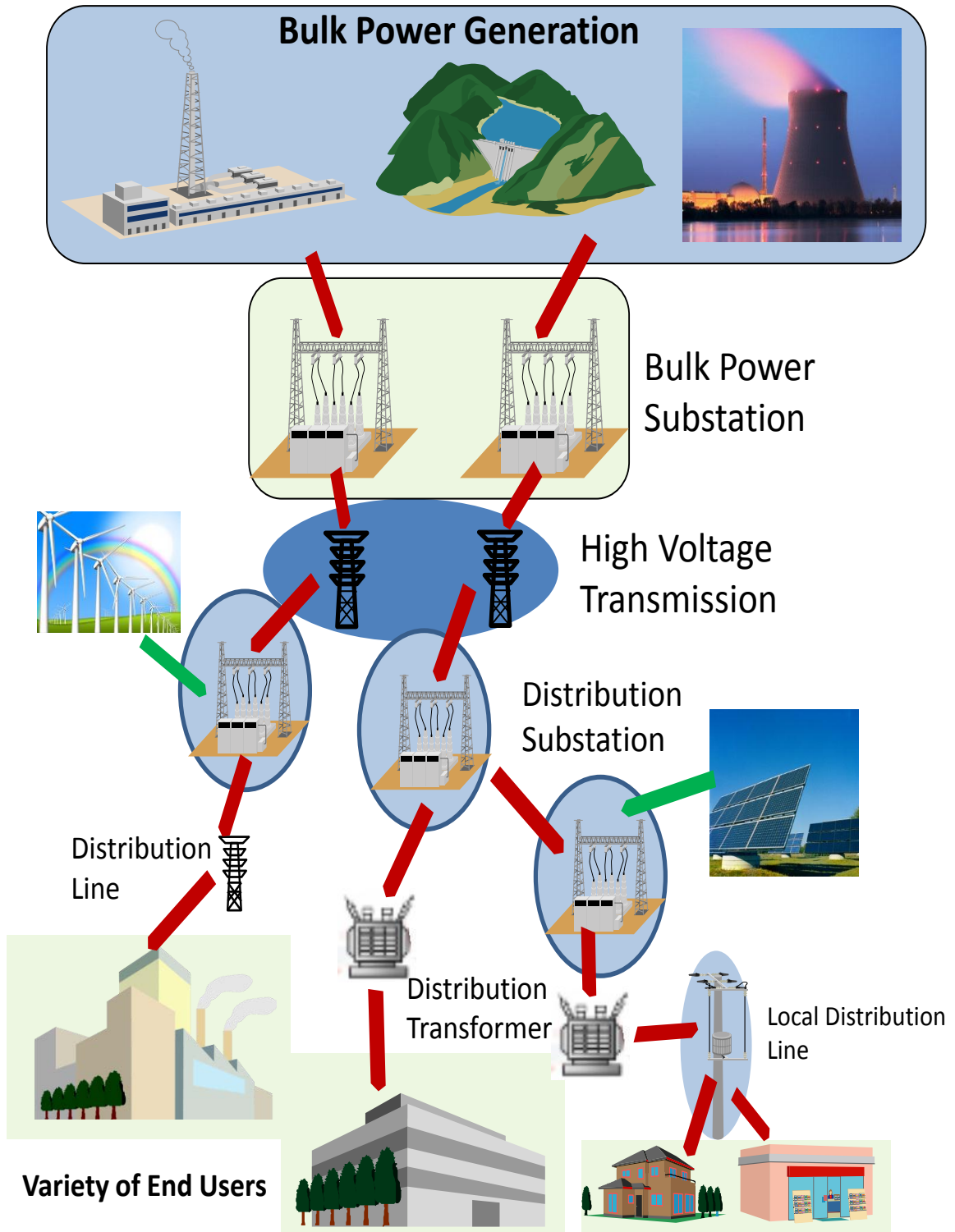


Fig. 1.1 A Typical Electrical Power System

1.3 The Role of Power Transformer in the Power System

The power transformer is a major power system component that permits economical power transmissions with high efficiency and low loss. It transfers energy from one circuit to another by means of a common magnetic field. In all cases except autotransformers, there is no direct electrical connection from one circuit to the other. According to the definition of ANSI/IEEE, a transformer is a static electrical device, involving no continuously moving parts, used in electric power systems to transfer power between circuits through the use of electromagnetic induction. The term power transformer is used to refer to those transformers used between the generator and the distribution circuits, and these are usually rated at 500 kVA and above [4].

Power systems typically consist of a large number of distributed generation plants, distribution points, and interconnections within the system or with nearby systems, such as a neighboring utility. The complexity of the system leads to a variety of transmission and distribution voltage levels. Power transformers must be used at each of these points where there is a transition between the different voltage levels. It is evidenced that transformers are one of the main devices in the electric utility grid. So power system reliability, power quality, economic cost and even the company image are influenced by the transformers health and performing. For this reason, norms and standards related to many different protection schemes are used and trying to make more specific and efficient standards for transformer protection as well as the other power system components.

1.4 Research Background

In high voltage electric power systems, especially 300 kV and 550 kV systems, very high capacity power transformers, up to 1500 MVA, have been used. When faults occur at the secondary sides of the transformer, circuit breakers (CB) interrupt the fault currents. Transient recovery voltages (TRV) appear across the CB due to the current interruptions. The TRV values may be in excess of the standard values and severely affect the CB. These phenomena are known, but the detailed characteristics of TRVs, such as amplitude factor (AF), rate of rise of recovery voltage (RRRV), peak value, and oscillation, have not been fully studied. Therefore, due to safety considerations, circuit breakers with higher voltage levels than the relevant system voltage have often been applied. To select suitable CB ratings, the TRV characteristics of the transformer limited

fault (TLF) current interrupting condition must be understood.

Since very high capacity power transformers are presently used in high capacity systems, there have been circumstances in which the TLF interrupting currents could not be fully covered by 10% of the rated terminal fault breaking currents (T10 duty). At present, TLF is presumed to be verified in accordance with T10 duty within the scope of the terminal faults (TF: T100, T60, T30, T10) under international electrotechnical commission (IEC) standards. The severity of TRV is expressed as amplitude factor. The current IEC standard of TLF-TRV amplitude factor is 1.7.

On the other hand, leakage inductance at the power-frequency domain cannot be applied for the TRV calculation, the frequency of which is generally far higher than several kHz.

In these indecipherable situations, transformer models of the high frequency region should be studied to identify clearly the TRV at TLF conditions.

1.5 Research Trend of Circuit Switching Phenomenon

At present, circuit breakers are to be installed on 245 kV to 1200 kV power system with short circuit ratings up to 120 kA [5]. Direct testing of high voltage CB, using with the power system or short circuit alternators is not feasible. A large scale experimental facility is needed for a CB development. To increase testing plant power is neither an economical nor a very practical solution. The main facility for CB testing and development experiment is a high current source. The current source is used to supply a high current with low voltage. It is used to inject the short circuit current during the test. A limited number of universities have a high current source, mainly by a capacitor bank, over the world. For a circuit interrupting test, a voltage source is additionally needed. The voltage source is a high voltage low current source. It provides transient recovery voltage. Two sources should be operated in a correct sequence. Furthermore a circuit breaker includes a lot of technical know-how. These aspects have made a university feel difficult.

In Japan, the yearly growth rate of an electric power consumption stays at a low level less than 1 per cent. Most of manufacturers for CBs have been forced to reduce a number of research workers due to the rapid decrease of a demand for substation equipments. Manufacturers tend to require fundamental researches out sourced in a university. By considering the circumstances, Professor Hikita Laboratory tried to make experimental setup in a small size for fundamental phenomena related to the CB development [5, 6]. Under the CB development topic, a precise transformer equivalent

circuit is investigated to calculate the TRV after interrupting the TLF current. This research study is performed with experimental and simulation methods. For the simulation, Electro-Magnetic Transient Program (EMTP) is used because it is widely used software for circuit switching phenomenon. For the experiment, synthetic testing

- (i) Current injection method (CIJ) and
- (ii) Capacitor current injection with diode as an interruption device

are used to measure the inherent TRV of TLF interrupting condition. Because synthetic testing is an alternative equivalent method for testing of high voltage equipment and it is accepted by the IEC standard [7]. The simulation, experiment results and constructed transformer equivalent circuit will be expressed in the chapter (3) and (4) of this dissertation.

1.6 Transient Recovery Voltage

When a circuit breaker interrupts a current, a voltage across the circuit breaker is generated to oppose the non-linear change of the interrupted current, due to a circuit transient phenomenon. This voltage is called the transient recovery voltage (TRV), which is the voltage difference between the source side and the load side of the circuit breaker. Generally the configuration of the network as seen from the terminals of the circuit breaker determines amplitude, frequency, and shape of voltage oscillations.

During normal system operation the energy stored in the electromagnetic field is equally divided over the electric field and the magnetic field. During the interruption process the arc rapidly loses conductivity as the instantaneous current approaches zero. When the short-circuit current is interrupted at current zero, there is still magnetic energy stored in the leakage inductance of the transformers in the substation, in the self-inductance of the stator and field windings of the supplying generators, and in the inductance of the connected bus bars, the overhead lines and the underground cables. Current interruption causes a transfer of the energy content to the electric field only.

Electromagnetic waves propagate through the system even after current interruption, which is caused by the sudden change in the configuration of the system. These voltage waves reflect against transformers, increase in amplitude, and travel back to the terminals of the interrupting device [7, 8]. This results in a voltage oscillation. The actual waveform of the voltage oscillation is determined by the configuration of the power system.

The duration of the TRV is in the order of milliseconds, but its rate of rise and its amplitude are of critical significance for a successful operation of the interrupting

device.

Figure 1.2 shows three typical transient voltages that are generated when interrupting simple resistive, capacitive and inductive circuits. In the case of resistive circuit interruption (figure 1.2 (a)), the TRV ($V_S - V_L$) is a simple sinusoidal system voltage with a maximum value of 1.0 p.u. In capacitive circuit interruption (figure 1.2 (b)), the TRV ($V_S - V_L$) will appear as a (1 - cosine) wave with a maximum value of 2.0 p.u. following current interruption. In inductive circuit interruption (figure 1.2 (c)), the TRV ($V_S - V_L$) will appear as a sinusoidal system voltage following a high frequency oscillatory voltage wave caused by the inductive circuit and the stray capacitance.

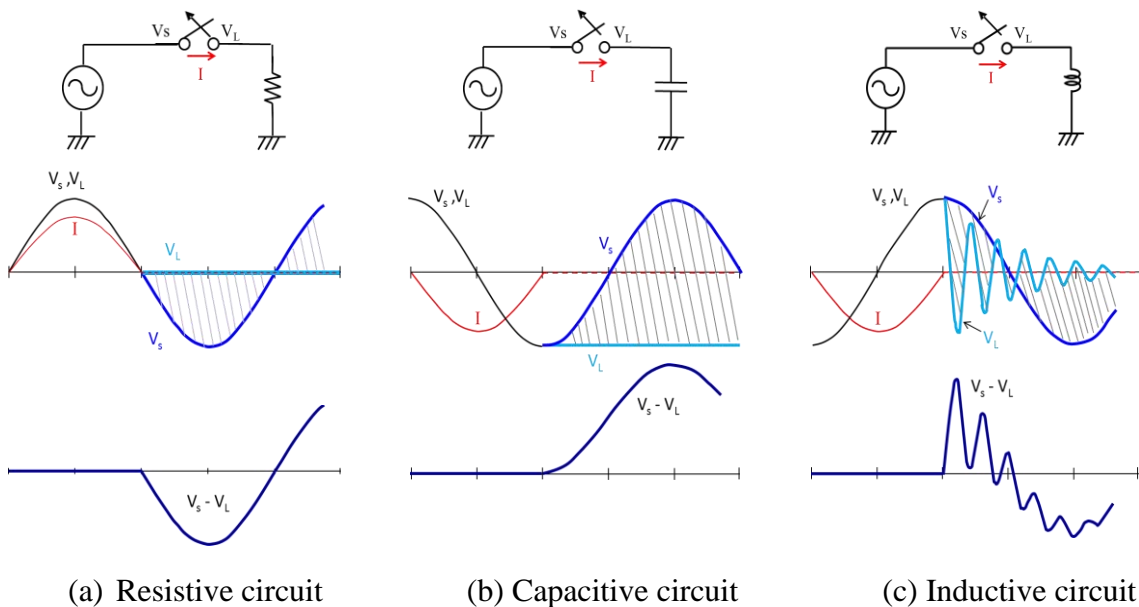


Fig. 1.2 Transient recovery voltage of simple circuit models

1.7 Transformer Limited Fault

The TRV in a power system is generally a combination of the three types shown in figure 1.2, depending on the circuit, where the circuit breaker interrupts the current. Transformer limited fault (TLF) interruption is defined as the case in which all interrupting currents are provided to the short-circuit fault point through a transformer, and are interrupted by a circuit breaker as shown in figures 1.3 (a) and (b).

The circuit is characterized by the source and the transformer impedance. After the circuit breaker interrupts the current, the source side voltage, which is the TRV in this case, is decided by the transformer impedance; the source impedance is generally about 10% of the transformer impedance. The transformer impedance consists of

resistances, inductances and capacitances. The high frequency oscillation due to the circuit components is super-imposed on the system voltage.

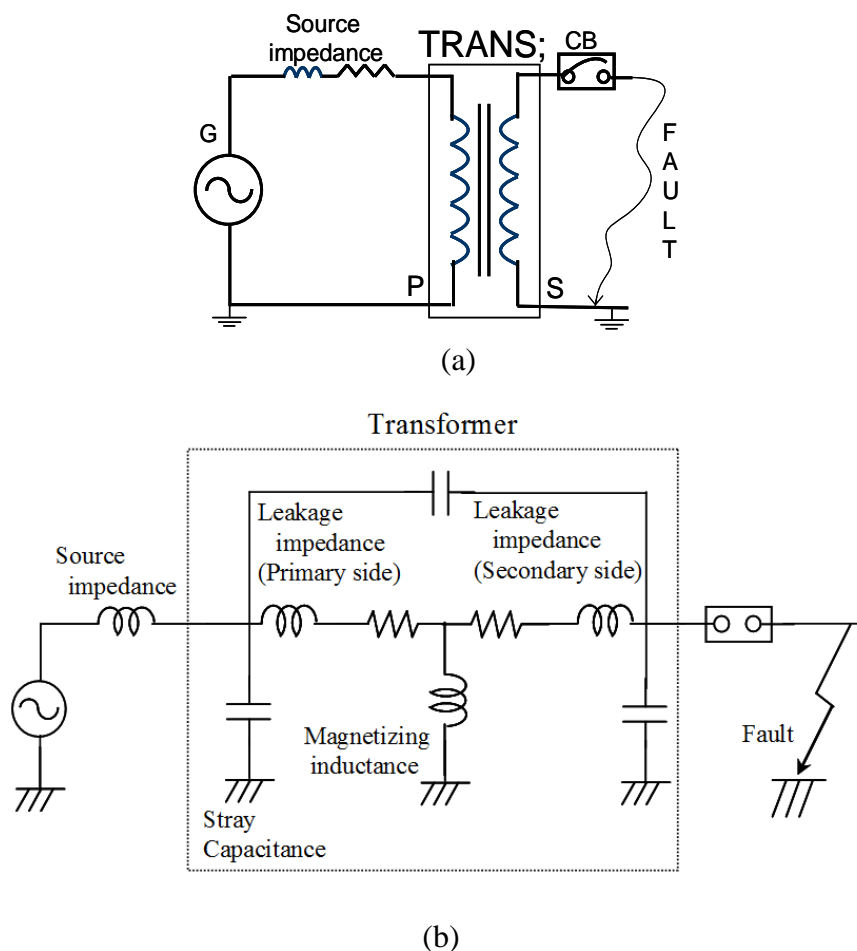
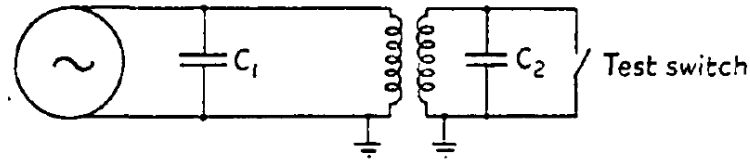
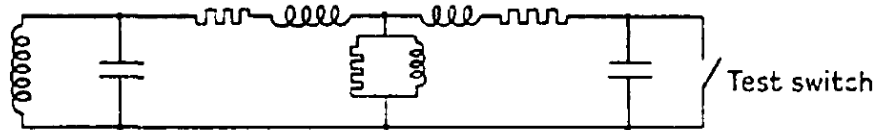


Fig. 1.3 Transformer limited fault interrupting

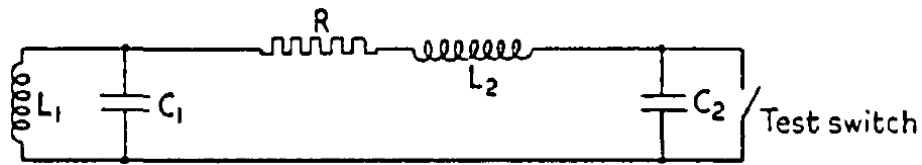
In 1939, L. Gosland reported to the British Electrical and Allied Industries Research Association (E.R.A. Report Ref. G/T102). This report dealing with measurements on re-striking-voltage transients (*the term re-striking-voltage transients is the former usage of transient recovery voltage (TRV) at that time of 1939*) at a transformer sub-station, using the re-striking-voltage indicator (R.V.I.), it was pointed out that the effective inductance per phase of the transformer determine the frequency of the transients appeared to be about 93% of the nominal leakage inductance, the resonance frequency of the system being from 8 to 14 kc./s. (*the unit kc./s was a once-common unit of frequency before 1960.*) Some evidence was also produced to the effect that measurements on another transformer showed this same type of reduction in effective inductance for resonance frequencies considerably higher than the power frequency [9].



(a) Schematic diagram of short-circuit test plant



(b) Equivalent circuit



(c) Simplified circuit

Fig. 1.4 Representation of test plant with transformer [9]

Figure 1.4 (a) is a typical circuit in which a transformer plays a large part in determining the transient of re-striking voltage. Figure 1.4 (b) is the conventional equivalent circuit. In most cases the exciting inductance of the transformer may be neglected in calculations of re-striking voltage. By neglecting this, the simple equivalent circuit of figure 1.4 (c) is obtained, where the inductance L_2 is that appropriate to the leakage reactance of the transformer, L_1 being that relating to the reactance of the generating plant [9].

L. Gosland et al. (1940) take an account of field short-circuit tests on transients of re-striking voltage, in which the phenomenon of variation of effective reactance of transformers was demonstrated to a very marked extent. In order to explain the results of these tests, a detailed investigation into the variation of effective transformer reactance was carried out, and as a result of this it is here shown that, so far as transients of re-striking voltage are concerned, L_2 is, for any transformer, a parameter such as resistance, inductance and capacitance which varies with frequency and with time from the start of the transient, and that the laws governing these variations can be calculated with reasonable accuracy from the dimensions of the transformer [9]. From this report it is evidence that transformer impedance mainly influence on the TLF-TRV.

The fault clearing case shown in figure 1.5 which seems to be, though not so frequent, provable in actual power system electrical stations. The equivalent circuit diagram related to the relevant circuit-breaker's fault-current interrupting is also shown in the figure. In most of such cases, the condition $Z_{Tr} \gg Z_s$ seems to be provable, where Z_{Tr} and Z_s present transformer impedance and system short-circuit impedance, respectively. Therefore, as the majority of the voltage distribution during the short-circuit fault exists on Z_{Tr} , and, also, Z_{Tr} exists just adjacent to the relevant circuit-breaker, the TRV during the fault current interrupting is mostly dominated by the relevant transformer constants, inductances and capacitances as Haginomori et al.(2008) have shown [9].

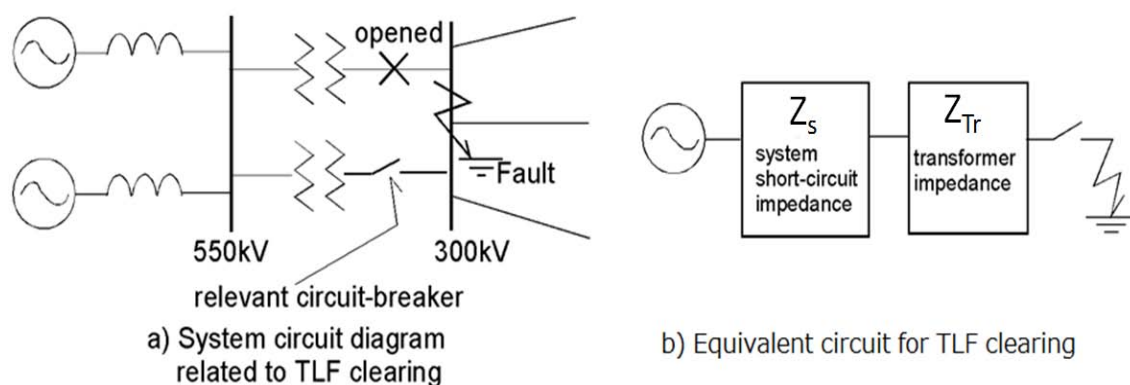


Fig. 1.5 Example of TLF clearing in power system

The TLF interruption features a high TRV rise rate and high TRV peak values, despite a low interrupting current. The former is due to the following reasons, which may introduce; extremely severe TRV conditions.

- The transformer's capacitance is relatively low, compared to the system circuits or apparatuses.
- The transformer may be located adjacent to the relevant circuit-breaker, so only less additional capacitance may exist.

But for the latter, the interrupting current is only a portion of the total bus fault current, e.g., 10 - 30%. This is because it is restricted by the leakage impedance of the transformer, and generally does not exceed 10% of the rated interrupting current in many cases. However, as described above, the interrupting current tends to increase as the capacity of the power transformer increases.

Since a few ten years ago, Parrott (1985) and Harner et al. (1972) have

investigated these phenomena, and the results have been introduced to the IEC circuit-breaker standard, i.e., IEC 62271-100, T10 (10% of rated breaking current) for high voltages and a special T30 for medium voltage circuit-breaker TRV ratings [11,12]. If the appropriate transformer constants related to the TRVs are available, the TRVs are easily calculated by applying EMTP.

Today's state of transformer constants is such that:

- For the power frequency region sufficiently accurate constants such as inductances, resistances, and capacitances are obtainable.
- For the lightning surge region, some studies have been done and sufficiently accurate values are, hopefully, available.
- For the TRV frequency region, less study has been done. So, in the past studies the same as power frequency's constants have been mostly applied.

In this study transformer constant models related to TLF current interrupting and applicable to EMTP are surveyed. Beforehand, the followings are supposed.

TRV frequencies are of several kHz --- several tens kHz.

Within more than several kinds of resonant frequencies of transformers, the primary resonant frequency seems to be the main part of the TRV wave shape.

For the primary resonant frequency of voltage oscillation, the voltage distribution is linear along the windings, so also rather simple physical and geometrical conditions as for the magnetic flux and electric field distribution could be applied in considering the constants.

As for the inductances dominating TRV in TLF case, leakage one seems to be effective, to which, whether skin effect in the iron core in TRV frequency is significant or not, is best interesting.

To get experimental data for TRV at TLF interrupting condition, current injection measurement (CIJ) method and capacitor injection with diode interruption are used. To obtain transformer constants at TRV frequency region, frequency response analysis (FRA) measurement is used.

1.8 Transformer Models and Frequency Range

Over the past decades, several studies have been conducted on parameters associated with the TLF current interrupting with the goal of drafting TRV standards. Several groups, such as [13], have proposed norms and standards related to TRV parameters for the highest levels of fault currents encountered. A valuable review has

been published on the subject of transformer TRV [12]. Most cases used a leakage inductance value of 50/60 Hz and a stray capacitance to analyze the TRV. The leakage inductance was calculated directly from the percent impedance, the transformer voltage, and power ratings. The values obtained were inductances at 50/60 Hz and were not necessarily effective inductance values for the TRV frequency of the transformer. These characteristic parameters for the TRV frequency region can hardly be determined analytically on the basis of transformer design data. In most studies, though these circuit constants were carefully chosen and minutely taken into account in calculations, the results were only close approximations of the actual system phenomena. So far, the transformer equivalent circuit has been satisfactory even at the TRV frequency range. On the other hand, a phenomenon is known in which magnetic flux will not be able to enter the iron core of a transformer in the high frequency regions. Therefore, the leakage inductance will change along with the frequency. A leakage inductance of 50/60 Hz may give a wrong TRV value [14]. A transformer consists of very complex components comprising a network of resistances, capacitances, and self or mutual inductances.

Moreover, although great advancements have been made in transient simulation software, the individual component models used in the transient simulations still need improvements. Transformer models are one of the components in need of advancement. Although power transformers are conceptually simple designs, their representations can be very complex due to different core and coil configurations and to magnetic saturation, which can markedly affect transient behavior. Eddy current and hysteresis effects can also play important roles in some transients [15].

For that reason, it is difficult to apply one acceptable representation for all possible transient phenomena in the power system throughout the complete range of frequencies. To study the TRV at TLF conditions, a transformer model using TRV-frequency-region impedance values is considered. A simulation model is constructed with the alternative transients program–electromagnetic transients program (ATP-EMTP). Because EMTP is probably the most widely-used power system transients simulation program in the world. In the EMTP there are four kinds of applicable transformers are represented in the menu [16- 20].

- XFORMER
- Saturable transformer component (TRANSFORMER)
- BCTRAN
- Hybrid model

However, any of these models cannot simulate the frequency dependency of inductance. So, frequency dependent equivalent circuit is constructed in this study. The best way to

confirm that the EMTP transformer model is accurate or not is by checking the simulation results and comparing them with the practical results of experiments.

1.9 Dissertation Outline

This dissertation presents the results of the investigation of EMTP transformer model for TRV calculation at TLF current interrupting condition. The investigated results of current injection experiment (CIJ) and capacitor current injection with diode as an interruption device with several transformers and simulation results of EMTP transformer model which correspond the experimented transformer are expressed. There are six chapters consists of in this dissertation including this chapter.

Chapter 1 is the introduction. The valued of electricity in our daily life and future trend of electric power generation which likely to change for long lasting of our earth are introduced. Overview of typical electrical power system and the importance of transformers are written. The background of this research study is expressed. The basic of transient recovery voltage, the phenomena of TRV and transformer limited fault are explained. Today condition of EMTP transformer models and applicable frequency range are also expressed in this chapter. Moreover, why frequency dependent equivalent circuit is needed for TRV study is also pointed out.

In **chapter 2** the popular diagnostic measurement method for transformer internal condition, frequency response analysis (FRA) measurement method, is expressed. FRA is used for detection of transformer winding condition which is failure or not after fault generated. It consists of measuring the impedance of transformer windings over a wide range of frequencies. This property is used well in our research to calculate the impedance of the tested transformers at high frequency region as it is essential for EMTP transformer construction.

In **chapter 3** analysis of the EMTP transformer model with the 4 kVA two windings low voltage transformer with the current injection (CIJ) measurement method to study a transient recovery voltage (TRV) at the transformer limited fault (TLF) current interrupting condition is presented. Tested transformer's impedance was measured by

the frequency response analyzer (FRA). From FRA measurement graphs leakage inductance, stray capacitance and resistance were calculated. The EMTP transformer model was constructed with those values. The EMTP simulation was done for a current injection circuit by using transformer model. The experiment and simulation results show a reasonable agreement.

Chapter 4 deals with the study of frequency dependent inductance and construction of frequency dependent equivalent circuit for transient recovery voltage (TRV) study. The TRV of the transformer limited fault (TLF) current interrupting condition has been investigated with several transformers by using current injection (CIJ) method. A transformer model for the TLF condition is treated as leakage impedance and a stray capacitance with an ideal transformer in a computation by EMTP. By using the frequency response analysis (FRA) measurement, the transformer constants were evaluated at high frequency regions. FRA measurement graphs showed that the leakage inductance value of the test transformers gradually decreases along with the frequency. From these results, frequency dependent transformer equivalent circuit was constructed. The inherent TRV was measured by using capacitor current injection with diode as an interruption device. The frequency responses and TRV results of the models are good agreement with measurements. The TRV amplitude factor of measured and simulation results are discussed in this chapter.

Chapter 5 concerns the study of transformer iron core characteristics at a high frequency. The frequency dependent transformer equivalent circuit for TRV under TLF condition was studied with the experiment and simulation methods. The capacitor current injection method is used to get the experimental TRV waveforms. The measured TRV results show the center of TRV oscillation is shifted. To analyze the TRV with simulation model, the frequency dependent equivalent circuit was constructed with EMTP. The simulation circuit elements such as short-circuit inductance, resistance and stray capacitance are calculated from the FRA measurement graph. The simulation results show the TRV wave shape is shifted to the center and good agreement with the measured ones. Short-circuit inductance of all tested transformers which is calculated from FRA graph is frequency dependence. To study this, frequency dependency impedance study was conducted. These results are presented in this chapter.

In **chapter 6** the composition of this dissertation is summarized. Establishment of research techniques for TLF-TRV study is pointed out. Moreover, the scope for the future research is also given.

References

1. Luces M. Faulkenberry, Walter Coffey, "Electrical Power Distribution and Transmission", Prentice-Hall, Inc, 1996.
2. L.L Grigsby, "Electric Power Engineering Handbook", Second Edition, Taylor & Francis Group, LLC, 2006.
3. Mohamed E. El-Hawary, "Introduction to Electrical Power Systems", John Wiley & Sons, Inc., Hoboken, New Jersey, IEEE Press, 2008.
4. James H. Harlow, "Electric Power Transformer Engineering", The Electrical Power Engineering Series; 9, CRC Press LLC, 2004.
5. J.G. Jamnani, and Mrs. S.A. Kanitkar, "TRV Rating Concepts and Generation of TRV Envelopes for Synthetic Testing of Extra High Voltage Circuit Breakers", International Journal of Computer and Electrical Engineering, Vol.3, No.1, pp. 24-29, February, 2011.
6. H. Ikeda, K. Harada, M. Kozako, S. Ohtsuka, and M. Hikita, "University Approach for Circuit Breaker Development", 20th International Conference on Electricity Distribution, CIRED, Paper 0794, Prague, June 8-11, 2009.
7. IEC 62271-100, "High-voltage switchgear and controlgear- Part 100: Alternating-current circuit-breakers", Second Edition, April, 2008.
8. Lou van der Sluis, "Transients in Power Systems", John Wiley & Sons Ltd, 2001.
9. L. Gosland, W.F.M. Dunne, "Calculation and Experiment on Transformer Reactance in Relation to Transients of Restriking Voltage", Journal of Institution of Electrical Engineers, Vol. 87, Issue 524, pp 163-177, May 8, 1940.
10. E. Haginomori, MyoMin Thein, H. Ikeda, S. Ohtsuka, M. Hikita, and T. Koshizuka, "Investigation of transformer model for TRV calculation after fault current interrupting," ICEE 2008, Panel discussion, Part 2, PN2-08, Okinawa, Japan, July 6-9, 2008.
11. Robert H. Harner, J. Rodriguez, "Transient Recovery Voltages Associated with Power-System, Three-Phase Transformer Secondary Faults," IEEE Trans. Power App. Syst., vol. PAS-91, pp. 1887-1896, Sept./Oct. 1972.
12. P.G. Parrott, "A Review of Transformer TRV Conditions," CIGRE WG 13.05, ELECTRA No. 102 pp 87-118, 1985.
13. Robert H. Harner, "Distribution System Recovery Voltage Characteristics: I-Transformer Secondary-Fault Recovery Voltage Investigation," IEEE Trans. Power Apparatus and Systems, Vol. PAS-87, No.2, pp. 463-487, Feb 1968.
14. M. Thein, H. Ikeda, K. Harada, S. Ohtsuka, M. Hikita, E. Haginomori and T.

-
- Koshizuka, "Investigation of Transformer Model for TRV Calculation by EMTP," IEEJ Transactions on Power and Energy, Vol.129, No.10, pp 1174-1180, Oct 2009.
15. Bruce A. Mork, Francisco Gonzalez, Dmitry Ishchenko, Don L. Stuehm, and Joydeep Mitra, "Hybrid Transformer Model for Transient Simulation-Part I: Development and Parameters," IEEE Transactions on Power and Delivery, vol. 22, No.1, pp. 248-255, Jan. 2007.
 16. A.Ametani, N.Kuroda, T.Tanimizu, H. Hasegawa and H.Inaba, "Field test and EMTP simulation of transient voltages when clearing a transformer secondary fault", Denki Gakkai Ronbunshi, Vol. 118-B, No.4, pp.381-388, April 1998.
 17. Eiichi Haginomori, "Applied ATP-EMTP to Highly-sophisticated electric power systems", August, 2003.
 18. Hans K. Høidalen, Bruce A. Mork, Francisco Gonzalez, Dmitry Ishchenko, Nicolas Chiesa, "Implementation and Verification of the Hybrid Transformer Model in ATPDraw", IPST 2007, Lyon, France, June 4-7, 2007.
 19. A.Ametani, N.Kuroda, T.Tanimizu, H. Hasegawa and H.Inaba, "Theoretical Analysis of Transient Recovery Voltages When Clearing a Transformer Secondary Fault", Denki Gakkai Ronbunshi, Vol. 119-B, No.11, pp.1308-1315, November 1999.

Chapter 2

Frequency Response Analysis

2.1 Introduction

The application of frequency response analysis (FRA) technology is the conditional assessment of transformers and it is a well-understood technique in electrical testing. It is the ratio of an input voltage or current to an output voltage or current. FRA is an exciting test technology which has been extensively used around the world over the past decades for detecting the integrity of winding structures of power transformers. This technique has been applied to power transformers to investigate mechanical soundness since the pioneering work of E. P. Dick and C. C. Erven at Ontario Hydro in Canada in the late 1970's.

In the 1980's the Central Electricity Generating Board (CEGB) in the UK took up the measurement technique and applied it to transmission transformers. The French also began to pursue measurements at the same time. On the break up of the CEGB in the early 1990's work in FRA was taken up by National Grid in the UK and resulted in several papers at Doble Client Conferences. The technique has been spread further through Euro Doble conferences and client meetings and several utilities took up the technique.

To check the winding deformation of the power transformer is difficult to determine by conventional measurements of ratio, impedance and inductance. However, deformation results in relative changes to the internal inductance and capacitance of the winding structure. These changes can be detected externally by FRA method.

Experience has shown how to make measurements successfully in the field and how to interpret results. With advent of sophisticated instrumentation, FRA is now a well established technique for factory and field measurements, sensitive, easy to perform with repeatability and becomes an effective monitoring and diagnostic tool for verifying the geometrical integrity of power transformers [1, 2, and 4].

2.2 General Application of FRA in the Power System Transformer

Power transformers are usually very reliable, but when faults or lightning strikes occur, the transformer can be affected disastrously. When a transformer is subjected to high through fault currents, it may suffer mechanical shock that gradually displaces and distorts the windings. In the process of winding movement, the insulation between the turns can be abraded, causing a short circuit and damage to the windings. Mechanical vibrations, initiated by short circuit forces, may cause the windings to lose their clamping pressure, eventually leading to collapse of the windings and transformers fail in-service. Most of these failures are caused by transformer winding faults and through faults generated by lightning and switching surges.

The other cause of winding movement may be extensive vibration during transformer transportation. As the windings experience vibration, they may slacken and subsequently become unable to withstand mechanical forces exerted during faults. Ageing also contributes to winding looseness. In addition, harmonics generated under normal operating conditions may cause winding and core vibration. Short circuit faults are potentially very destructive because if the clamping pressure is not capable of restraining the forces involved, substantial permanent winding deformation or even collapse can occur almost instantaneously, often accompanied by shorted turns. A common cause of failure is a close-up phase to earth fault resulting from a lightning strike.

It is expected that a transformer will experience and survive a number of short circuits during its service life, but sooner or later one such event will cause slight winding movement, and the ability of the transformer to survive short circuits in future will then be severely reduced. As the transformer ages, its components deteriorate and the likelihood of a failure increases.

Frequency Response Analysis (FRA) has become a popular technique used to externally monitor and assess the condition and mechanical integrity of transformer windings for short-circuits, open-circuits, deformation, winding insulation breakdown and loss of clamping pressure. The FRA technique can help maintenance personnel identify suspect transformers, enabling them to take those transformers out of service before failure. This FRA technique calculates and computes frequency-dependent

variables of the transformer's windings, i.e. inductance and capacitance. It is these distributed winding parameters that will change when the windings are; short-circuited, open-circuited, deformed, or loose [2 and 3].

2.3 Property of FRA Measurement

As transformers are one of the main devices in the power utility grids, advanced techniques have been developed in recent years in order to improve the transformer life assessment. The main aims are:-

- To check the actual health state of a particular transformer in order to predict the breakdown before it occurs, and
- To decide whether to repair or not a transformer without opening it.

FRA measurement technique became widely used technique because of:-

- There is a direct relationship between the geometric configuration of the winding and core within a transformer and the distributed network of resistances, inductances and capacitances that make it up.
- This RLC network can be identified by its frequency dependent transfer function.

They are especially useful for detecting winding displacements inside the transformer and are based on the fact that if something occurs inside the transformer. However, the main problem about FRA techniques is to interpret the observed evolution of the frequency response in order to identify both failures and failure tendencies in the transformer [4 and 6]. These are briefly expressed in the following session 2.4.

2.4 Detectability of Faults by FRA Device

The transformers using in the power system have a 35 year design life and usually very reliable, however, the in-service failure of a transformer is very dangerous to utility personnel through explosion and fire, potentially damaging to the environment through oil leakage, is costly to repair or replace and consequently it may affect in loss of revenue. Lightning strikes, faults arise in the power system and aging of transformer can lead the risk and failure. To prevent these failures and to maintain transformers in good operating condition, maintenance engineers usually used routine preventative maintenance programs and schedules by making regular testing. FRA test becomes increasingly used to detect transformer winding movement or looseness by comparing the fingerprint FRA data and currently measurement data. From this comparison,

differences may indicate damage to the transformer, which can be investigated further using other techniques or by an internal examination [5].

Different kinds of fault give different changes between fingerprinted FRA data and investigated FRA measurement results. Some of these changes are highly distinguishable and allow the fault to be identified (e.g. loosened turns). Others can be confused with different faults having a similar effect (e.g. multiple core earths and closed loops in the tank). Simon A. Ryder had done which faults can be detected using FRA and how different faults may be distinguished. There are nine different types of faults are simulated. The summarize results are expressed in Table 2.1 [5].

Table 2.1 Detectability of Faults Using FRA [5]

Fault	Detectability
Poor tank ground	Easily detectable
No core ground	Not detectable
Multiple core grounds	Detectable Cannot be distinguished from closed loops in tank
Foreign objects in tank	Not detectable
Closed loops in tank (Circulating current)	Detectable Cannot be distinguished from multiple core grounds
Poor contact	Easily detectable
Additional turns	Easily detectable
Short-circuited turns	Easily detectable
Loosened turns	Detectable

2.5 Application of FRA Measurement in our Research

The purpose of this study is a transformer model construction to investigate transient recovery voltage (TRV) at transformer limited fault (TLF) current interrupting condition. A transformer model is treated as leakage impedance and a stray capacitance with an ideal transformer by EMTP. A leakage impedance value at a commercial power frequency is generally used in most of TRV studies. The phenomenon that a magnetic flux will not able to enter an iron core of a transformer at high frequency regions, a leakage impedance at high frequency region will not give a same value as that at a commercial power frequency. So that, the TRV calculation with the leakage impedance

value at a commercial power frequency may not give correct results.

FRA technique can be measured the transformer impedance in wide frequency range. By applying this property, we tried to introduce and evaluated the transformer constants (leakage inductance and stray capacitance) at high frequency region, between 10~100s kHz, for TRV calculation [6]. To find transformer impedance values at TRV frequency region it was considered that:-

- (1). Is it possible to calculate the transformer impedance from FRA measurement?

- (2). Is it possible to use the transformer impedance which were calculated from the FRA measurement for TRV study?

EMTP transformer model is constructed with impedance values which are evaluated from FRA measurement and simulation results show agreeable with the experiment results.

The transformer impedance calculations from FRA measurement graphs are expressed in detail in Chapters 3 and 4 of this dissertation.

References

1. E.P.Dick, C.C.Erven, "Transformer Diagnostic Testing by Frequency Response Analysis", IEEE Trans, PAS-97, No.6, pp. 2144-2153, Nov-Dec, 1978.
2. Charles Sweetser, Dr. Tony McGrail, "Sweep Frequency Response Analysis Transformer Applications: A Technical Paper from Doble Engineering", Version 1.0, Jan 27, 2003.
3. M. de Nigris, R. Passaglia, R. Berti, L. Bergonzi and R. Maggi, "Application of Modern Techniques for the Condition Assessment of Power Transformers", CIGRE Session 2004, Paris, Paper A2-207.
4. J.Pleite, E.Olias, A.Barrado, A.Lazaro, J.Vazpuez, "Modeling the Transformer Frequency Response to Develop Advanced Maintenance Techniques", Paper 4, Session 13, 14th PSCC, Sevilla, 24-28 June, 2002.
5. Simon A. Ryder, "Transformer Diagnosis Using Frequency Response Analysis: Results from Fault Simulations," IEEE Power Engineering Society Summer Meeting, Volume 1, Issue , Pg. 399 - 404 vol.1, 25-25 July 2002.
6. M. Thein, H. Toda, M. Hikita, H. Ikeda, E. Haginomori and T. Koshiduka, "Investigation of Transformer Impedance for Transformer Limited Fault Condition by using FRA Monitoring Technique", the International Conference on Condition Monitoring and Diagnosis 2010 (CMD 2010), paper A7-2, pp. 197-200, Shibaura Institute of Technology, Japan, September 6-11, 2010.

Chapter 3

Investigation of Transformer Model for Transient Recovery Voltage Calculation at Transformer Limited Fault Condition by EMTP

3.1 Introduction

An interrupting performance of a high voltage circuit breaker (CB) is tested under various conditions which reflect different fault conditions. Among this conditions transformer limited fault (TLF) interrupting condition becomes a supplementing issue as a particular case in the recent years. In the past time, the TLF interrupting performance of the CB was usually tested by the 10% terminal fault (T10) interrupting because the transformer impedance was usually very large compared to the short circuit impedance of other fault conditions such as a bus terminal fault. Since the capacity of electricity power system has been increased to fulfill the consumer demand, very large capacity power transformers up to 1500 MVA have been introduced in high voltage electricity system.

On the other hands, winding impedance of large capacity power transformers are being reduced not only regarding on the losses point of view but also the development of transformer design technology in some special case. In this circumstance, when a fault occurs in the power system, the TLF current became to exceed an interrupting current of the condition defined in the relevant international electrotechnical commission (IEC) standard (IEC62271-100, T10) because transformer leakage impedance became to decrease. Since a fault current of the TLF condition becomes to exceed the “T10 duty” condition, a separate test has been adopted with a current level higher than that at “T10 duty” for terminal fault (TF). Moreover the transient recovery voltage (TRV) which appears across the CB due to current interruption may exceed the standard value and severely effect on CB. This is well known phenomenon but the detail

characteristics of TRV such as amplitude factor, rate of rise of recovery voltage, peak value and oscillation are unknown. Therefore higher voltage level CB is used for that condition.

To select suitable CB rating, TRV characteristics of TLF current interrupting condition is needed to understand. The accurate TRV should be investigated carefully at the TLF condition in order to present a suitable TRV standard. The TRV investigation transformer model at TLF interrupting condition was studied applying the current injection (CIJ) measurement method. Several transformers which have different capacities and insulation medium were used in the CIJ experiments.

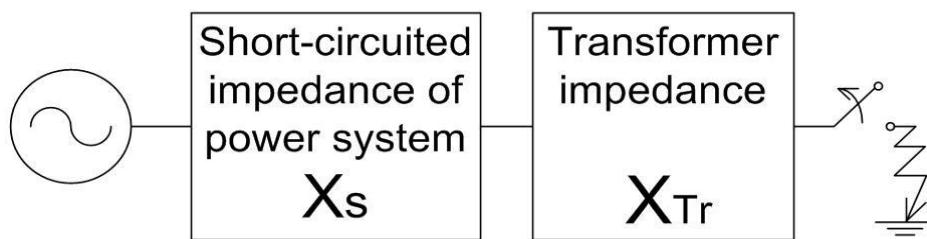
In the past, the interrupting condition analyses with the EMTP are performed with a transformer which is equivalently expressed in terms of leakage inductance, calculated based on percent impedance and stray capacitance. Several examples have been presented in which the TLF interruption condition was analyzed [1-4].

It is considered that leakage inductance at a commercial frequency domain cannot be used by extending to the TRV frequency domain. This is because inductance changes as magnetic flux cannot penetrate an iron core at a high-frequency domain such as TRV frequency domain. To study TRV at TLF condition, high frequency transformer model is preferred. Now a day the study of a transient phenomenon due to a circuit interrupting can be studied well developed software such as Electro-Magnetic transients program (EMTP). In this study a transformer model for the TLF condition is treated as leakage impedance and a stray capacitance with an ideal transformer in a computation by EMTP. The transformer constants were evaluated at high frequency regions, by using the frequency response analysis (FRA) measurement. The TRV experiment results with CIJ method, transformer impedance calculation from frequency response analysis (FRA) measurement, EMTP transformer models and its simulation results will be presented in this chapter [5-8].

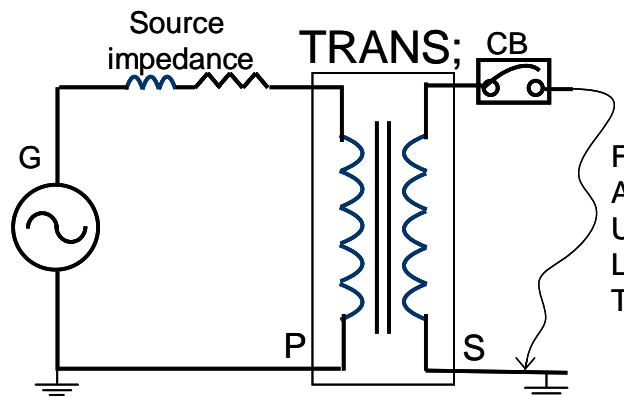
3.2 Transformer Limited Fault in the Power System

The TLF is one of fault that occurs in an electric power system. The fault clearing case in an actual power system is shown in figures 3.1(a) and (b). The TLF interrupting is defined as a fault where all fault currents are supplied through a transformer. Figure 3.1(b) represents the equivalent circuit diagram of the TLF interrupting condition in an electric power system. In the case of a TRV related to the TLF current interrupting condition, while short-circuit currents are generally much smaller than the rated short-circuited current but it is certain that a severe TRV may

result on CB contacts because of low impedances mainly due to the transformer stray capacitance [1,7,10]. The transformer stray capacitance occurs from winding to winding, from turn to turn, from windings to core and from winding to ground. The capacitance from winding to ground is the most dominant parameter on TRV than the other transformer capacitances. During the TLF, the majority of the voltage shares by the transformer impedance X_{Tr} , so that TRV after the fault current interrupting is mostly generated by the relevant transformer constants [5, 13]. To construct EMTP transformer model it was needed to know the test transformer impedance.



(a) Equivalent circuit for TLF clearing



(b) TLF interrupting in power system

Fig. 3.1 TLF interrupting circuit diagram

3.3 Impedance measurement

3.3.1 FRA Measurement

Frequency response analysis (FRA) is a powerful diagnostic technique and it has become popular for the examination of transformer internal conditions [9]. It can measure the impedances of transformer windings over a wide range of frequencies. This

property can be used for determining the circuit parameters by converting the FRA measurement raw data to impedances in ohm values versus frequency. The impedance values are calculated by converting the FRA output values (dB) with the following equation.

$$dB = 20 \cdot \log_{10} Z \quad \dots\dots\dots (3.1)$$

The transformer impedance was measured by a frequency response analyzer (NF FRA 5095). The measurable frequency range of this device is between 0.1 mHz to 2.2 MHz. The schematic diagram of transformer winding impedance measurement is shown in figure 3.2. The FRA measurement is done at both sides of the test transformer. FRA is measured at one side of the transformer while the other side is short-circuited condition. Figures 3.3 (a) to (c) are typical FRA results of 4 kVA two winding transformer. This is the relation between impedance and frequency obtained for the primary winding in different frequency regions, while the secondary is short-circuited. These results are used to calculate the transformer impedance for TRV study. The results are converted to the secondary side values by the test transformer's turn ratio. This is because, for instance, the FRA measurement from the secondary winding does not show the resonance point up to 2.2 MHz while the primary side is short-circuited. The measured impedance near the resonance frequency region is shown in figure 3.3 (b) and the measured impedance below 10 Hz is shown in figure 3.3 (c) respectively. Photographs of FRA device (NF FRA 5095) are shown in figures 3.4.

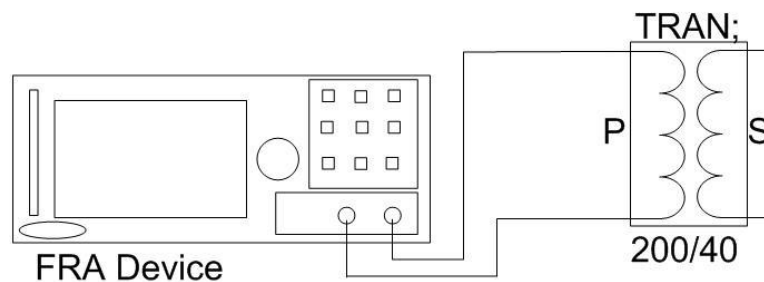
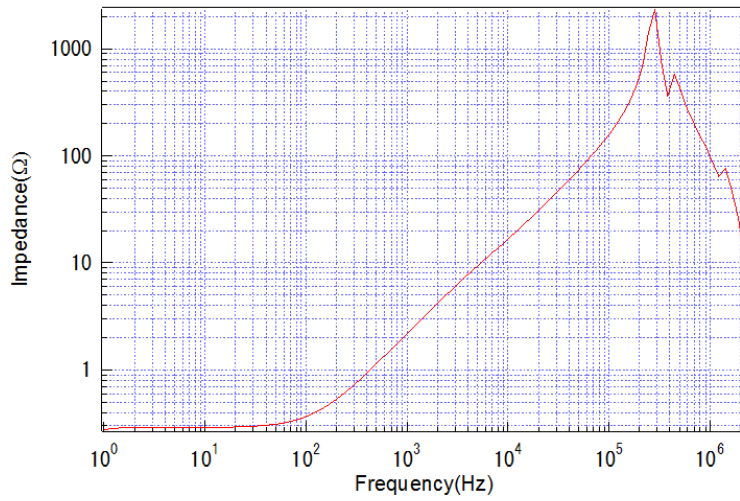
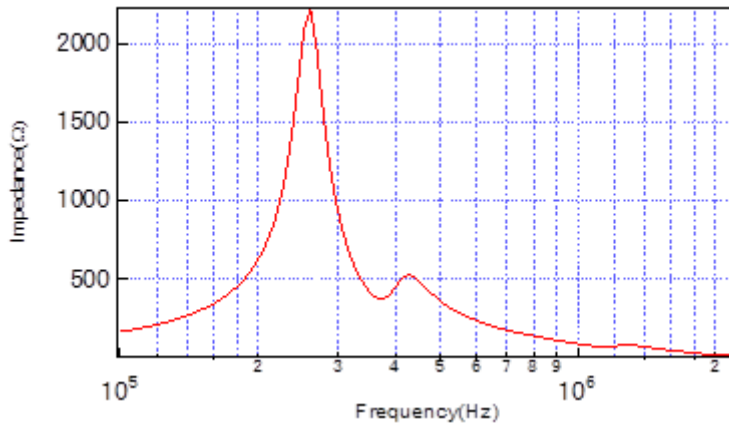


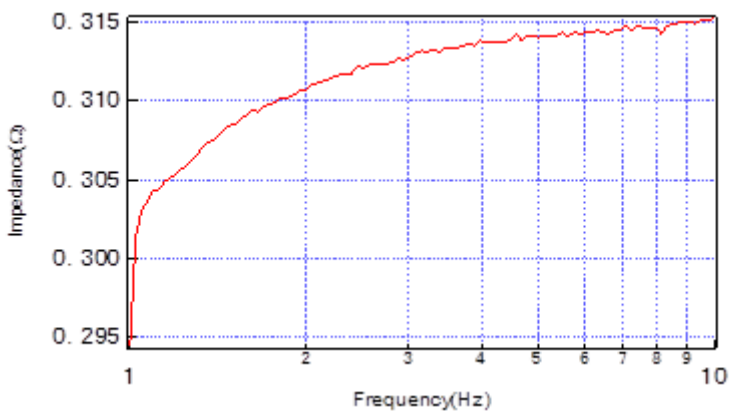
Fig. 3.2 FRA measurement setup diagram



(a) FRA graph used to calculate transformer impedance (1 Hz ~ 2.2MHz)

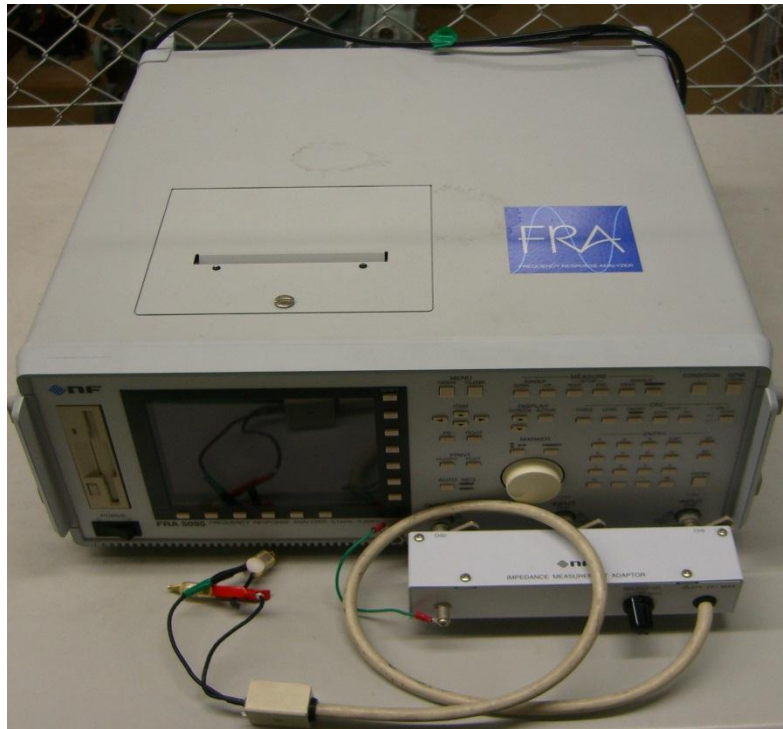


(b) FRA graph used to calculate damping resistor (100 kHz ~ 2.2MHz)

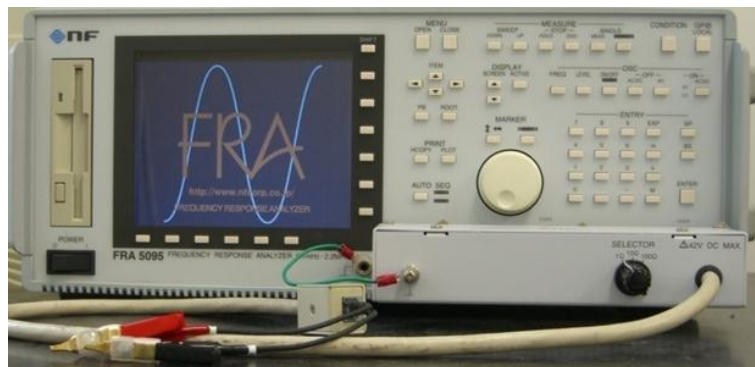


(c) FRA graph used to calculate winding resistance at very low frequency (1Hz ~10Hz)

Fig. 3.3 Typical FRA measurement graphs of test transformer in different frequency values



(a) Photograph of FRA device (NF FRA 5095)



(b) Photograph of FRA device (NF FRA 5095)



(c) Probe cable of NF FRA 5095

Fig. 3.4 Photographs of FRA measuring device

3.3.2 Impedance Calculation Procedure

Actually it is better if a frequency dependent inductance model can be used in TRV investigation. At the moment there is no EMTP inductance model of frequency dependence. For the first step of our study, the leakage inductance (L_t) is evaluated by averaging the impedance values. The stray capacitance (C_t) was calculated from a resonance point of the FRA graph (at 0.27 MHz) by applying the calculated leakage inductance value. Figure 3.5 shows one procedure to determine the impedance (transformer constants) calculated from the FRA graph. The first EMTP transformer model of the tested low voltage, 4 kVA two windings transformer is constructed from these values. Figure 3.6 is the equivalent transformer model circuit that was used in the first step EMTP simulation. In figure 3.6, L_t is the leakage inductance and C_t is the stray capacitance of the tested transformer. The stray capacitance C_t is assumed to include all stray capacitance related to the TRV. R_t is the winding resistance in the very low frequency region and it is obtained from the FRA measurement shown in figure 3.3(c). R_d is adopted for a damping resistance in the TRV oscillation to adjust the amplitude ratio. In the first step EMTP transformer model, the damping resistance value is derived as shown in the next section.

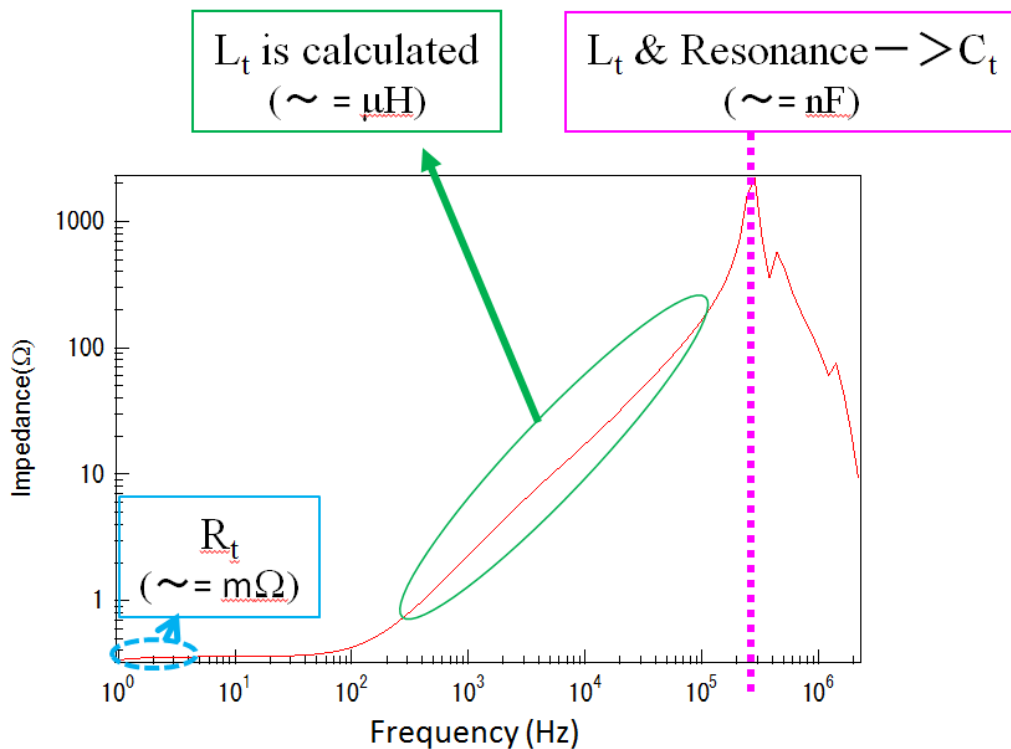


Fig. 3.5 The impedance calculation from FRA graph

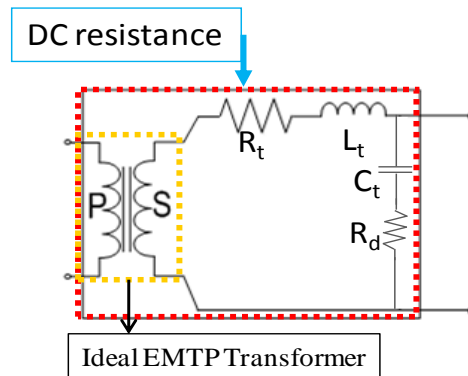
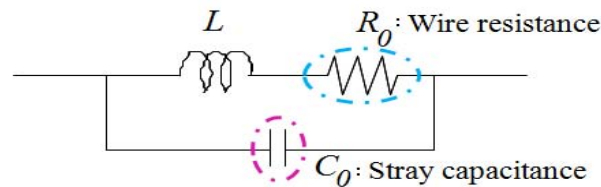


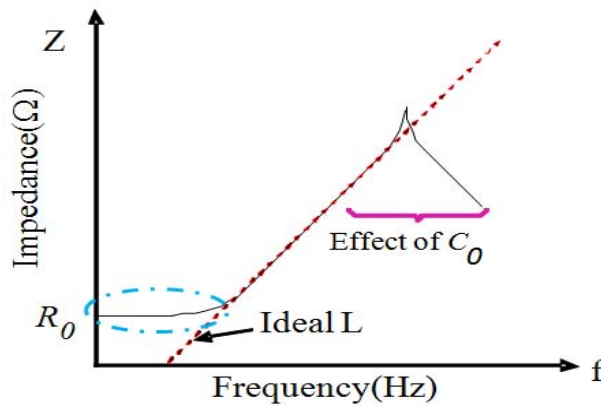
Fig. 3.6 First step model transformer circuit of EMTP simulation

3.3.3 Precise Calculation Analysis

As expressed in figure 3.7, the first calculated inductance will contain a winding resistance R_0 , which appears dominantly at the very low frequency region. In the high frequency region, the transformer impedance appears as a parallel circuit of the inductance L_t and the parallel stray capacitance C_t . The first calculated leakage inductance value L_t from the FRA measurement becomes equivalent to the parallel circuit of the stray capacitance C_t and the accurate inductance L_t^* . L_t^* can be determined from the relation of $j\omega L_t = Z = 1/(j\omega C_t^* + 1/j\omega L_t^*)$.



(a) Winding impedance equivalent circuit



(b) Frequency response of inductor

Fig. 3.7 The frequency response of general inductor

To get an accurate impedance value of the transformer, the following calculation is performed, based on equation (3.2) and the test transformer winding circuit configuration shown in figure 3.8.

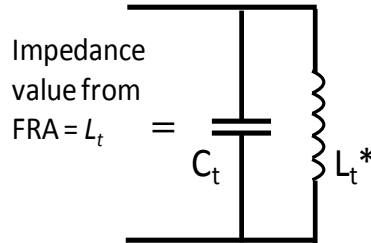


Fig. 3.8 Equivalent impedance circuit to calculate precise impedance values from FRA measurement

$$L_t^* = \frac{L_t}{1 + \omega^2 L_t C_t} \dots\dots\dots (3.2)$$

where L_t^* = leakage inductance calculated from equation (3.2),
 L_t = leakage inductance calculated from FRA graph,
 C_t = stray capacitance calculated from FRA graph.

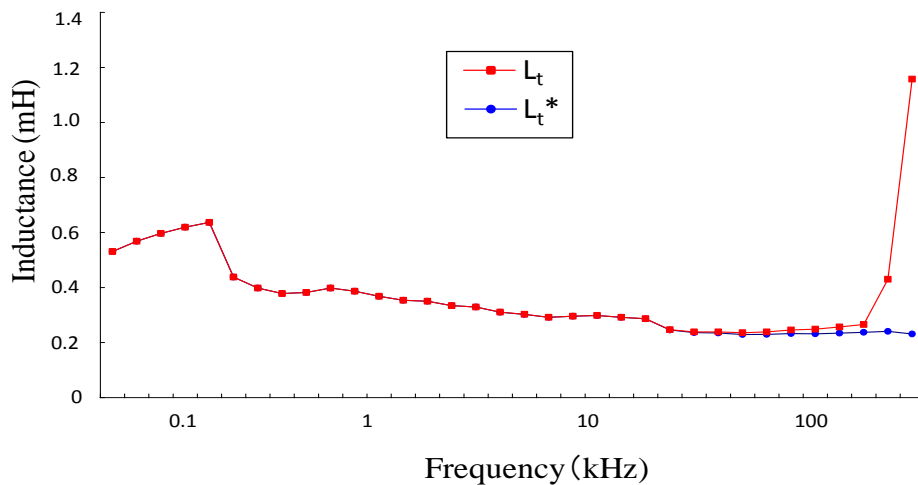


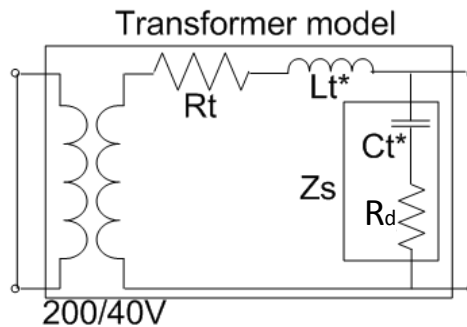
Fig. 3.9 Inductances from FRA measurement (L_t) and precise calculation (L_t^*)

In the inductance graph shown in figure 3.9, two inductance values are coincide up to 30 kHz. After 30 kHz, L_t^* value becomes smaller than L_t . It is considered the inductance values below 30 kHz correspond to the leakage inductance and the resistance.

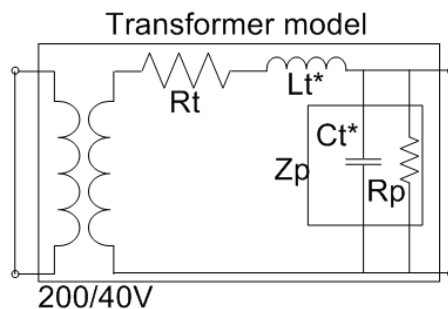
The values above 30 kHz include the capacitance effect since $1/j\omega C_t$ becomes equivalent to $j\omega L_t$ at one specific frequency. The inductance value that is calculated from the FRA graph suddenly changes at around 0.1 kHz and 100 kHz in figure 3.9. The change in the impedance around 100 kHz arises from the effect of the stray capacitance. The capacitance of the test transformer at the resonance point C_t^* is calculated from the resonance point frequency and L_t^* . The impedance values calculated from the FRA graph and calculated from equation (2) are expressed in Table 3.1. The differences are very small, as the simulation by EMTP with L_t^* and C_t^* values gives the same results as that with L_t and C_t [7].

Table 3.1. Summarized Impedance Values of 4 kVA Transformer

	FRA Graph		Precise Calculation	
	L_t	C_t	L_t^*	C_t^*
Primary	0.3mH	1.16nF	0.295mH	1.18nF
Secondary	12 μ H	29nF	11.8 μ H	29.4nF



(a)



(b)

Fig. 3.10 Ideal transformer winding circuits

Finding a way to calculate the damping resistance value is essential in the EMTP model. To obtain an accurate model of the tested transformer, the ideal equivalent

models shown in figures 3.10(a) and (b) are considered. Figure 3.10(b) is considered because there will be some parallel resistance with the stray capacitance, due to a skin effect of the windings and an iron loss in the high-frequency region. R_t is the winding resistance in the very-low-frequency region, which is obtained from the FRA measurement shown in figure 3.3(c).

EMTP simulation is done using both models in figures 3.10(a) and (b). Simulation results from figure 3.10(a) give agreeable results with the experiment. The simulation results from figure 3.10(b) show a very short decay of oscillation compared with the experiment.

It is necessary to find the damping resistor value used in this model instead of a fitted value. According to the FRA graph in figure 3.3(a), the transformer winding impedance varies with the frequency. At the resonance point (0.27 MHz), the impedance value will be same as R_d in figure 3.10(a) because $j\omega L_t^* = 1/j\omega C_t^*$ when R_t is negligibly small. Then, the resistance R_p of the test transformer at the resonance point is determined from the resonance point (peak impedance value) of the FRA graph in figure 3.3(b).

By equating the parallel portion Z_p (C_t^* and R_p) and the series portion Z_s (C_t^* and R_d) of figures 3.9(a) and (b), a reasonable value of R_d is obtained. The calculation process is expressed as follows [7].

$$\left. \begin{aligned}
 Z_p &= \frac{1}{\frac{1}{R_p} + j\omega C_t^*} \\
 &= \frac{R_p}{1 + (\omega R_p C_t^*)^2} - \frac{j\omega R_p^2 C_t^*}{1 + (\omega R_p C_t^*)^2} \\
 Z_s &= R_d - \frac{j}{\omega C_t^*} \\
 R_d &= \frac{R_p}{1 + (\omega R_p C_t^*)^2}
 \end{aligned} \right\} \dots\dots\dots(3.3)$$

where R_p = resistance of the test transformer at the resonance point, as obtained from the FRA graph in figure 3.3(b),
 C_t^* = capacitance of the test transformer at the resonance point,
 R_d = damping resistor.

3.4 Experiment

3.4.1 Transformer for Experiment

A low-voltage, 4 kVA two windings transformer is used as the first example of determining the circuit parameters in an equivalent circuit because of its simple winding configuration. The transformer specifications are expressed in Table 3.2. Figure 3.11 is the photograph of tested 4 kVA transformer.

Table 3.2. Specifications of 4 kVA Transformer

Rated kVA	4 kVA
Number of phases	Single
Number of windings	2 windings
Rated voltage	200/40 V
Rated current	20/100 A
% Impedance	2.4 % at 75 ° C



Fig. 3.11 The photograph of tested 4 kVA transformer

3.4.2 Current Injection Measurement

The TRV can be investigated by both current interrupting and current injection (CIJ) methods. The former includes various factors affecting the TRV shape, such as current chopping and the arcing voltage of the interrupting equipment, as Harner (1968) and Ametani et al. (1998) have shown [1,11,12]. To investigate the inherent TRV, the CIJ method is preferable. The current interrupting can be expressed by a phenomenon where the opposite polarity current is injected after the current zero point. The opposite current is only injected in the current injection method, which is theoretically the same as the current interrupting.

As shown in figure 3.12, the power source G supplies a fault current through the source-side impedance and the transformer at the TLF current interrupting condition. The circuit breaker CB interrupts the fault current. The experimental circuit is constructed by this phenomenon. To investigate the TRV at TLF, the CIJ measurement circuit shown in figure 3.13 is used.

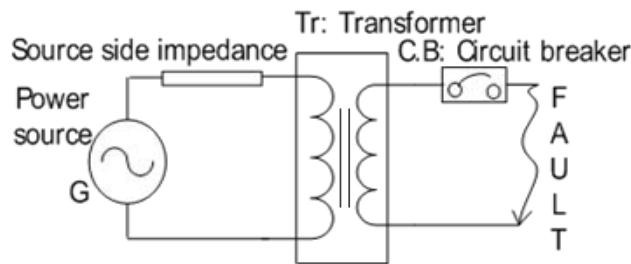


Fig. 3.12 TLF interrupting circuit diagram in power system

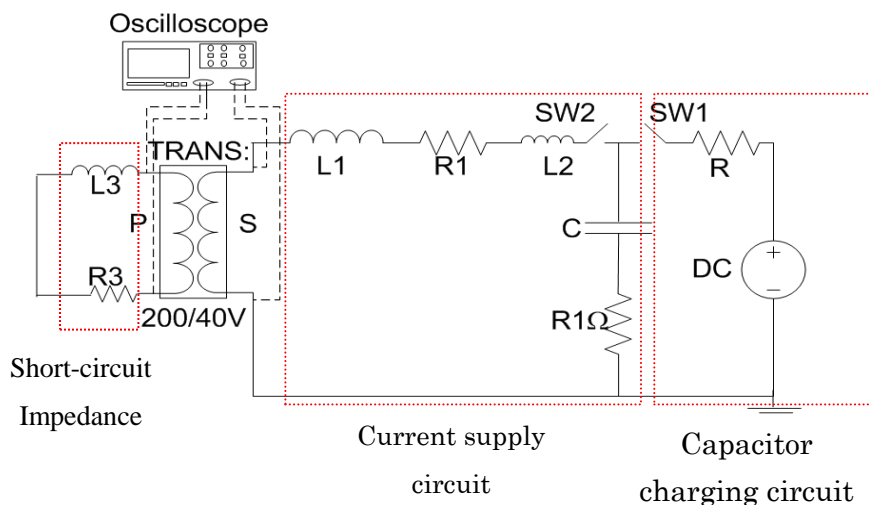
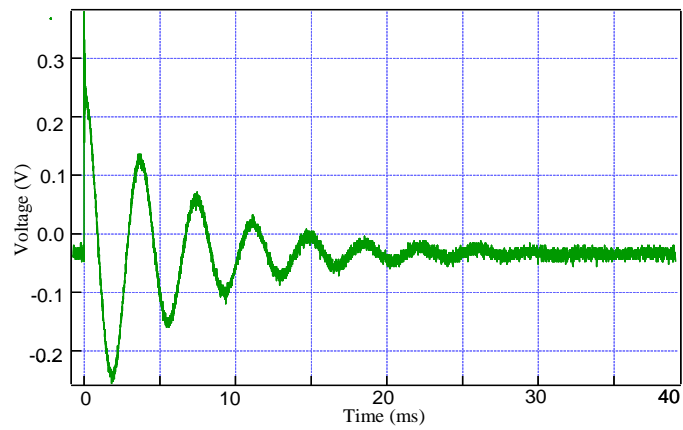
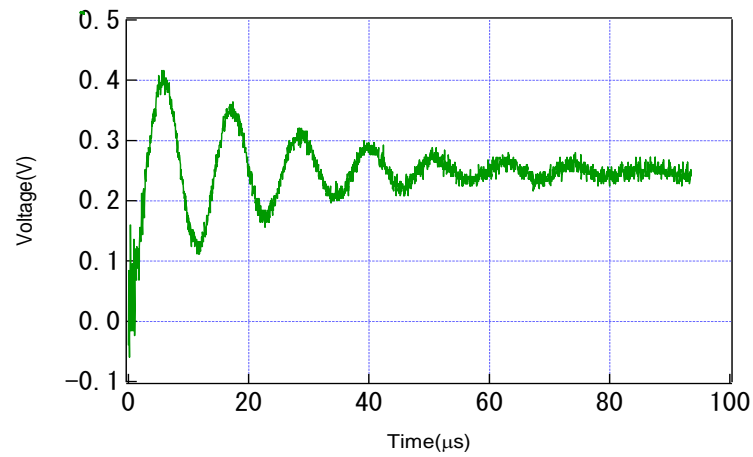


Fig. 3.13 Schematic diagram of CIJ experiment

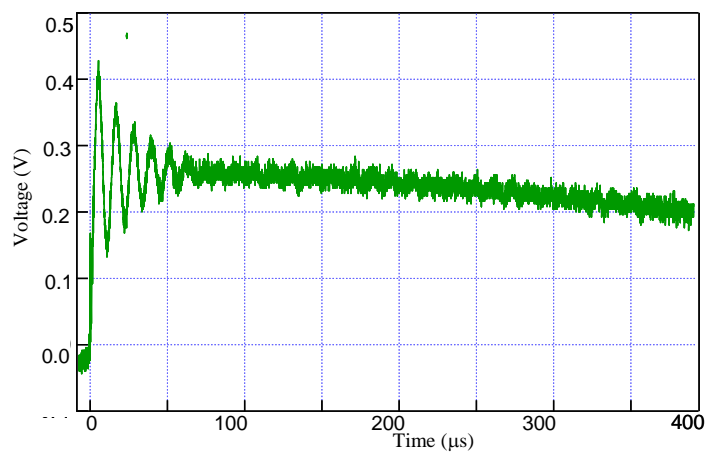
When the power source G is short-circuited, $L3$ and $R3$ in figure 3.13 represent the source-side impedance. The fault is replaced by a current supply circuit, which is energized by a DC supply. First, the capacitor C is charged by the DC voltage supply by switching $SW1$. After charging the capacitor C , current injection is done with $SW2$ (mercury switch). The values $L1$, $L2$, and $R1$ are current injection circuit elements. The voltages at the transformer primary and secondary sides are measured with an oscilloscope. The wave shapes of the two voltages are the same, while the magnitudes are different due to the turn ratio of the transformer. $R_1\Omega$ is a resistor for detecting the current. Figures 3.14(a) to (c) are example experimental results. Figure 3.14(a) is time duration of 40 ms (main voltage oscillation) and figures 3.14(b) and (c) are time durations of 100/400 μs (TRV oscillation wave). The TRV oscillation appears in the first 400 μs of the main voltage oscillation.



(a) Main oscillation



(b) TRV oscillation



(c) TRV oscillation

Fig. 3.14 Wave shapes of experiment

3.5 EMTP Model with CIJ Circuit

Figure 3.15 shows a constructed EMTP simulation model circuit for the TRV investigation at the TLF current interrupting condition. It is found that the EMTP simulation results for the model circuit are in agreement with the experimental results shown in figure 3.14. The EMTP results are shown in figures 3.16(a) to (c). Figure 3.16(a) is the main voltage oscillation corresponding to the frequency that gives the closed circuit formed by the capacitor C , the inductances $L1+L2$, the short-circuit impedance $L3$, and the transformer leakage impedance L_t^* . Figure 3.16(b) is the TRV oscillation that corresponds to the TRV determined from L_t^* , $L3$, and the transformer stray capacitance C_t^* from EMTP simulation with damping resistance R_d .

To obtain EMTP results that agree with the experimental TRV wave shape, the damping resistor R_d is essential in the EMTP model circuit shown in figure 3.15. It was found that the damping resistor determined from the resonance peak could not completely adjust the amplitude ratio. The EMTP simulation result for the TRV without a damping resistance is shown in figure 3.16(d).

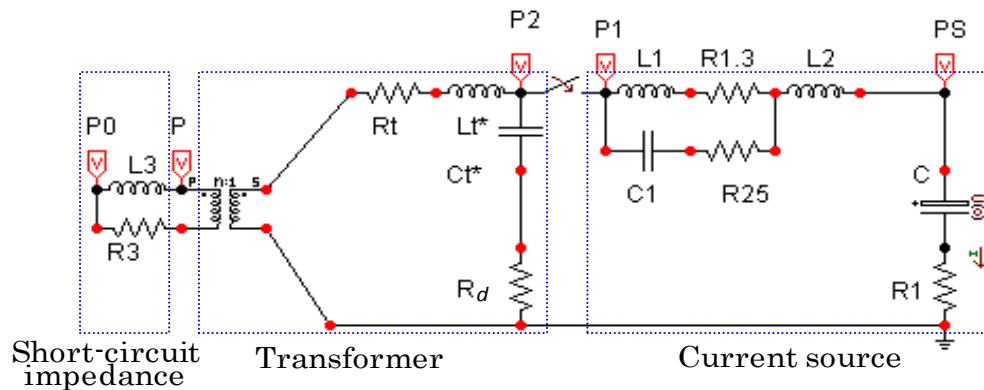
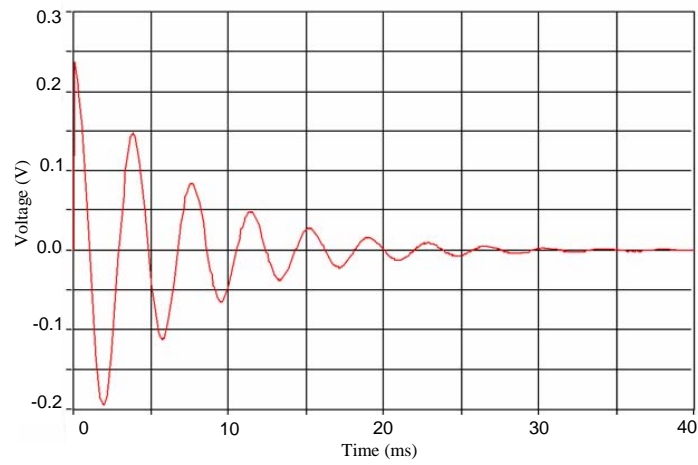
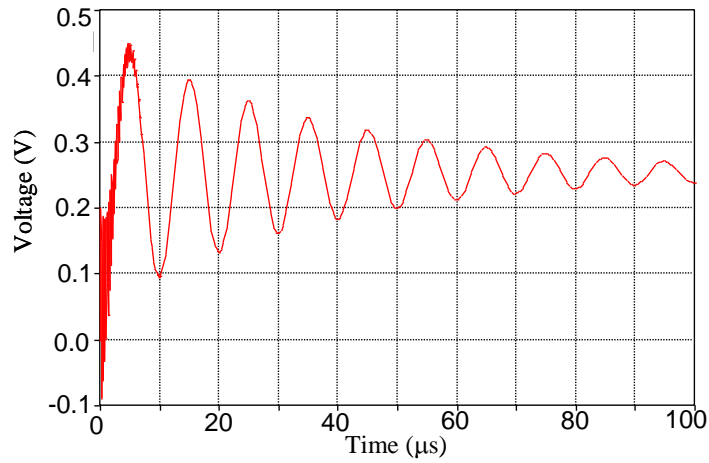


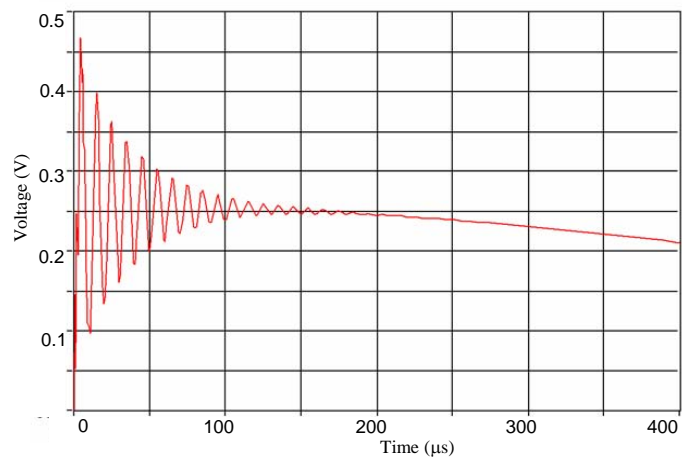
Fig. 3.15 EMTP model with CIJ circuit



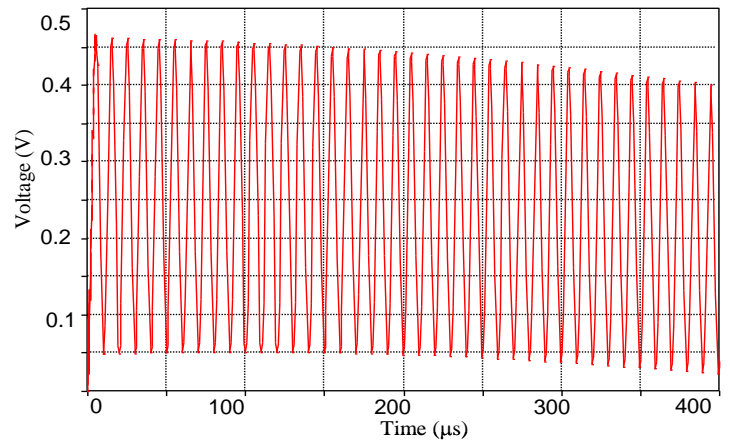
(a) Main oscillation



(b) TRV oscillation



(c) TRV oscillation



(d) TRV oscillation without damping resistance

Fig. 3.16 Voltage graphs of accurate EMTP model

3.6 Discussion

Discuss of the results of the experiment and EMTP simulation results are as follow:-

From the main voltage oscillation, figures 3.14(a) and 3.16(a), it is obvious that good agreeable results with the experiment and the simulation. From the EMTP simulation it was understood that the inductance and the capacitance of current supply circuit mainly influenced on the main voltage oscillation wave.

From the TRV oscillation wave, figures 3.14(b) and 3.16(b), agreeable results are seen between the experiment and the simulation. From EMTP simulation it was understood that the leakage inductance and the stray capacitance of the test transformer mainly influenced on this TRV oscillation wave. Furthermore, the damping resistor is indispensable in the EMTP model. Its resistance value determines the TRV oscillation to be damped.

3.7 Conclusion

From this study, the following conclusions for the accurate TRV calculation by EMTP at the TLF condition are obtained.

For the transformer model:-

- (1). The leakage impedance can be obtained from FRA by averaging between the frequency range of 500 Hz to 100 kHz.
- (2). A stray capacitance can be obtained from the resonance frequency and calculated leakage impedance.
- (3). A damping resistor can be obtained from impedance at the resonance frequency.

For current injection method:-

- (1). By using the transformer model the EMTP calculation and the experiment give an agreeable results.
- (2). Current injection is not suffered from current chopping and arcing voltage which are main difficulties in an interrupting method.

For the future it is desirable to identify the more precise impedance calculation from FRA measurement graph to use TRV investigation EMTP model for TLF condition. Next step study of TLF-TRV with capacitor current injection with diode as an interruption device is presented in chapter 4 of this dissertation.

References

1. Robert H. Harner, "Distribution System Recovery Voltage Characteristics: I-Transformer Secondary-Fault Recovery Voltage Investigation," IEEE Trans. Power Apparatus and Systems, Vol. PAS-87, No.2, pp 463-487, Feb 1968.
2. Robert H. Harner, J. Rodriguez, "Transient Recovery Voltages Associated with Power-System, Three-Phase Transformer Secondary Faults," IEEE Trans. Power App. Syst., vol. PAS-91, pp. 1887-1896, Sept./Oct. 1972.
3. P.G. Parrott, "A Review of Transformer TRV Conditions," CIGRE WG 13.05, ELECTRA No. 102 pp 87-118.
4. "Transient Recovery Voltage Conditions to be Expected when Interrupting Short-circuit Currents limited by Transformers," CIGRE Report 13-07, 1970.
5. E. Haginomori, M. Thein, H. Ikeda, S. Ohtsuka, M. Hikita, and T.Koshiduka, "Investigation of transformer model for TRV calculation after fault current interrupting," ICEE 2008, Panel discussion, Part 2, PN2-08, Okinawa, Japan, July 6-10, 2008.
6. M. Thein, H. Ikeda, K. Harada, M. Hikita, S. Ohtsuka, E. Haginomori and T. Koshiduka, "Transformer Model for TRV Calculation at the Transformer Limited Fault Condition by EMTP", ICEE 2009, HF1-08, I9FP0196, Shenyang, China, July 6-9, 2009.
7. M. Thein, H. Ikeda, K. Harada, S. Ohtsuka, M. Hikita, E. Haginomori and T. Koshiduka, "Investigation of Transformer Model for TRV Calculation by EMTP," IEEJ Trans; on Power and Energy, Vol.129, No.10, pp 1174-1180, Oct 2009.
8. M. Thein, H. Toda, K. Harada, M. Hikita, S. Ohtsuka, H. Ikeda, E. Haginomori and T. Koshiduka, "Investigation of TRV at Transformer Limited Fault by using Transformer Impedance Calculated by FRA Measurement", The joint technical meeting on Electrical Discharges, Switching and Protection Engineering and High Voltage Engineering, IEE Japan, ED-09-167, SP-09-38, HV-09-47, pp 77-81, Nov 19-20, 2009.
9. Ryder, S.A., "Transformer diagnosis using frequency response analysis: results from fault simulations," IEEE PES Summer Meeting, Volume 1, Issue, 25-25, vol.1, pp. 399 - 404 July 2002.
10. Cigre Working Group 33.02 (Internal Over voltages), "Guidelines for Representation of Network Elements when Calculating Transients,".
11. A.Ametani, N.Kuroda, T.Tanimizu, H. Hasegawa and H.Inaba, "Field test and EMTP simulation of transient voltages when cleaning a transformer secondary

- fault”, Denki Gakkai Ronbunshi, Vol. 118-B, No.4, April 1998, pp.381-388.
12. A.Ametani, N.Kuroda, T.Tanimizu, H. Hasegawa and H.Inaba, “Theoretical Analysis of Trnasient Recovery Voltages When Clearing a Trnasformer Secondary Fault”, Denki Gakkai Ronbunshi, Vol. 119-B, No.11, pp.1308-1315, November 1999.
 13. L. Gosland, W.F.M. Dunne, “Calculation and Experiment on Transformer Reactance in Relation to Transients of Restriking Voltage”, Journal of Institution of Electrical Engineers, Vol. 87, Issue 524, pp 163-177, May 8, 1940.

Chapter 4

Investigation of TRV under Transformer Limited Fault Condition by Frequency Dependent Equivalent Circuit

4.1 Introduction

In chapter 3, the simple transformer model for transient recovery voltage (TRV) investigation at transformer limited fault (TLF) condition is constructed. The frequency responses of the transformer impedance were measured by frequency response analyzer (FRA). The measured results show short-circuit inductance of the all tested transformers are frequency dependent. To analyze the phenomena the construction of frequency dependent equivalent circuit is considered. To get the experimental TRV waves capacitor current injection with diode as an interruption switch is used. These results will be presented in this chapter 4.

Figure 4.1 is a single-phase equivalent circuit diagram of the TLF condition in an electric power system. In this figure, a transformer is expressed as the commonly used T-shaped equivalent circuit. When studying the TRV using the current injection (CIJ) method, a reverse-polarity current instead of an interrupting current is injected from two terminals of a breaker into a circuit where the power supply is short-circuited. In this case, the magnetizing inductance of the transformer becomes parallel to the leakage impedance at the primary side and the source impedance. As a general rule, the magnetizing inductance of a transformer at a commercial frequency may be neglected because the inductance is higher than the aforementioned impedances. However, in the range of several to several hundred kHz, which corresponds to the TRV frequency, the magnetizing inductance is considered to diminish due to such factors as an increase of eddy current inside the iron core, a reduction of flux inside the core due to the skin effect, and the frequency dependence of relative permeability [1].

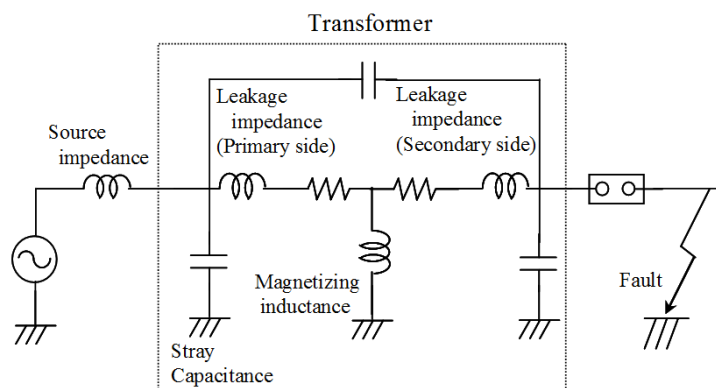


Fig. 4.1 Typical equivalent circuit for TLF condition

4.2 Example of Experiment Setup

To study the inherent TRV at the TLF interrupting condition, a TRV measurement circuit with a diode as an interrupting switch is used. Figure 4.2 illustrates the schematic diagram of the experiment. Current is provided to a transformer through a capacitor connected to the secondary side of the transformer via a mercury switch (SW2). The primary side of the transformer is short-circuited using a diode, and current is interrupted at the half-wave point. The mercury switch is adopted to prevent chattering when the switch is turned on. The diode used to interrupt the current is capable of high-speed switching when the current is interrupted at a reverse recovery time of 2 ns. The impact of the diode on the TRV after current interruption can be neglected because its terminal-to-terminal capacity of 2 pF is quite low compared to the stray capacitance of the transformer. The voltage and current are measured across the transformer terminals. Figure 4.3 shows example of the current flowing in the diode and the voltage that occurs due to the current interruption.

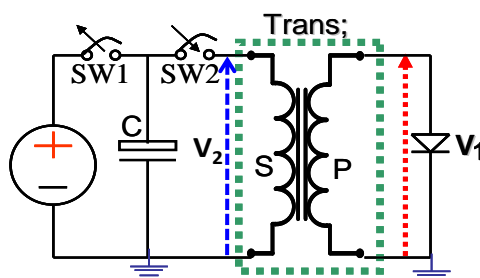


Fig. 4.2 Experimental circuit for diode interruption

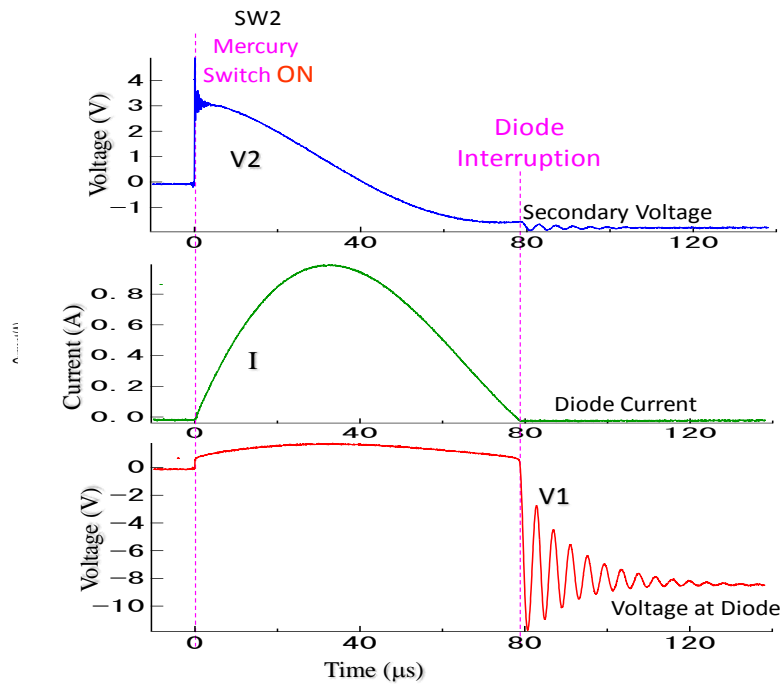


Fig. 4.3 Example experiment result of diode interruption

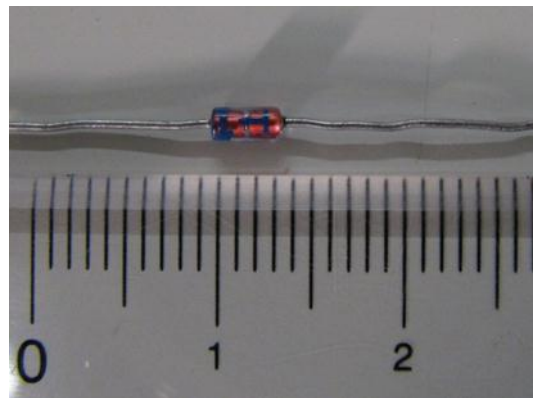


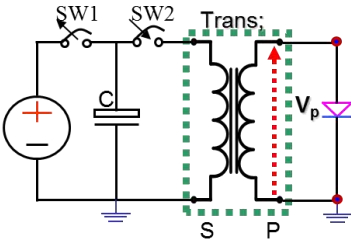
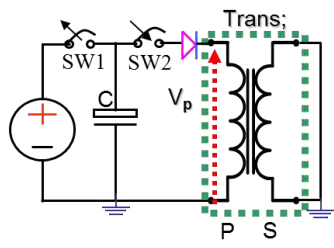
Fig. 4.4 Photograph of diode which is used in the experiment

As shown in figure 4.3, current is injected to the test transformer by switching on the SW2 (mercury switch). Injected current (I) is flow in the transformer and as soon as that current reaches the zero point, diode interrupts this and voltage oscillation (V1) occurs across the diode. This voltage (V1) is the investigated TRV and experimental inherent TRV wave of TLF condition is obtained. Figure 4.4 is the photograph of a diode which is used in this experiment. It is a small signal silicon diode (**1S1585**) made by Toshiba.

Table 4.1. Specifications of 50 MVA transformer

	High Voltage Side	Low Voltage Side
Rated Voltage	28000 V	11000 V
Rated Current	1790 A	4550 A
Rated Capacity	50 MVA	
Frequency	50 Hz	
Type	Single phase Two windings Short-circuit Test Transformer	
% Impedance	1.76 % At 75°C	

Table 4.2. Experiment setup of current injection

	Case 1	Case 2
Case	Simple, Small turn ratios	Large turn ratios, Connection circuit capacitance
Application of transformer	4 kVA, 300 kVA	5 kVA, 50 MVA
Experiment Set up	 <p style="text-align: center;">Setup 1</p>	 <p style="text-align: center;">Setup 2</p>
Remark	<ul style="list-style-type: none"> ■ If the test transformer has large turn ratios and connection circuit capacitance, setup 2 is preferable. ■ Because the stray capacitance of Diode affects on the current zero interruption. 	

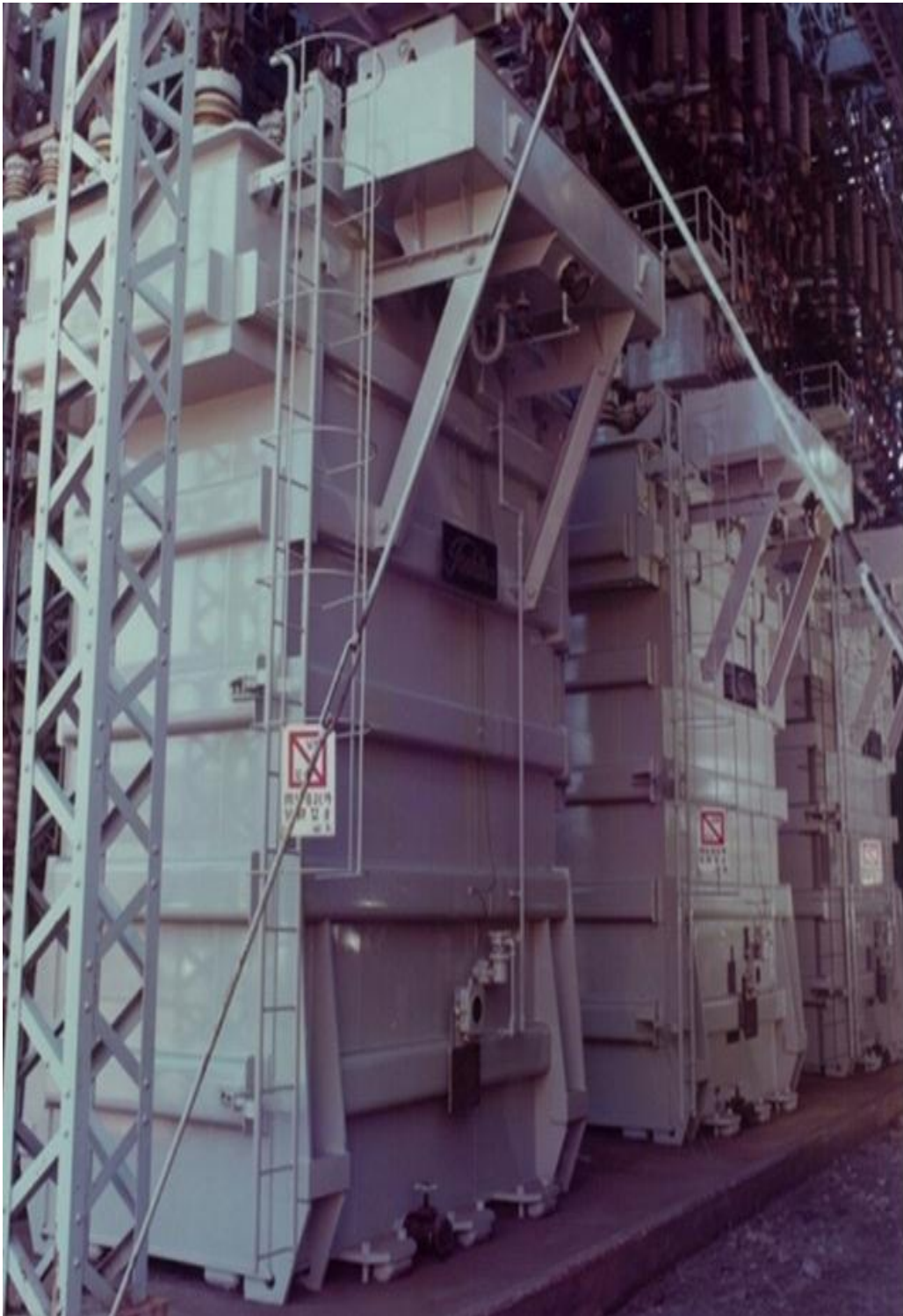


Fig. 4.5 Photograph of 50 MVA short-circuit test transformer (Hamakawasaki, Toshiba)

4.3 Experiment Results

The experiment was done with three kinds of transformer which have different capacities and different winding configurations (4 kVA two winding transformer, 300 kVA two winding oil-immersed transformer and 50 MVA two winding short-circuit test transformer). Table 4.1 is the specifications of 50 MVA transformer. Table 4.2 is the summarized table of experiment setups which were used in TRV measurements. Figure 4.5 is the photograph of 50 MVA transformer.

Figures 4.6(a) and (b) are the TRV measurement circuit of three tested transformers. The experiment results of 50 MVA transformer is expressed in figure 4.7. Since the tested 50 MVA transformer is connected with the bus-bar of test bay, setup 2 is used. TRV and amplitude factor measurement result of 50 MVA transformer is shown in figure 4.8. Since another two tested transformers (4 kVA and 300 kVA) have simple and small turn ratio, setup 1 is used. The experiment results of these two transformers are expressed in figures 4.9 and 4.10.

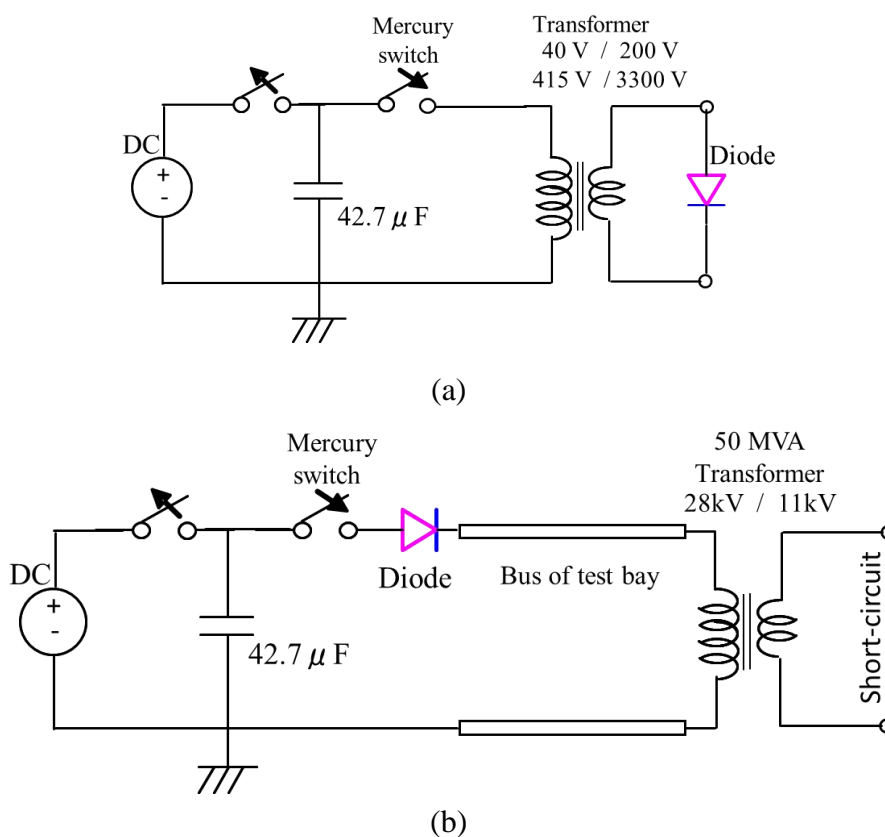


Fig. 4.6 TRV measurement circuit of tested transformers

From the experiment result the following points have been confirmed.

(1) Figure 4.7 shows that a current with a peak value of approximately 4 A flows in the transformer, and the current is interrupted at the half-wave point. The voltage drop of the transformer has appeared at the time of current flowing.

(2) After the current interruption, a TRV of approximately 40 kHz appears and it is decreased gradually, and voltage has become 0.

(3) Figure 4.8 shows that the TRV amplitude factor is 1.3, which is lower than the value of 1.7 specified by applicable standards i.e., IEC and JEC. The TRV amplitude factor is 1.4 for both 4 kVA transformer and 300 kVA transformer. It is expressed in figures 4.9 and 4.10.

(4) Sabot (1985) [2] mentions the relationship between amplitude factor and TRV frequency and reports an amplitude factor of 1.4 at the frequency of 40 kHz. This is in reasonable agreement with the measurement in (3) above.

(5) The center of oscillation is not constant, as can be seen in figures 4.8, 4.9 and 4.10. The center is low just after the current interruption and gradually increases thereafter. This may be due to the fact that the short-circuit inductance of transformers is frequency dependent, and the inductance is apparently low just after the current interruption but gradually increases thereafter.

(6) The small value of the first TRV wave is caused by the inconstant center of oscillation described in item (5) above.

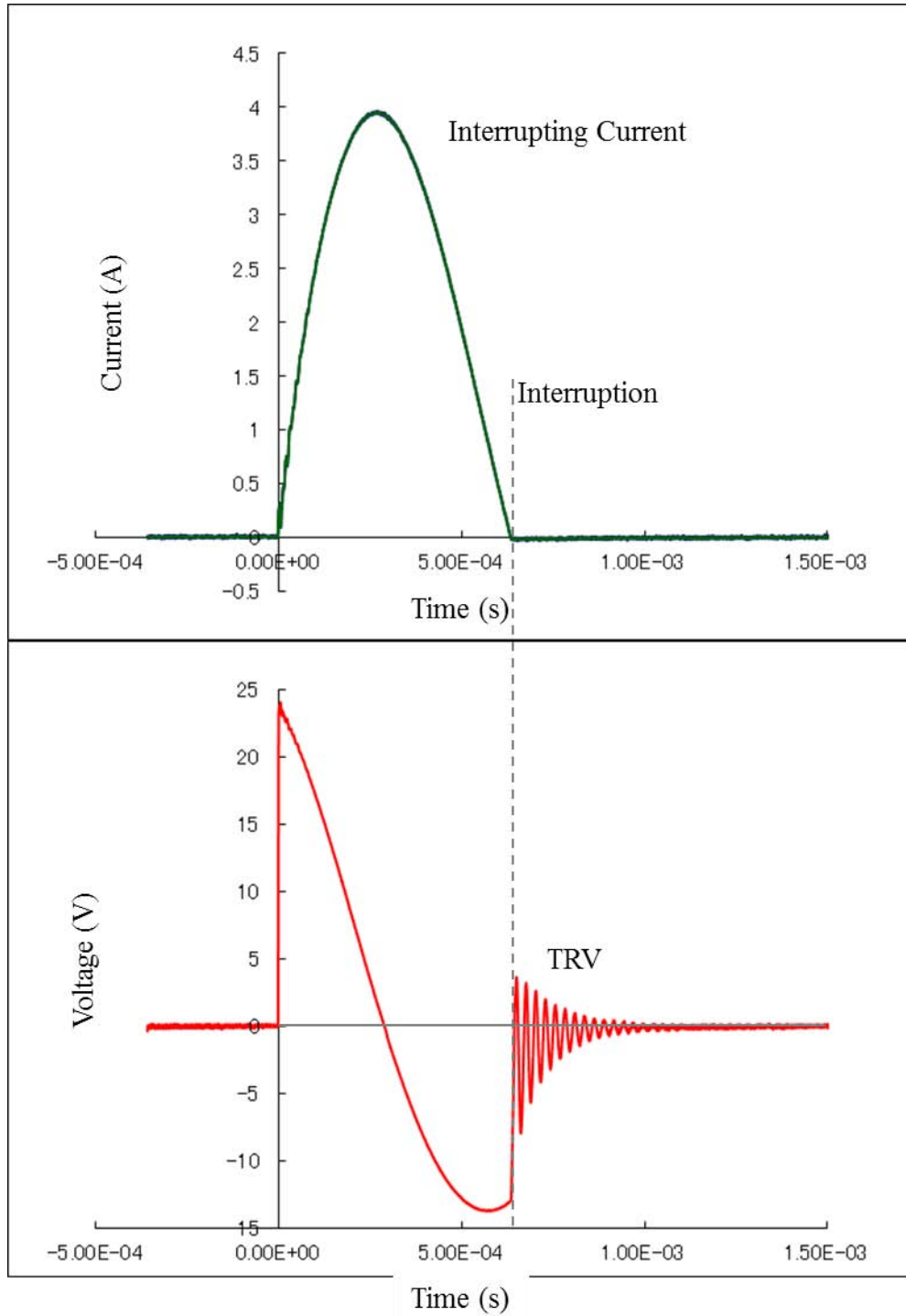


Fig. 4.7 TRV measurement result of 50 MVA transformer

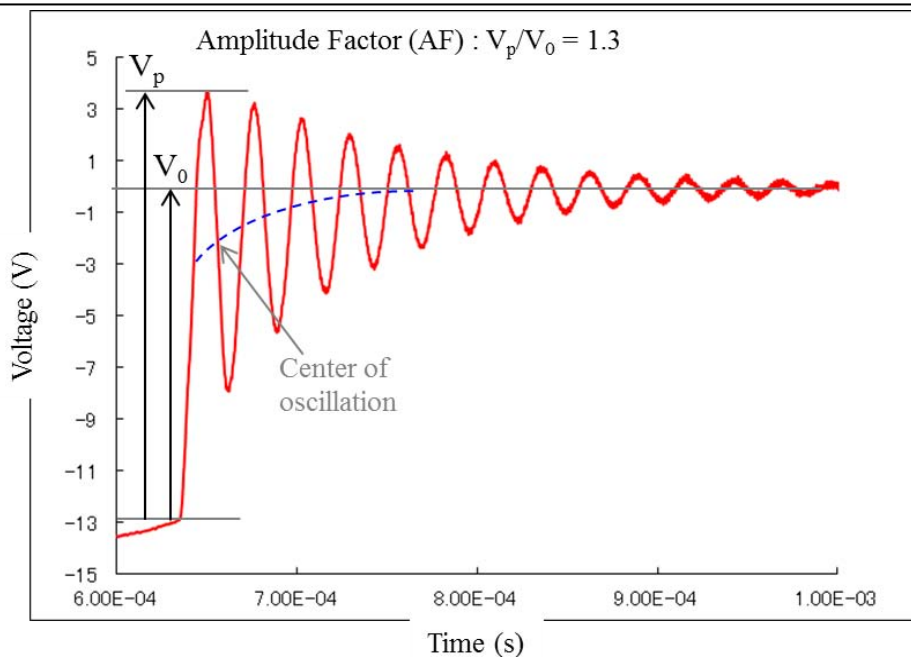


Fig. 4.8 TRV and amplitude factor measurement result of 50 MVA transformer

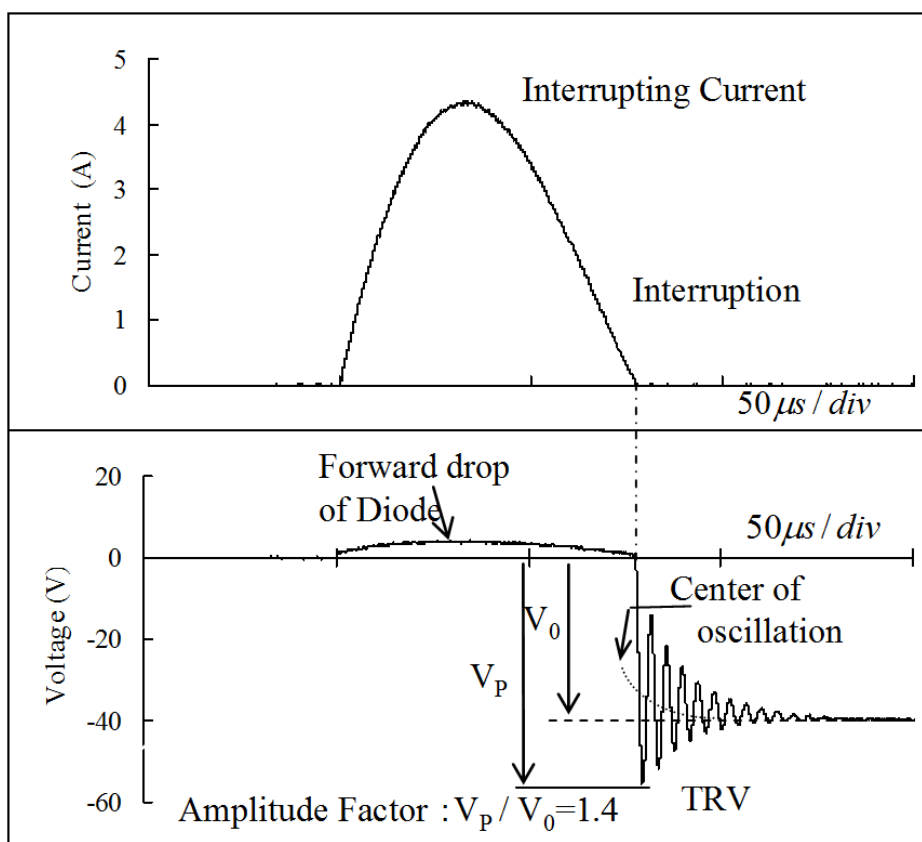


Fig. 4.9 TRV and amplitude factor measurement result of 4 kVA transformer

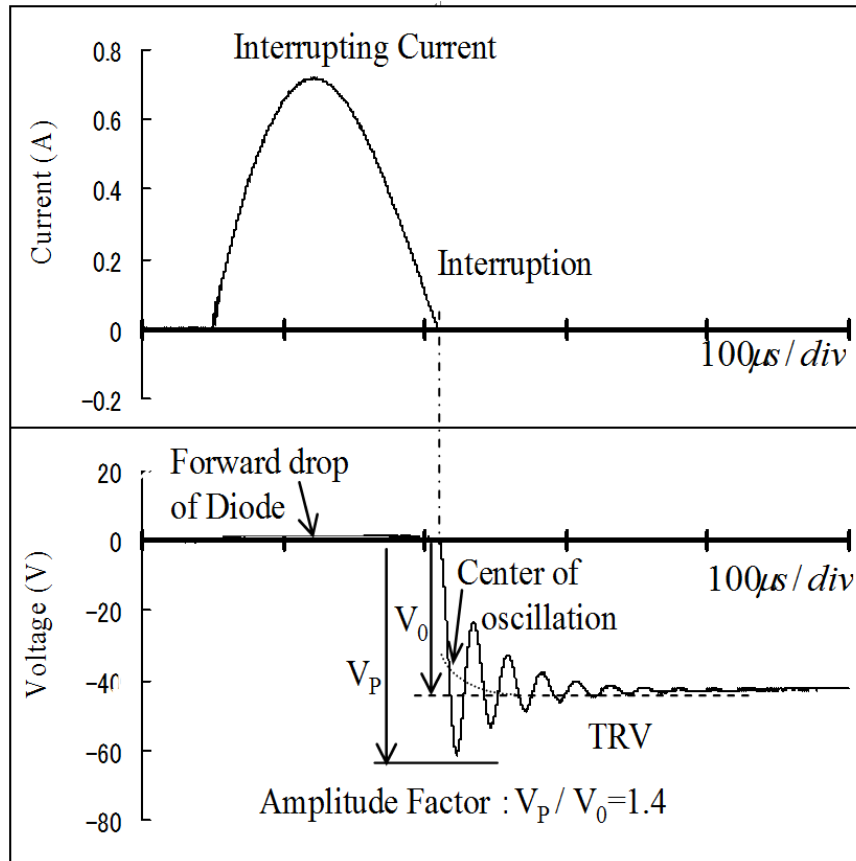


Fig. 4.10 TRV and amplitude factor measurement result of 300 kVA transformer

4.4 Examination of Frequency Dependency

4.4.1 Impedance Frequency Response

In the preceding section, the TRV amplitude factor of the transformer is found to be 1.3 for 50 MVA transformer and 1.4 for 4 kVA transformer and 300 kVA transformer. The cause of this small value is investigated and the investigated results will be presented for the 300 kVA transformer. Table 4.3 is the specifications of 300 kVA transformer. The frequency response of the impedance of a 3.3 kV, 300 kVA transformer has been investigated using a frequency response analysis (FRA) device (NF - FRA 5095).

For the 300 kVA test transformer, the secondary side (415 V) is short-circuited to take measurements from the primary side (3.3 kV). Figure 4.11 shows the impedance measurement obtained with the FRA device.

Figure 4.11 presents both the real and imaginary parts of the impedance. The real and imaginary parts are calculated using the phase angle, which is simultaneously measured with the impedance by FRA.

Figure 4.11 reveals the following points.

- (1) The total impedance is identical to the real part at up to the 10 Hz frequency level due to the dominant effect of the winding resistance. This impedance is considered to be caused by the 0.9 Ω resistance of the transformer windings.
- (2) The impedance reaches a maximum at 46 kHz, indicating the resonance point. This frequency corresponds to a parallel resonance between the inductance and the stray capacitance of the transformer.
- (3) The impedance from approximately 100 Hz to the resonance point is the same as the imaginary part, and the impedance gradient equals that of the imaginary part. The imaginary part corresponds to the reactance of the impedance and is composed of the inductance and the stray capacitance of the transformer. However, the impact of stray capacitance can be neglected in the low-frequency domain.

Here, let L_1 and L_2 be the self-inductance of the primary and secondary side of the transformer, respectively, R_2 the resistance of the secondary side, and M the mutual inductance between the primary and secondary side. Then the imaginary part of the total impedance is expressed by the following equation

$$X = \omega(L_1 - \frac{(\omega M)^2}{R_2^2 + \omega^2 \cdot L_2^2} \cdot L_2) \dots\dots\dots (4.1)$$

When ω is very large and $R_2 \ll \omega L_2$, the above equation becomes

$$X \cong \omega(L_1 - \frac{M^2}{L_2} \cdot L_2) \dots\dots\dots (4.2)$$

Therefore, the imaginary part may be considered to be the inductance of the transformer. This inductance X is called “Short-circuited inductance”.

- (4) The impedance gradient is clearly different between the frequency domain of approximately 1 kHz or greater and the domain of less than 1 kHz.

Figure 4.12 shows the short-circuit inductance calculated by dividing the imaginary part in figure 4.11 by ω (angular frequency). The inductance is almost constant at approximately 4 mH up to a frequency level of approximately 1 kHz, but the inductance decreases linearly at subsequent higher frequencies. This means that the short-circuit inductance of the transformer is certainly frequency dependent. Meanwhile, the inductance rapidly diminishes near the resonance point, which would suggest the effects of stray capacitance.

Figure 4.13 is the photograph of 300 kVA oil-immersed transformer.

Table 4.3. Specifications of 300 kVA transformer

Rated kVA	300 kVA
Number of phases	Single
Number of windings	2 windings
Rated voltage	3300/414 V
Rated current	91/723 A
%Impedance	3.69 %

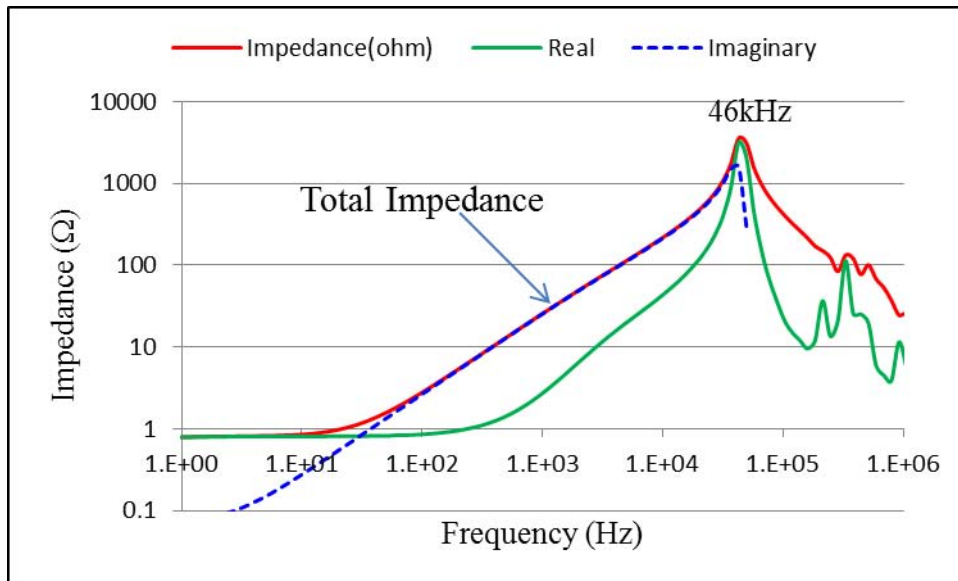


Fig 4.11 FRA measurement graph of 300 kVA test transformer

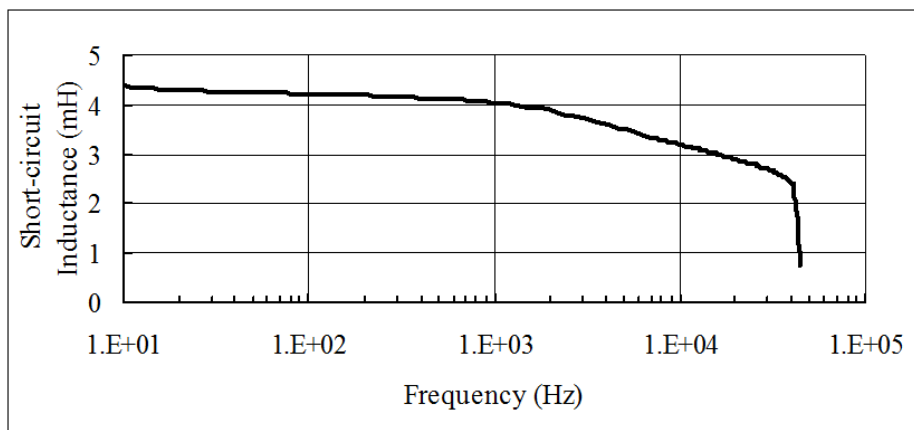


Fig 4.12 Frequency-dependent inductance of 300 kVA test transformer



Fig. 4.13 Photograph of 300 kVA oil-immersed transformer (Hamakawazaki, Toshiba)

4.5 Frequency Dependent Equivalent Circuit

As shown in figure 4.12, the short-circuit inductance of transformer is not constant and tends to decrease with an increase of frequency. Such that a frequency-dependent short-circuit inductance equivalent circuit (model) is constructed and shown in figure 4.14. The model is constructed by the following steps.

- (1) General equivalent circuits such as a transformer, a winding resistor, and a leakage inductance are expressed as serial connections, while stray capacitance is connected in parallel. Following this procedure, the resistor and the inductance are connected in series and a capacitor is connected in parallel as a stray capacitance.
- (2) Based on the results presented in the previous sections, the winding resistance of 300 kVA transformer is set to 0.9Ω .
- (3) The inductance is divided into three parts to represent a commercial frequency domain, a domain of approximately 10 kHz, and the

resonance point.

- (4) An inductance value of 4.05 mH is obtained from the inductance at a frequency of 50 Hz in figure 4.12. All the inductances in item (3) above are added together for a total inductance value of 4.05 mH.
- (5) An inductance value of 3.25 mH is obtained from the inductance at approximately the 10 kHz frequency domain in figure 4.12. It is adjusted so that the $L_a + L_b$ value in figure 4.14 equals this inductance value of 3.25 mH.
- (6) An inductance value of 2.5 mH at the resonance point is obtained by linearly approximating the range of 2–20 kHz in figure 4.12. This is represented by setting the L_a value in figure 4.14 to 2.5 mH.
- (7) The stray capacitance is set to 4.5 nF by taking into account the frequency of 46 kHz at the resonance point and $L_a = 2.5$ mH.
- (8) Resistors are placed in parallel to L_b and L_c to eliminate the effects of L_b and L_c at the 10 kHz frequency domain and at the resonance point.

Figure 4.15 shows a comparison of the frequency responses between the simulated result calculated from the circuit in figure 4.14 using the Frequency Scan function of EMTP and the measured impedances shown in figure 4.11. The simulation values for the model are in good agreement with the measured values in terms of frequency response, frequency at the resonance point, and impedance at the resonance point.

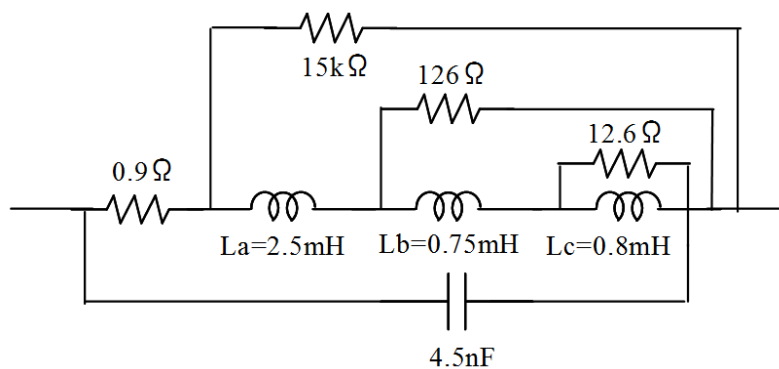


Fig. 4.14 Frequency-dependent equivalent circuit

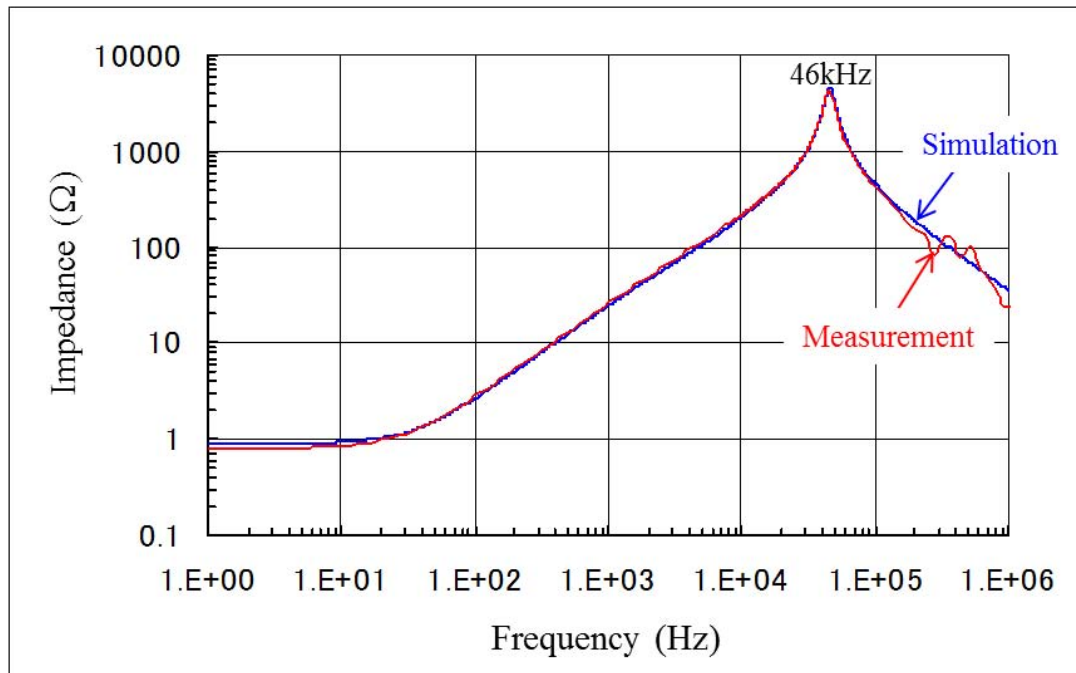


Fig. 4.15 Comparison of frequency response between FRA measurement and model for 300 kVA transformer

4.6 TRV Calculation Using Frequency-Dependent Equivalent Circuit

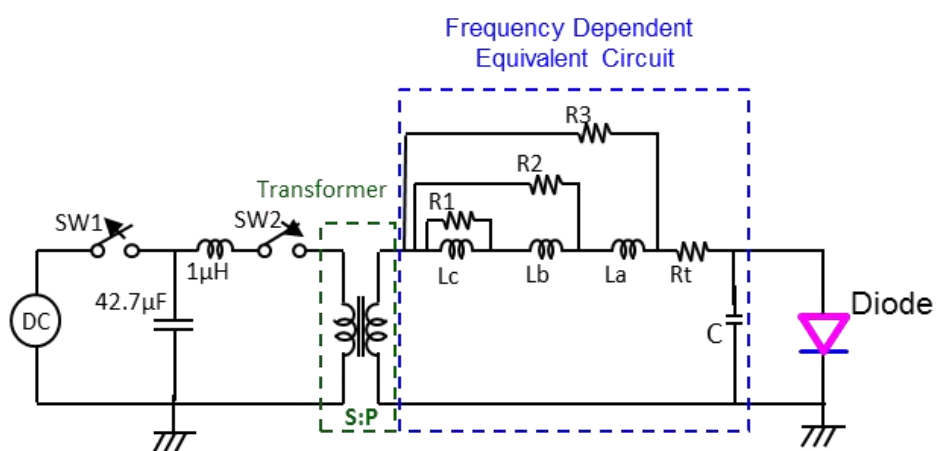
TRV is calculated using the frequency-dependent equivalent circuit constructed in figure 4.14 and simulating the TRV measurement circuit in figure 4.6. A diode is assumed to be an ideal switch. The forward voltage drop is measured separately and is serially connected to this switch as a nonlinear resistance. Figures 4.16 (a) and (b) are the schematic equivalent circuits of EMTP simulation for three tested transformers.

Figure 4.17 shows the waveforms resulting from the TRV calculation for 300 kVA transformer. The aspects of the TRV waveforms, especially the aspect of TRV attenuation, are in good agreement with the similar aspects in figure 4.10. The TRV frequency of approximately 40 kHz and TRV amplitude factor of 1.5 are also in good agreement with their counterparts in figure 4.10. It is also found that the center of oscillation is small just after the current interruption and gradually increases thereafter, as is the case with the measured waveform in figure 4.10.

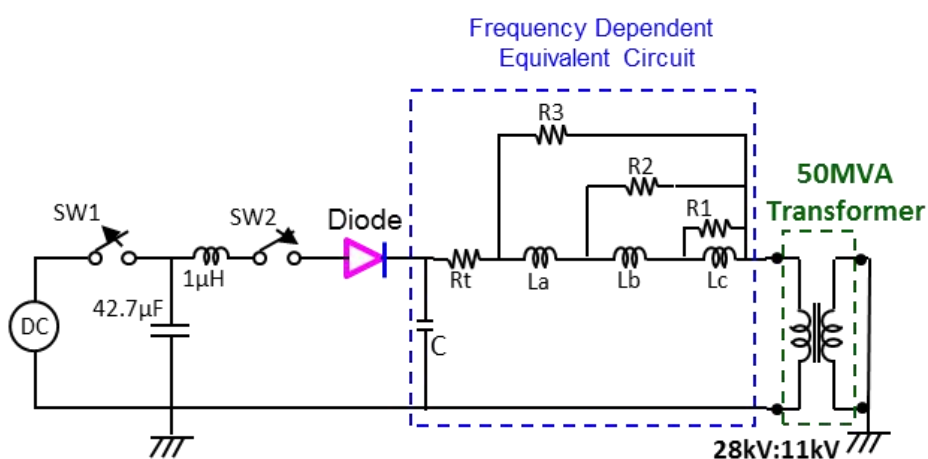
Figure 4.18 shows the waveforms of 300 kVA transformer resulting from the

TRV calculation, after removing L_b and L_c as well as the 12.6Ω and 126Ω resistors, in other words, by eliminating the frequency dependence. Compared to figure 4.17, the peak values of the interrupting current become higher due to the decreasing inductance of the transformer, and the frequency of the interrupting current increases.

The TRV amplitude factor is 1.9, which is larger than that in figure 4.17. In addition, the attenuation of the TRV oscillations is also delayed. The center of oscillation is constant because the inductance of the transformer model is constant.



(a) EMTP simulation circuit for 4 kVA and 300 kVA transformers



(b) EMTP simulation circuit for 50 MVA transformer

Fig. 4.16 Schematic TRV-TLF equivalent circuits of EMTP simulation

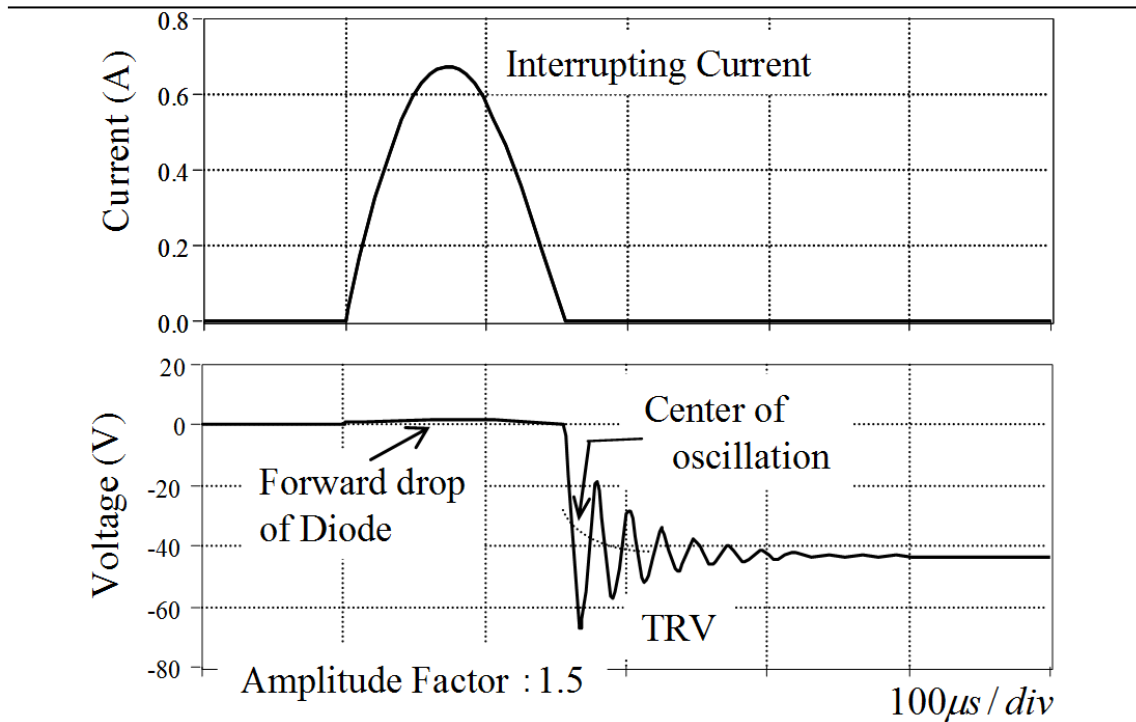


Fig. 4.17 TRV calculated result for 300 kVA transformer by using frequency-dependent transformer model

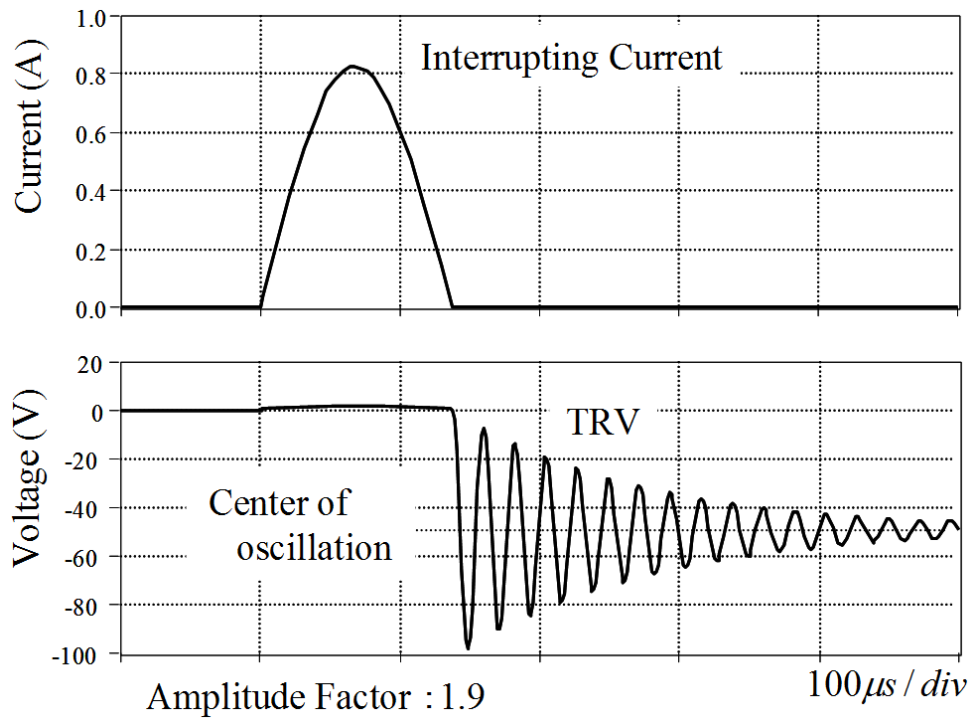
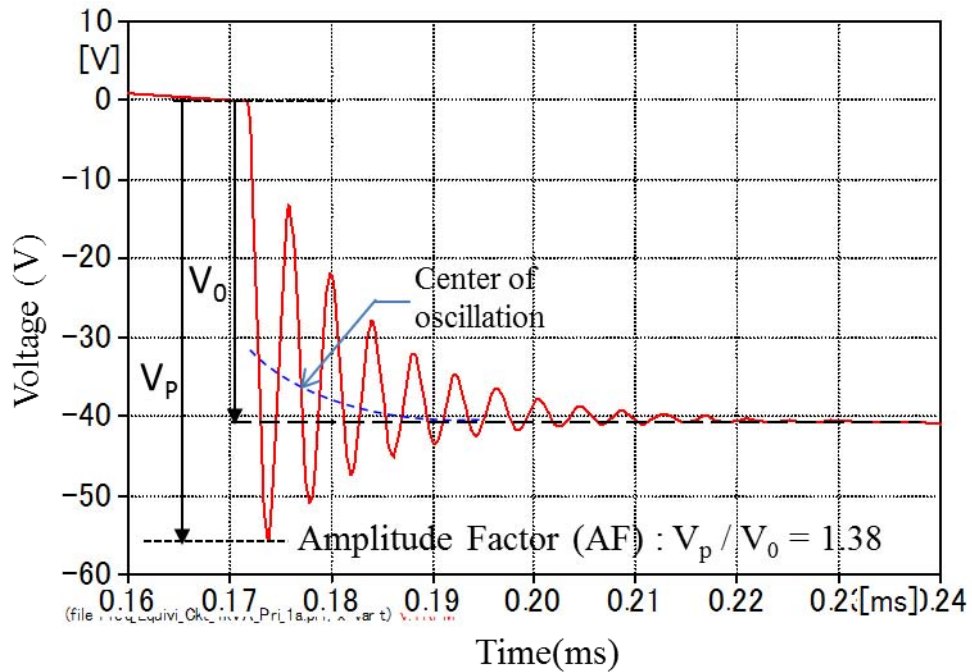
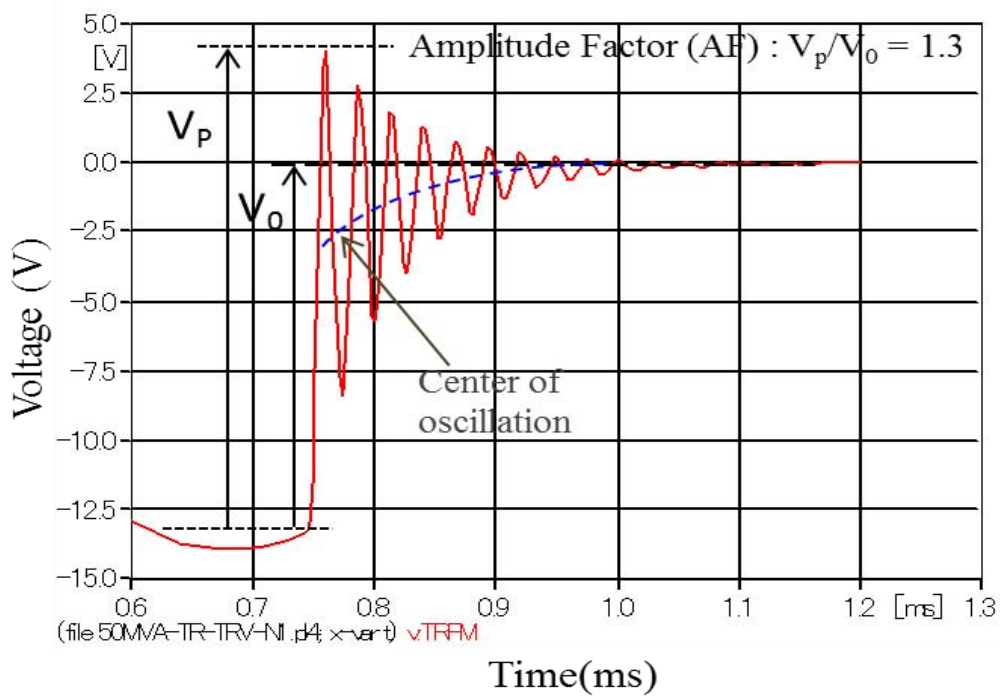


Fig. 4.18 TRV calculated result for 300 kVA transformer by using frequency-independent transformer model



(a) TRV calculated result and amplitude factor for 4 kVA transformer



(b) TRV calculated result and amplitude factor for 50 MVA transformer

Fig. 4.19 TRV calculated results and amplitude factors by using frequency-dependent equivalent circuit

Figures 4.19(a) and (b) shows the TRV waveforms resulting from the TRV calculation for 4 kVA transformer and 50 MVA transformer. The simulation results using the frequency-dependent equivalent circuit show amplitude factor of 4 kVA transformer is 1.38 and 50 MVA transformer is 1.3. The constructed EMTP model gives good agreement results with the measurement results. Table 4.4 is the TRV amplitude factors summarize for experiment and simulation results for three tested transformers.

Table 4.4. Summarize of amplitude factor

	Transformer Capacity	Amplitude Factor (AF)	
		Experiment	Simulation
1	4 kVA	1.4	1.38
2	300 kVA	1.4	1.5
3	50 MVA	1.3	1.3

4.6.1 Discussion

Frequency-dependent equivalent circuit for TRV at TLF condition can be constructed. By using this model simulation were done and the calculated TRV results show good agreement with the experiment results for all tested transformers up to 50 MVA capacity level. The circuit elements for constructed frequency-dependent equivalent circuit were calculated from the short-circuit impedance measurement graphs which were measured by FRA device. So the merit of the constructed model is that, if the short-circuit impedance measurement graphs could be provided the TRV at TLF condition can be calculated.

4.7 Study of TRV Characteristics with Extra Capacitance

Values at TLF Condition

To study TRV characteristics at TLF condition, diode interruption experiment have been performed. In TLF condition, frequency and attenuation of oscillation are mostly influenced by the leakage inductance and stray capacitance of transformer. Base on the previous study results, it was tried to measure the TRV amplitude factor (AF) characteristics, depending on the TRV frequency by connecting the extra capacitance. The results showed AF is related with the TRV frequency. These will be reported in this section.

4.7.1 Experiment Setup

The transformer impedance is the main influence factor on TRV of TLF condition. However, in the actual electric system there has some connecting equipment between transformer and interrupting device such as bus bar or cable and these include some capacitance. This study examines the inherent TRV and amplitude factor due to the influence of extra capacitance. To study this, current injection (CIJ) experiment with a diode as an interrupting switch was performed.

Figure 4.20 is the schematic diagram of experiment. The test transformer is 4kVA two windings low voltage one. The CIJ test circuit was connected at the secondary side of the transformer. Diode was connected at the primary side. Firstly the capacitor C was charged by SW1. After that capacitor injection was done by SW2 (Mercury Switch). The voltage (V_p) and current were measured across the diode. In order to reduce the TRV frequency, the extra capacitors were connected in parallel to the primary side. The connected values were 5000 pF (C_1) for the second measurement, 2 x 5000 pF (C_1+C_2) for the third measurement and 3 x 5000 pF ($C_1+C_2+C_3$) for the fourth measurement respectively and the results were measured.

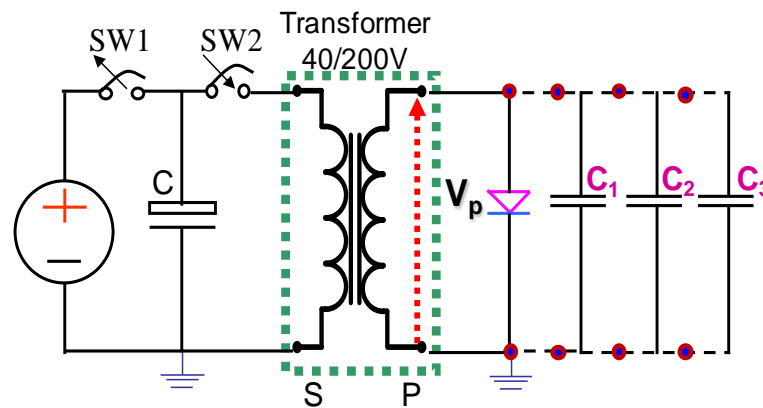
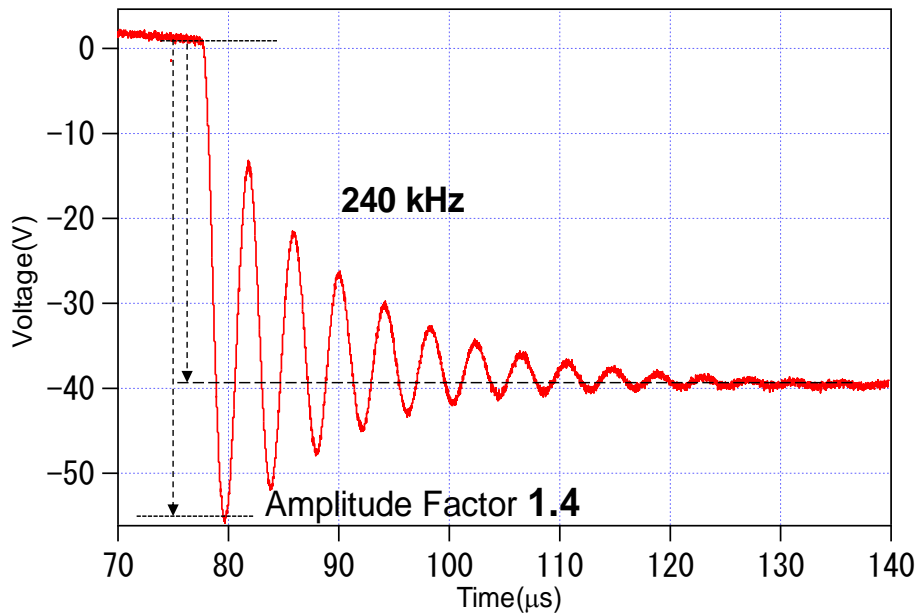


Fig. 4.20 Schematic diagram of experiment circuit

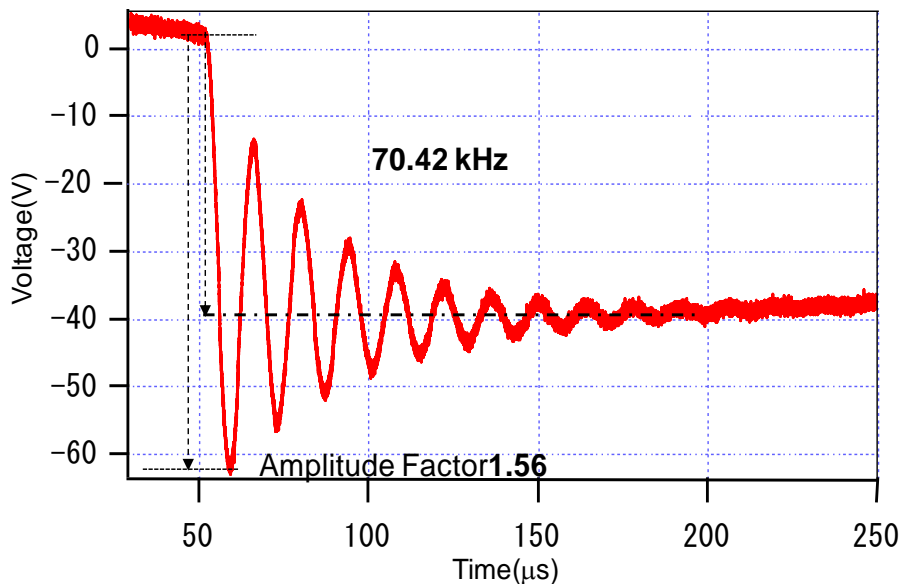
4.7.2 Experiment Results

Figure 4.21(a) is the voltage oscillation of transformer only, which is TRV and it is relevant to the tested transformer impedance. The frequency oscillation is 240 kHz and amplitude factor is 1.4 for this condition. Figure 4.21(b) is the TRV measurement result of 4 kVA transformer while three capacitors ($C_1+C_2+C_3$) were parallel connected condition. The frequency oscillation is 70.42 kHz and amplitude factor is 1.56 for this condition.

The four different experiment conditions and their correspond results: amplitude factor and frequency are summarized in Table 4.5. The results show if the TRV frequency becomes higher, the amplitude factor becomes smaller.



(a) TRV measurement result of 4kVA transformer only



(b) TRV measurement result of 4kVA transformer with three capacitors($C1+C2+C3$)

Fig. 4.21 TRV measurement results

4.7.3 EMTP Simulation Result

Frequency dependent transformer equivalent circuit for TRV of TLF investigation has been introduced and the results for 4 kVA, 300 kVA and 50 MVA transformers were reported in the above sessions. The transformer impedances such as leakage inductance, stray capacitance and winding resistance are used in this special equivalent circuit. These values are evaluated from FRA measurement graph. Figure 4.22 is the schematic diagram of EMTP simulation circuit.

By using this equivalent circuit, simulation was done. Figure 4.23(a) is the simulation result of TRV waveform while tested 4 kVA transformer impedance only is used in the equivalent circuit. The amplitude factor is 1.38 and TRV oscillation is 239 kHz for this condition. Figure 4.23(b) is the simulation result of TRV waveform while tested 4 kVA transformer impedance and additional capacitance $3 \times 5000 \text{ pF}$ (15 nF) are used in the equivalent circuit. This capacitance values were added at the equivalent circuit to get the same situation with the experiment that is three 5000 pF extra capacitors are parallels connected to the transformer. The amplitude factor is 1.51 and TRV oscillation is 80 kHz for this condition. The simulation results show agree well with the experiment results. The four different simulation conditions and their correspond results: amplitude factor (AF) and frequency are summarized in Table 4.5.

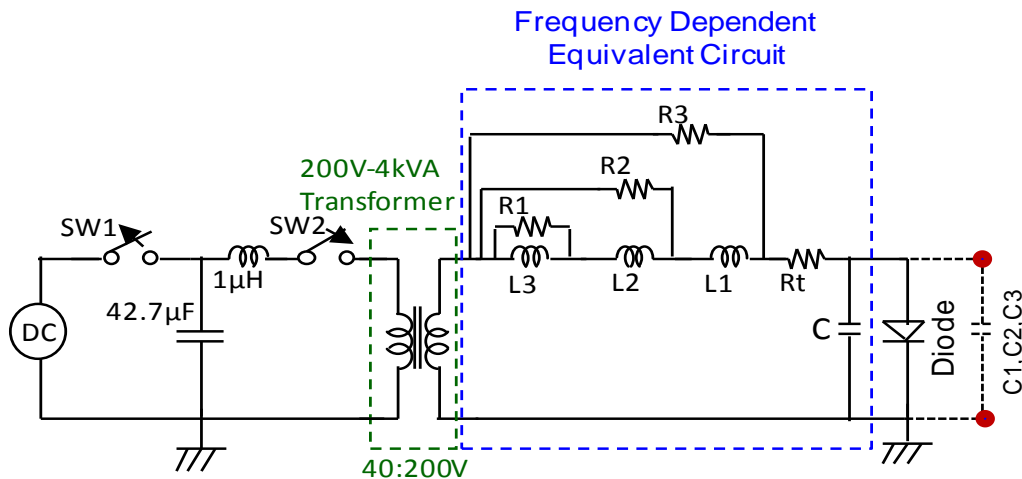
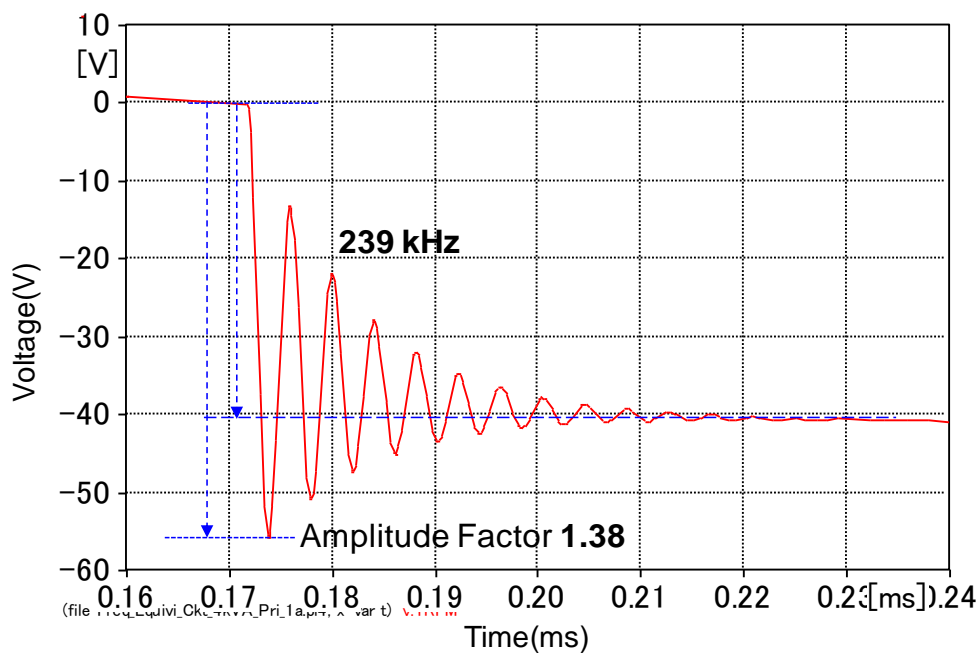
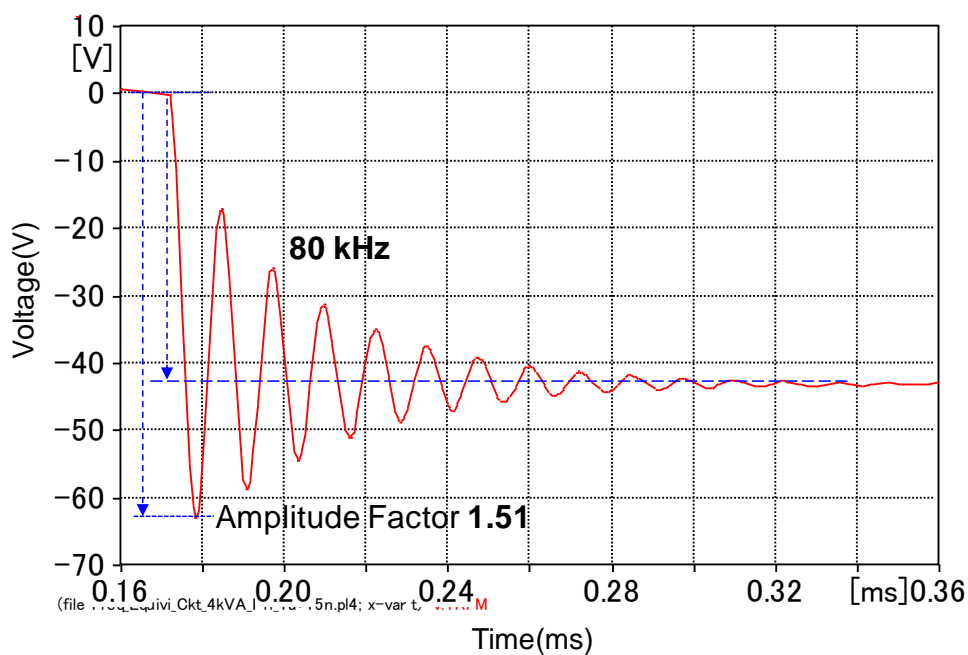


Fig. 4.22 EMTP simulation circuit



(a) EMTP simulation result of 4kVA transformer only



(b) EMTP simulation result of 4kVA transformer with three capacitors($C1+C2+C3$)

Fig. 4.23 EMTP simulation results

Table 4.5 TRV results of Experiment and EMTP Simulation with different conditions

No.	Condition	Amplitude Factor		Frequency	
		Experiment	EMTP	Experiment	EMTP
1.	Transformer only	1.4	1.38	240 kHz	239 kHz
2.	Transformer + (C1)	1.5	1.46	115 kHz	125 kHz
3.	Transformer + (C1+C2)	1.54	1.49	84.75 kHz	93 kHz
4.	Transformer + (C1+C2+C3)	1.56	1.51	70.42 kHz	80 kHz

4.7.4 Discussion

To understand the inherent TRV and influence of additional capacitance on TRV at TLF interrupting condition, experiment and simulation were done. From this study the following conclusions can be summarized.

(1). For the CIJ experiment with diode interruption:-

The measured results show the relation between the TRV waveform and the TRV amplitude factor. If more extra capacitance value is added to the transformer impedance, TRV waveform amplitude factor is increased meanwhile the waveform frequency is decreased.

(2). For the EMTP simulation:-

The simulation results using constructed frequency dependent transformer equivalent circuit gave well agreement with the experiment. Moreover the accuracy of this circuit for TRV study could be checked.

4.8 Conclusion

This chapter presents the study of TRV at TLF condition using capacitor injection with a diode interruption circuit. Frequency-dependent equivalent circuit can be constructed by EMTP. Transformer constants for simulation models are calculated from short-circuit impedance graphs measured with FRA device.

Experiment and simulation results give good agreement. From these results it was found that center of TRV oscillation was shifted, that might give an effect on the TRV amplitude. As expressed in Table 4.4, TRV amplitude factor is lower than the standard value of 1.7 which is defined in IEC and JEC.

Moreover, the effect of extra capacitance on TRV waves are also studied. The study results show if more extra capacitance value is added to the transformer impedance, TRV waveform amplitude factor is increased meanwhile the waveform frequency is decreased.

References

1. T. Koshizuka, T. Nakamoto, E. Haginomori, M. Thein, H. Toda, M. Hikita and H. Ikeda, "TRV under Transformer Limited Fault Condition and Frequency-Dependent Transformer Model," 2011 IEEE PES General Meeting, Detroit, Michigan, USA, 2011GM0415, July 26-29, 2011.
2. A.Sabot " Transient Recovery Voltage behind Transformer: Calculation and Measurement" IEEE Trans. Power Apparatus and Systems, Vol. PAS-104, No.7, 1985.
3. M. Thein, H. Toda, M. Hikita, H. Ikeda, E.Haginomori and T. Koshiduka, "Study of TRV Characteristics with Extra Capacitance Values at TLF Condition", the Annual Conference of Power & Energy Society, IEE of Japan, paper 33-288, pp.3-4, Fukui University, Japan , August 30 - September 1, 2011.

Chapter 5

Study of Transformer Iron Core Characteristics at a High Frequency

5.1 Introduction

Frequency dependent transformer equivalent circuit for transient recovery voltage (TRV) under transformer limited fault (TLF) condition was investigated by using small capacity transformers (4 kVA, 300 kVA and 50 MVA). The study was performed with experiment and simulation methods. The capacitor current injection method was used to obtain the experimental TRV waveforms. The measured TRV results show that the center of TRV oscillation is shifted. The TRV first peaks are low just after the current interruption and gradually increase thereafter. It is considered that short-circuit inductance of transformers is frequency dependent and inductance is apparently low just after the current interruption, but gradually increases thereafter. To analyze the TRV with simulation model, the frequency dependent equivalent circuit was constructed with electromagnetic transients program (EMTP). This circuit is constructed by short-circuit inductance, resistance and stray capacitance which are calculated from frequency response analysis (FRA) measurement graph. The simulation model was constructed by using these elements which feature the frequency dependency. The simulation results show the TRV wave shape is shifted to the center and good agreement with the measured ones [1-4].

The FRA measurement gives the frequency response of the transformer impedance. The measured FRA results show that the short-circuit inductance of all tested transformer is frequency dependence; that is, short-circuit inductance decreases along with the frequency. The phenomenon is known that magnetic flux cannot penetrate an iron core in the high frequency region. To study the frequency dependency of transformer impedance, the study of current ratio measurement that is secondary side current to primary side current (I_s/I_p) of transformer in the high frequency region up to

several tens kHz and magnetic flux versus current (ϕ - I) measurement at the high frequency region are done.

The experiment results of the current ratio study show that the current ratio of the tested transformers decreases along with the frequency. The experiment results of the magnetic flux versus current show that (ϕ - I) values decrease along with the frequency. These results are presented in the following section.

5.2 Current Ratio Measurement Experiment

Current ratio measurement is done to study current value at the secondary side which relative on the primary side along with the frequency increasing. In this study, two low voltage transformers with 4 kVA, 200/40V and 1 kVA, 100/100V were used. Figures 5.1 are photographs of 4 kVA transformer. Figures 5.2 are photographs of 1 kVA transformer. Specifications of transformers are expressed in Tables 5.1 and 5.2, respectively.

5.2.1 Experiment Setup

Figure 5.3 is the experiment setup. Capacitor C is charged by DC supply by SW1. The transformer is energized by the charged capacitor by SW2. Voltage V_p and current I_p at primary side and secondary current I_s were measured. There are nine different capacitors are used to obtain different frequencies of voltage and current waveforms.



(Front view)



(Side view)

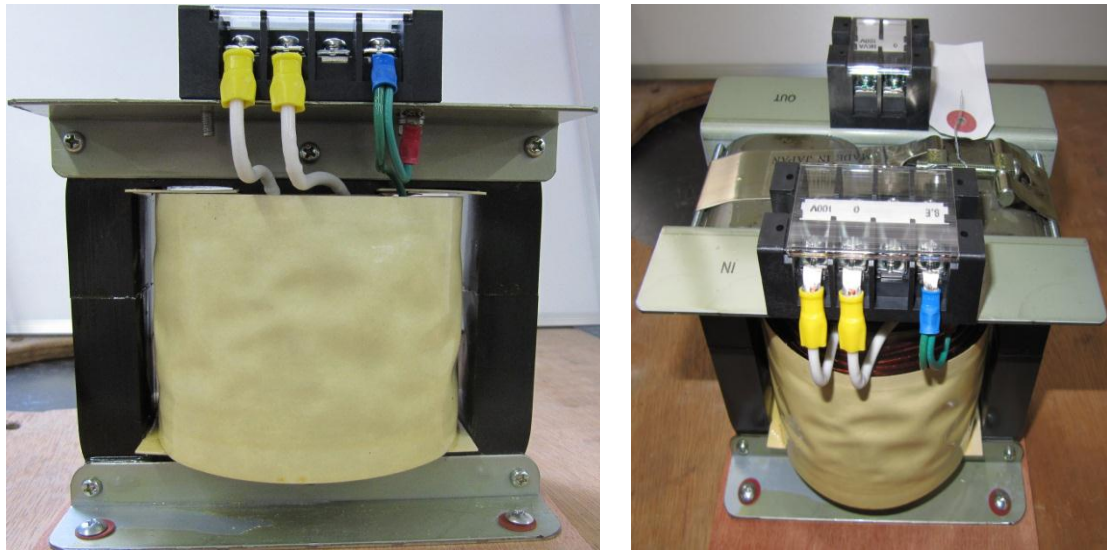


(Top view)

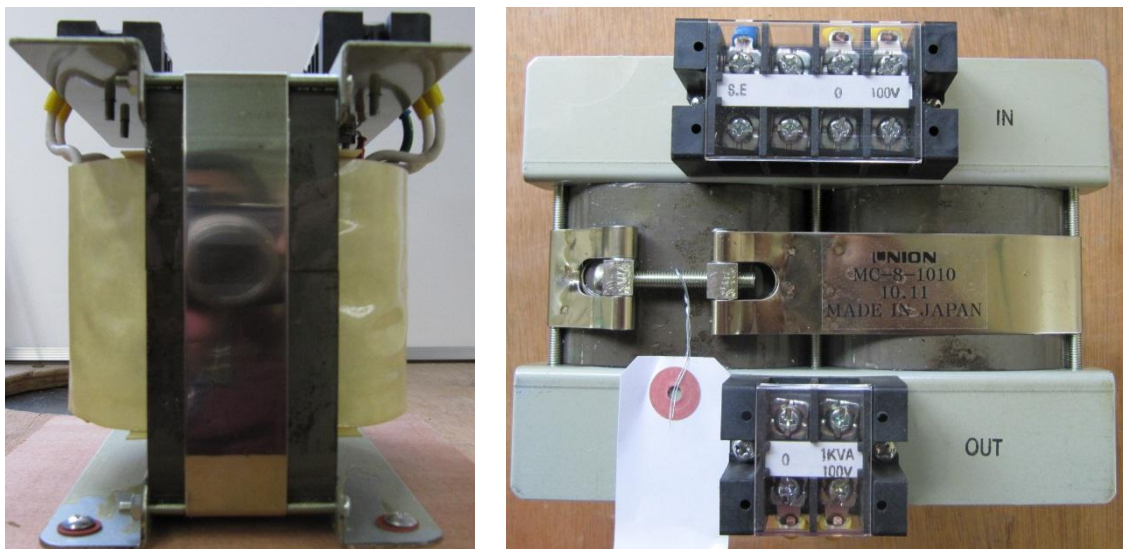
Fig. 5.1 The photograph of 4 kVA two windings transformer

Table 5.1. Specification of 4 kVA two windings transformer

	Primary	Secondary
Rated Voltage	200 V	40 V
Rated Current	20 A	100 A
Rated Capacity	4 kVA	
Frequency	50/60 Hz	
Type	Single phase Two windings	
% Impedance	2.4 % At 75°C	



(Front view)



(Side view)

(Top view)

Fig. 5.2 The photograph of 1 kVA two windings transformer

Table 5.2. Specification of 1 kVA two windings transformer

	Primary	Secondary
Rated Voltage	100 V	100 V
Rated Current	10 A	10 A
Rated Capacity	1 kVA	
Type	Single phase Two windings	
Frequency	50/60 Hz	
Type of Iron Core	Silicon steel	

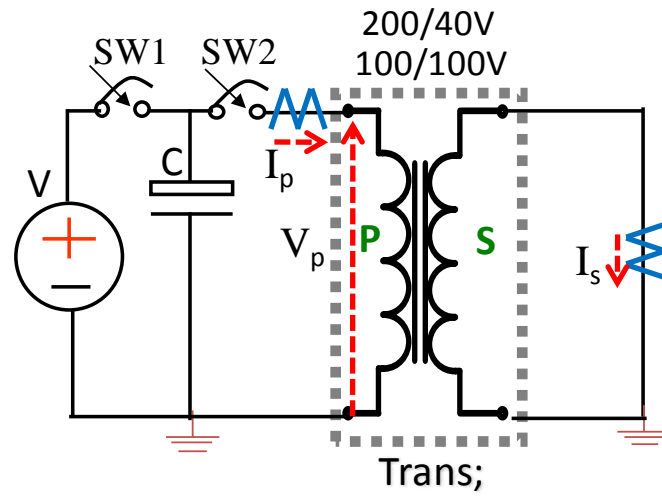


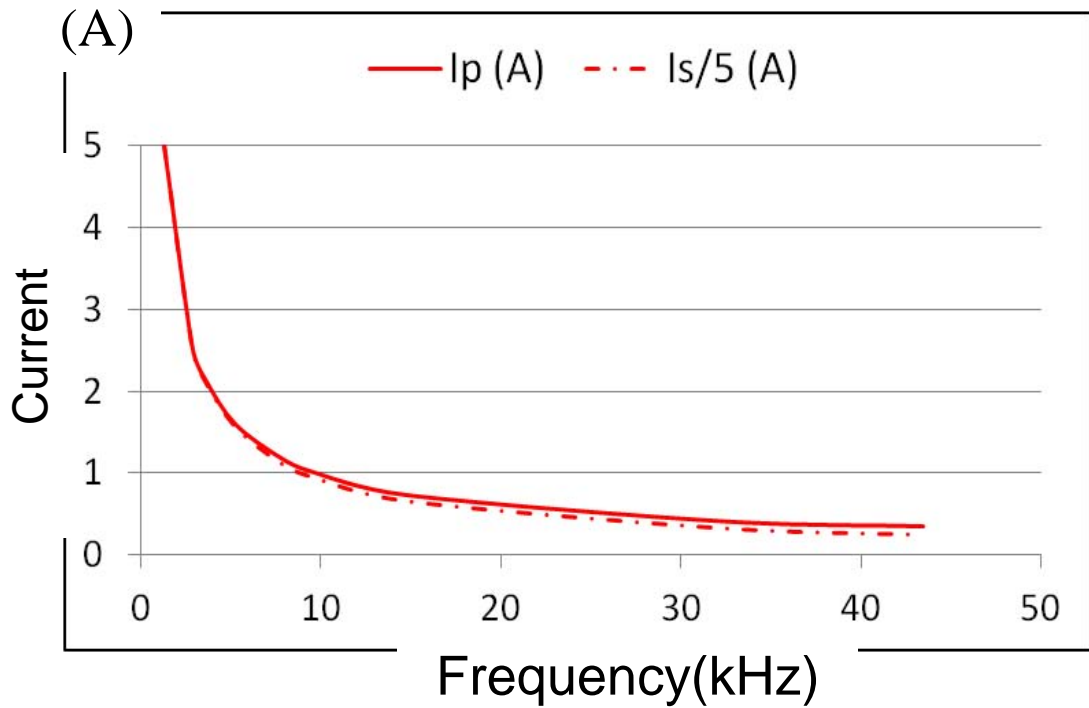
Fig. 5.3 The experiment circuit for current ratio measurement

Table 5.3. Current Ratio Results of 4 kVA Transformer with Nine Different Capacitors

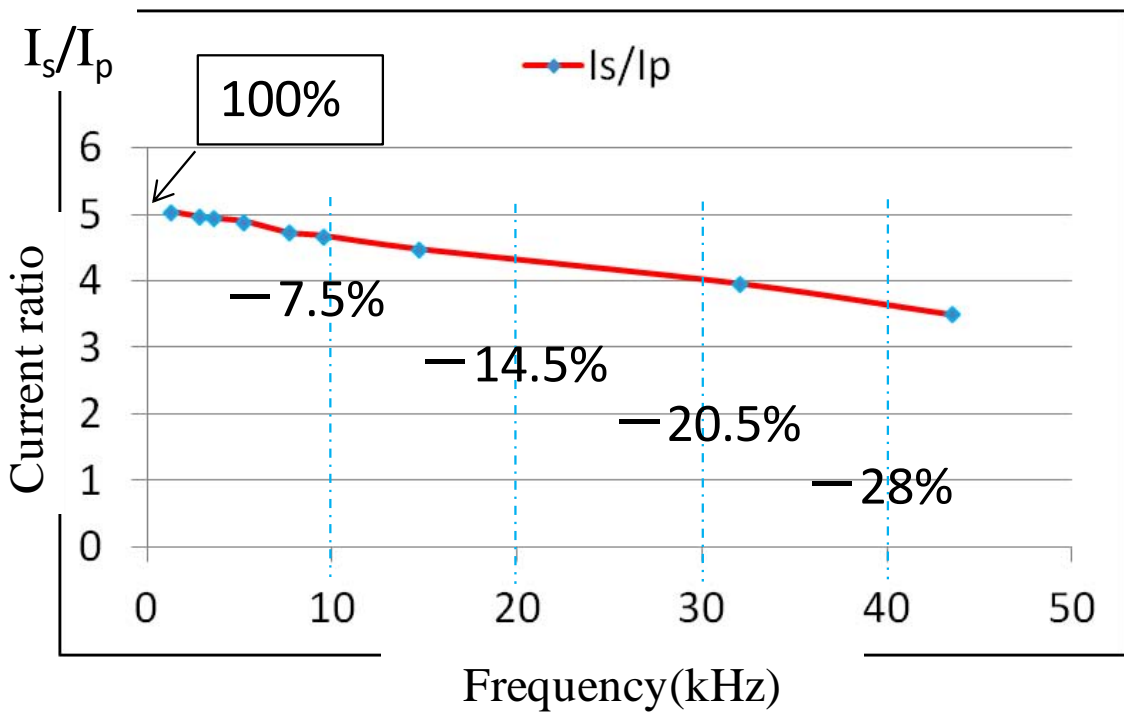
No.	Capacitor (μF)	Frequency (kHz)	I_p (A)	I_s (A)	I_s/I_p
1	42.7	1.26	5.000	25.006	5.000
2	9	2.83	2.537	12.588	4.961
3	6	3.57	2.138	10.554	4.936
4	3	5.21	1.602	7.834	4.890
5	1.5	7.69	1.197	5.650	4.721
6	1	9.52	1.018	4.757	4.675
7	0.47	14.7	0.737	3.302	4.477
8	0.1	32.05	0.419	1.661	3.959
9	0.056	43.48	0.354	1.235	3.494

Table 5.4. Current Ratio Results of 1 kVA Transformer with Nine Different Capacitors

No.	Capacitor (μF)	Frequency (kHz)	I_p (A)	I_s (A)	I_s/I_p
1	42.7	0.886	2.075	2.025	0.976
2	9	1.9	0.973	0.921	0.947
3	6	2.3	0.803	0.752	0.936
4	3	3.4	0.586	0.536	0.915
5	1.5	5	0.425	0.375	0.883
6	1	6.5	0.358	0.308	0.859
7	0.47	10.33	0.253	0.204	0.808
8	0.1	25.77	0.127	0.075	0.592
9	0.056	35.71	0.090	0.040	0.449

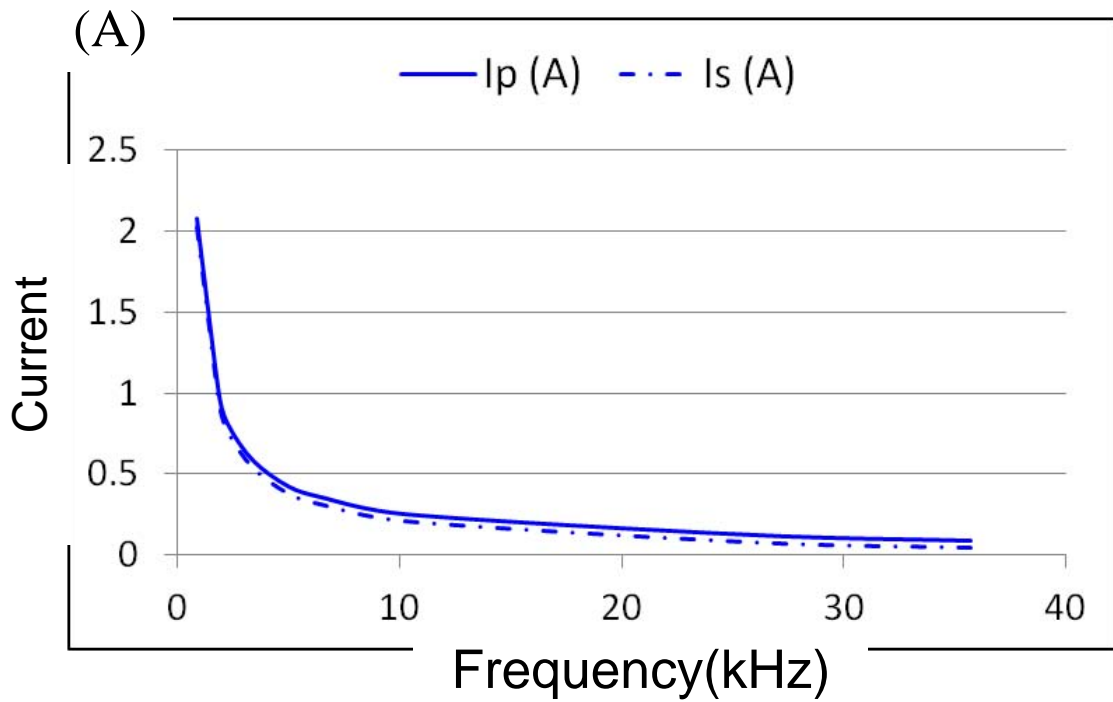


(a) Current values of 4 kVA transformer

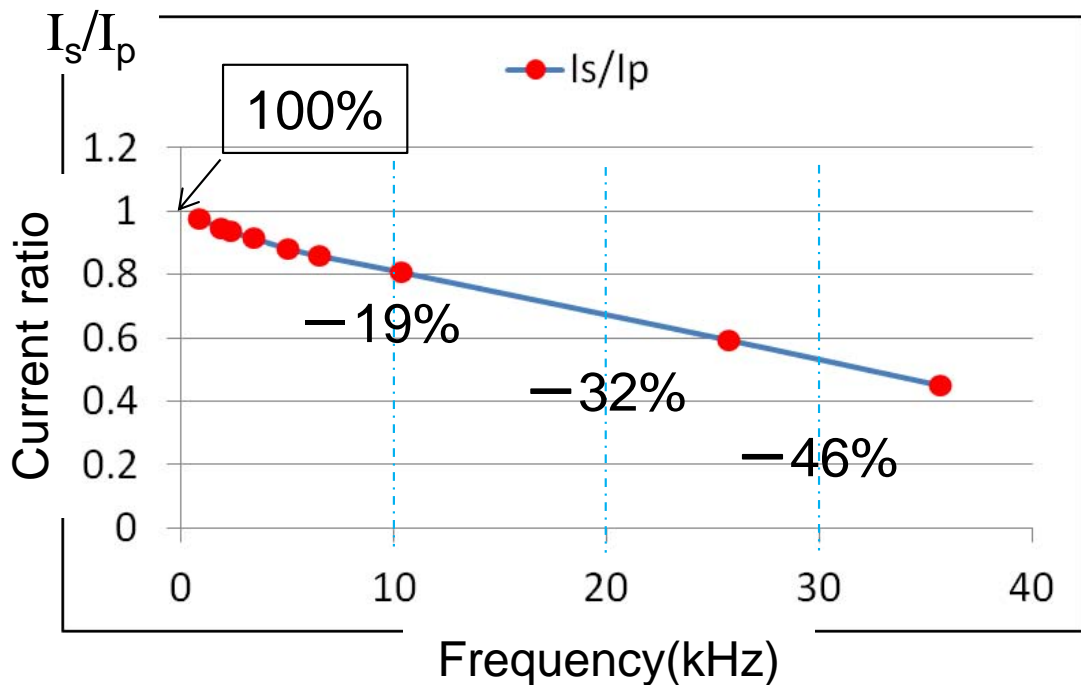


(b) Current ratio of 4 kVA transformer

Fig. 5.4 Measurement results of 4 kVA transformer



(a) Current values of 1 kVA transformer



(b) Current ratio of 1 kVA transformer

Fig. 5.5 Measurement results of 1 kVA transformer

5.2.2 Experiment Results

Measured current values I_p and I_s of 4 kVA transformer are showed in figure 5.4(a). Figure 5.4(b) is current ratios (I_s/I_p) of 4 kVA. It is evident that the current ratio decreases along with the frequency. Measured result of 1 kVA transformer shows same character with the 4 kVA transformer [5]. Figures 5.5(a) and (b) are the measurement results of 1 kVA transformer. Measurement data of two transformers are expressed in Tables 5.3 and 5.4. Current ratio decreasing percent of the two transformers in high frequency region are listed in Table 5.5. Figure 5.6 is the current ratio decreasing percent of two tested transformers.

Table 5.5. Current ratio decreasing % of two transformers

kHz	Is/Ip Decreasing %	
	4kVA	1kVA
10	7.5	19
20	14.5	32
30	20.5	46
40	28	-

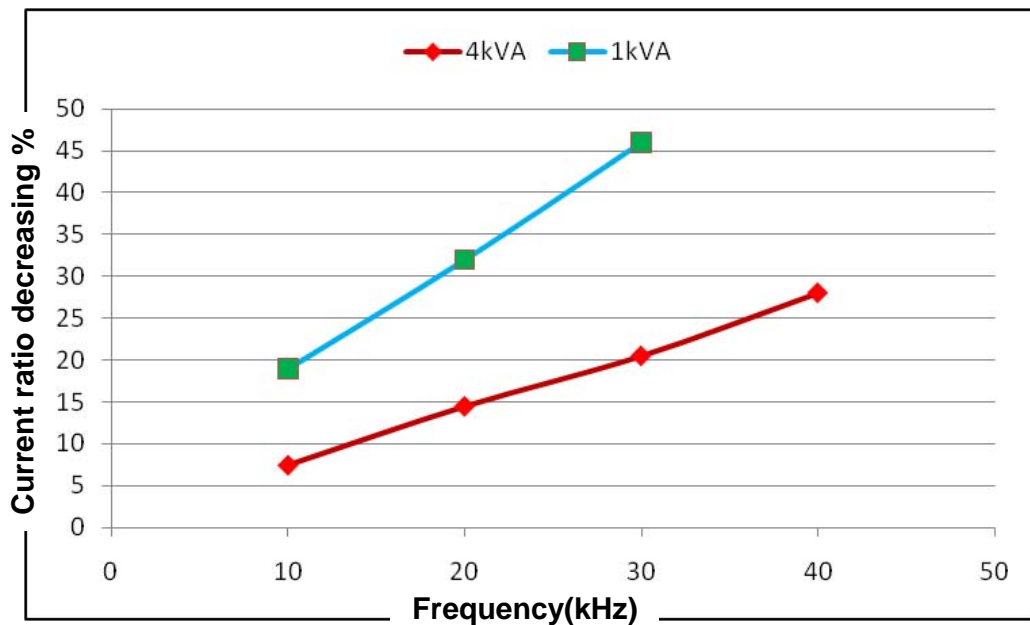
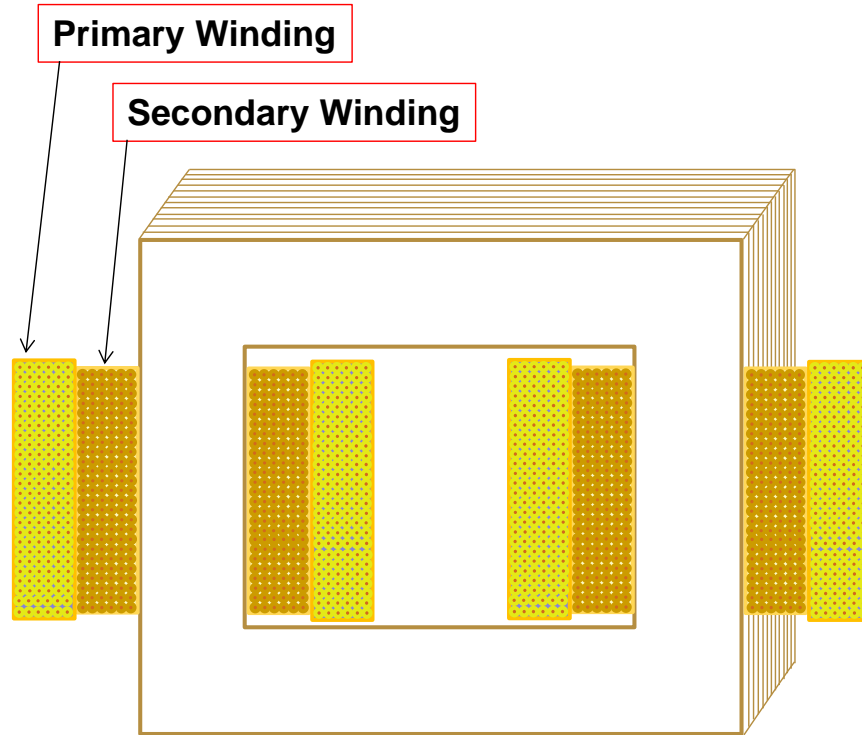


Fig. 5.6 Current ratio decreasing percent of two tested transformers

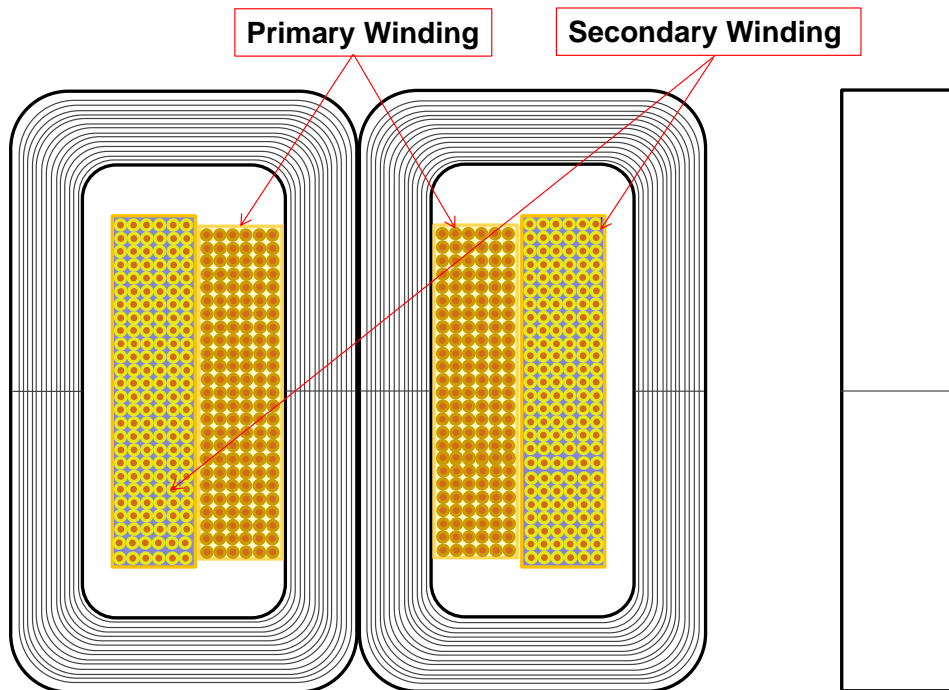
5.2.3 Consideration

Figures 5.4(a) and 5.5(a) show decreasing of current at secondary side is slightly larger than primary side. It is considered that if the magnetic flux within the iron core changed, an eddy current is generated within the iron core, in such a manner that it counters the effect of the magnetic flux change. When frequency increases, this phenomenon becomes evidenced and eddy current loss occurred. It results in the secondary side current more decrease than primary side and I_s/I_p ratio decreases along with the frequency.

Current ratio decreasing percent of 1 kVA transformer is larger than 4 kVA transformer. It might be related with the iron core stacking pattern and iron core and windings configuration of two tested transformers. Further study is needed to clearly understand the frequency dependency of current ratio. Schematic diagram of iron core stacking patterns and winding arrangement are shown in figures 5.7 (a) and (b).



(a) Winding and iron core stacking pattern of 4 kVA transformer



(b) Winding and iron core stacking pattern of 1 kVA transformer

Fig. 5.7 Winding and iron core sketch diagrams for two tested transformer

5.3 Current Injection Experiment with Charging Capacitor

To understand the magnetic flux distribution of transformer in high frequency region and the frequency dependency of the relative permeability, magnetic flux and current measurement (ϕ - I) study is done.

5.3.1 Current Injection with Different Capacitors

Figure 5.8 is the experiment setup. Capacitor C is charged by DC supply by SW1. The transformer is energized by the charged capacitor by SW2. Voltage and current were measured at primary side while secondary side is opened condition. There are four different capacitors are used to obtain different frequencies of voltage and current waveforms. Magnetic flux is calculated from the measured voltage by using equation (5.1).

$$\phi = \int_0^{\tau} V dt \quad (5.1)$$

Calculated magnetic flux and measured current values are plotted in the same graph. To confirm the influence of applied voltage and injected current on the ϕ - I curves, two types of measurement were done that is (i) applied voltage is fixed condition, and (ii) injected current is fixed condition. In this study, two low voltage transformers with 1 kVA, 100/100V and 4 kVA, 200/40V were used. The experiment results are presented as follow.

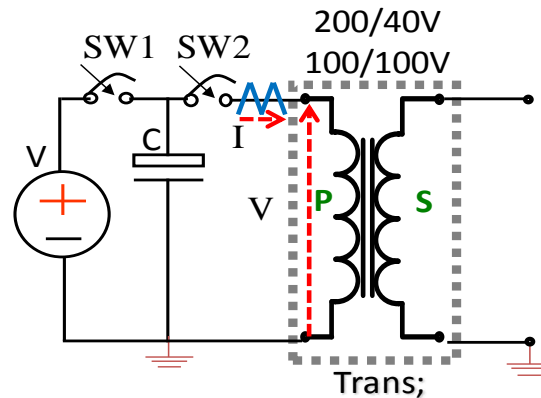
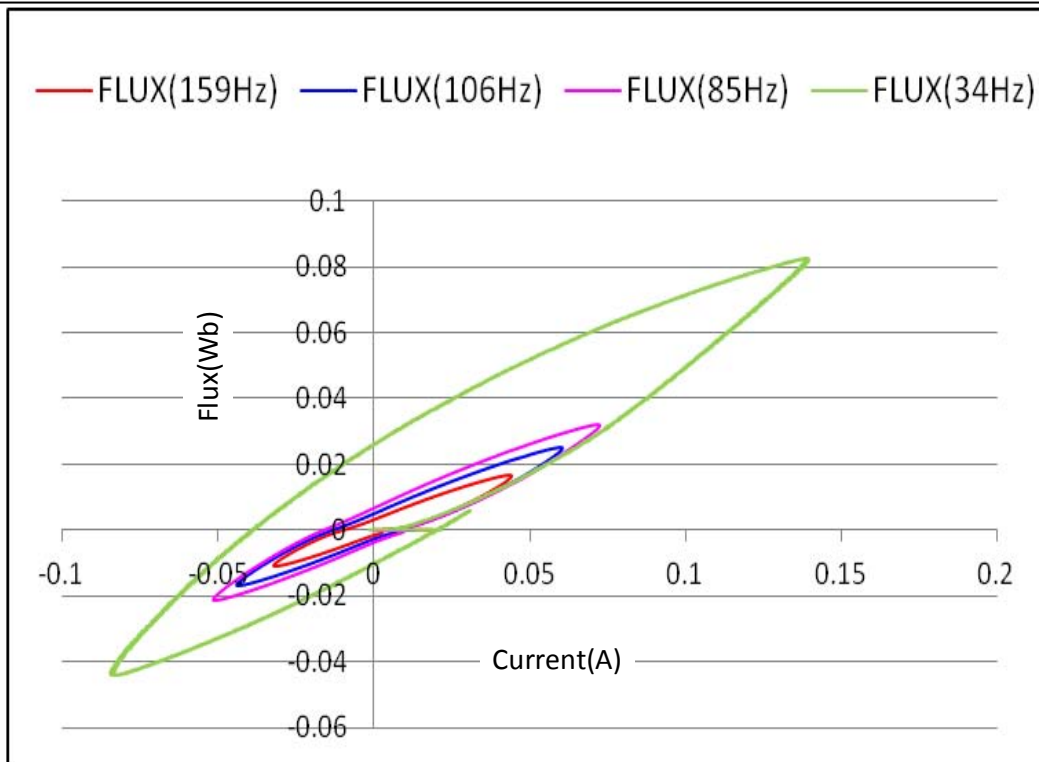
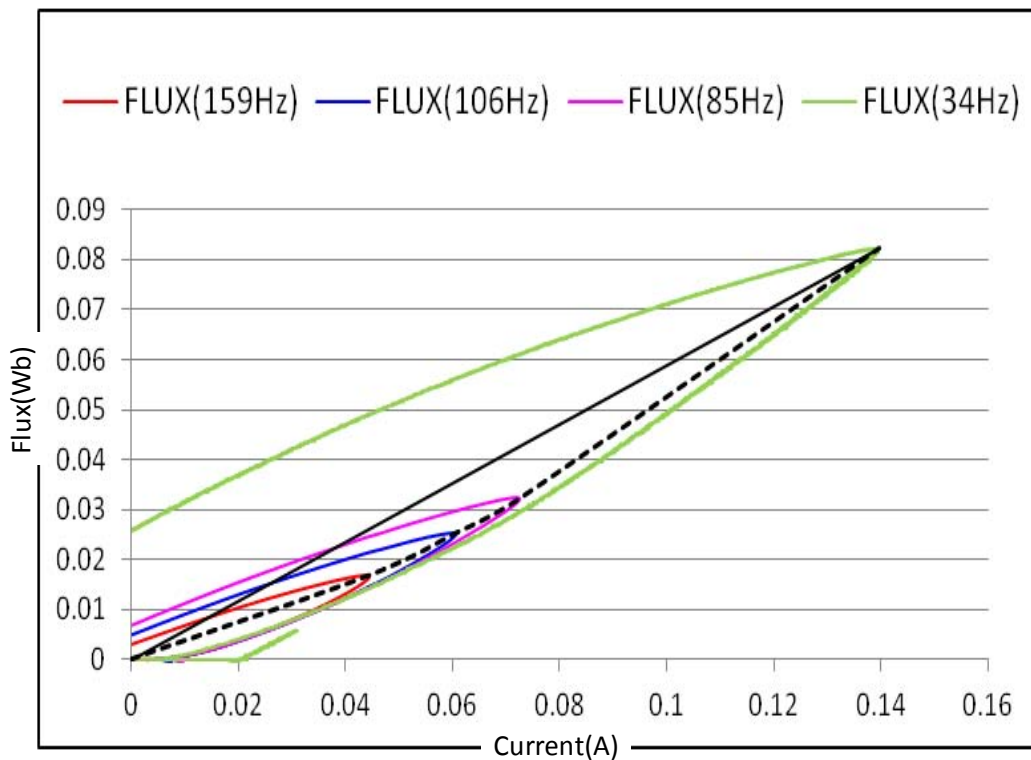


Fig. 5.8 The experiment circuit for ϕ - I study

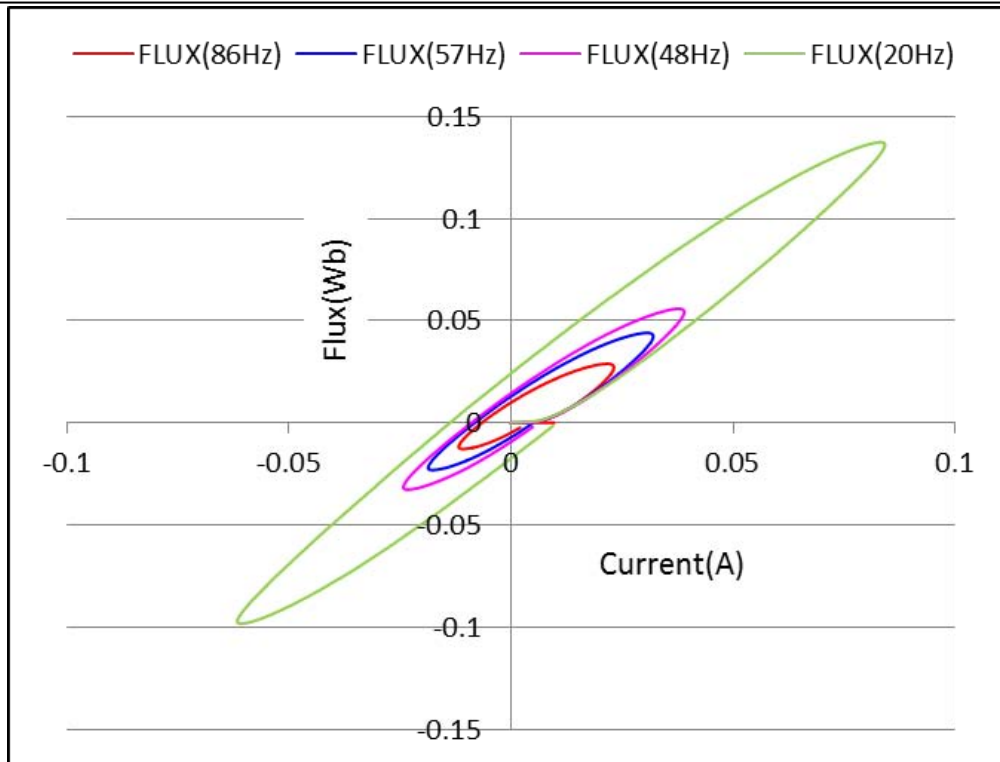


(a)

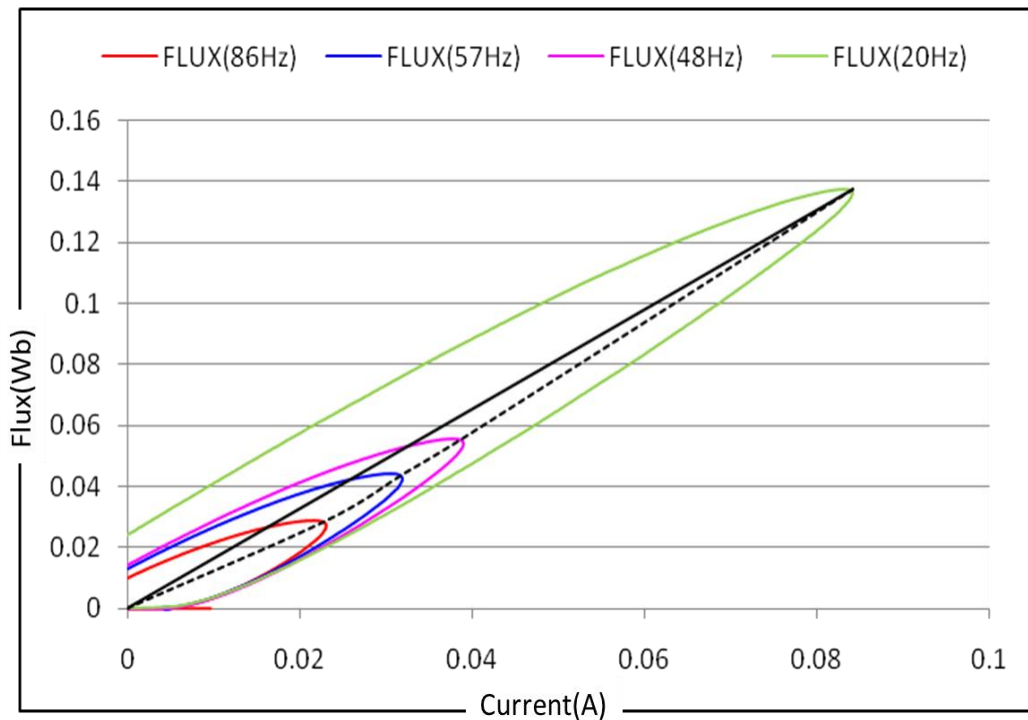


(b)

Fig. 5.9 The ϕ - I curves of 4 kVA transformer while applied voltage is fixed



(a)



(b)

Fig. 5.10 The ϕ - I curves of 1 kVA transformer while applied voltage is fixed

Table 5.6. The ϕ -I values of 4 kVA transformer (voltage is fixed)

No.	Capacitor (μF)	Frequency (Hz)	Applied Voltage (V)	Current (A)	Flux (Wb)	ϕ / I
1	42.7	34	18	0.1396	0.0823	0.5894
2	9	85	18	0.0726	0.0322	0.4440
3	6	106	18	0.0607	0.0253	0.4169
4	3	159	18	0.0444	0.0168	0.3782

Table 5.7. The ϕ -I values of 1 kVA transformer (voltage is fixed)

No.	Capacitor (μF)	Frequency (Hz)	Applied Voltage (V)	Current (A)	Flux (Wb)	ϕ / I
1	42.7	20	18	0.0842	0.137	1.631
2	9	48	18	0.039	0.0558	1.432
3	6	57	18	0.032	0.044	1.375
4	3	86	18	0.0232	0.0289	1.245

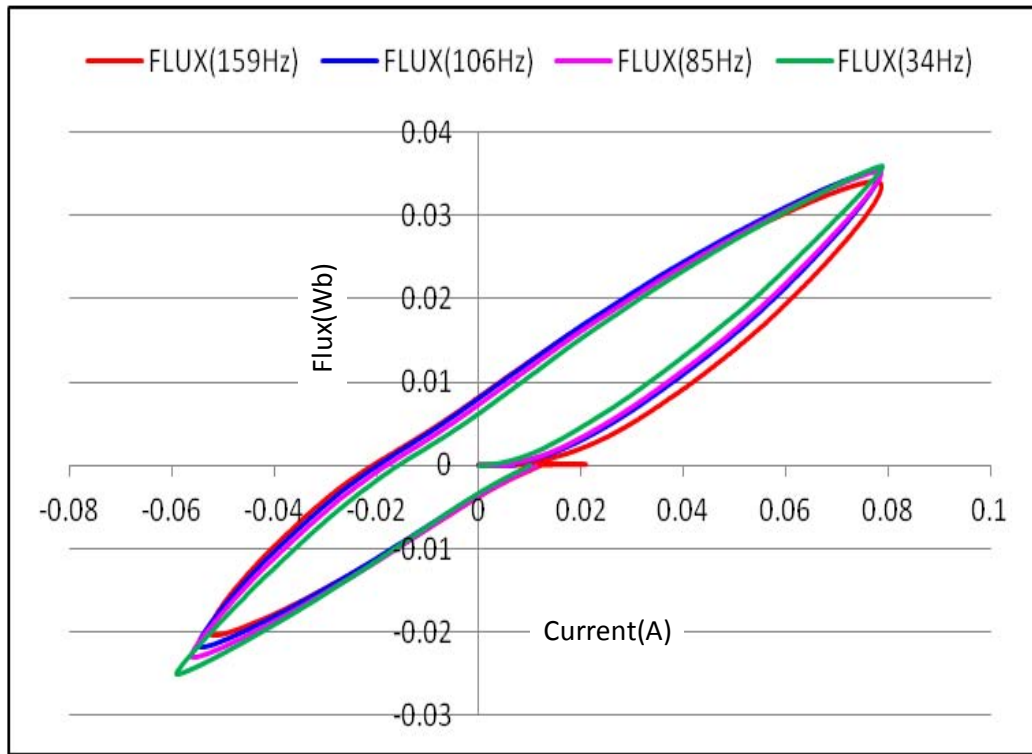
5.3.2 Experiment Results

The ϕ -I curves of 4 kVA transformer in different frequencies while the applied voltage is fixed condition are showed in figures 5.9 (a) and (b). Measured values are summarized in Table 5.6.

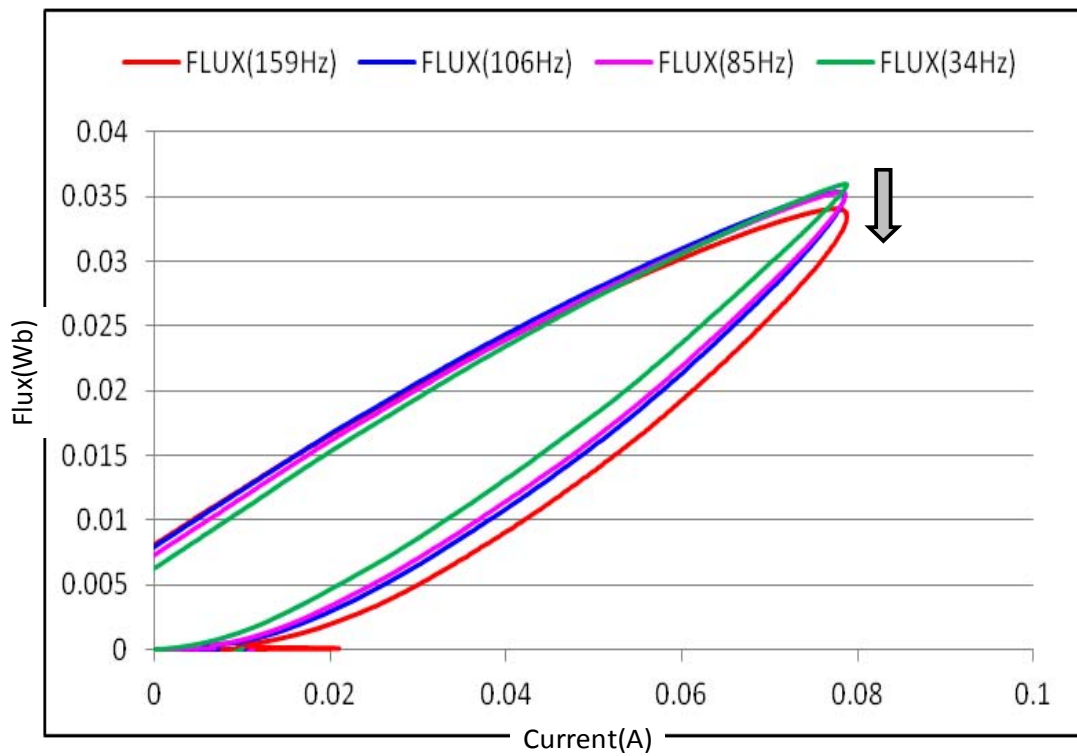
The ϕ -I curves of 1 kVA transformer in different frequencies while the applied voltage is fixed condition are showed in figures 5.10 (a) and (b). Measured values are summarized in Table 5.7. Experiment results of both transformers show ϕ/I ratio decreases when frequency is increased.

The ϕ -I curves of 4 kVA transformer in different frequencies while the injected current is fixed condition are showed in figures 5.11 (a) and (b). Measured values are summarized in Table 5.8.

The ϕ -I curves of 1 kVA transformer in different frequencies while the injected current is fixed condition are showed in figures 5.12 (a) and (b). Measured values are summarized in Table 5.9. Experiment results of both transformers show ϕ/I ratio decreases when frequency is increased.

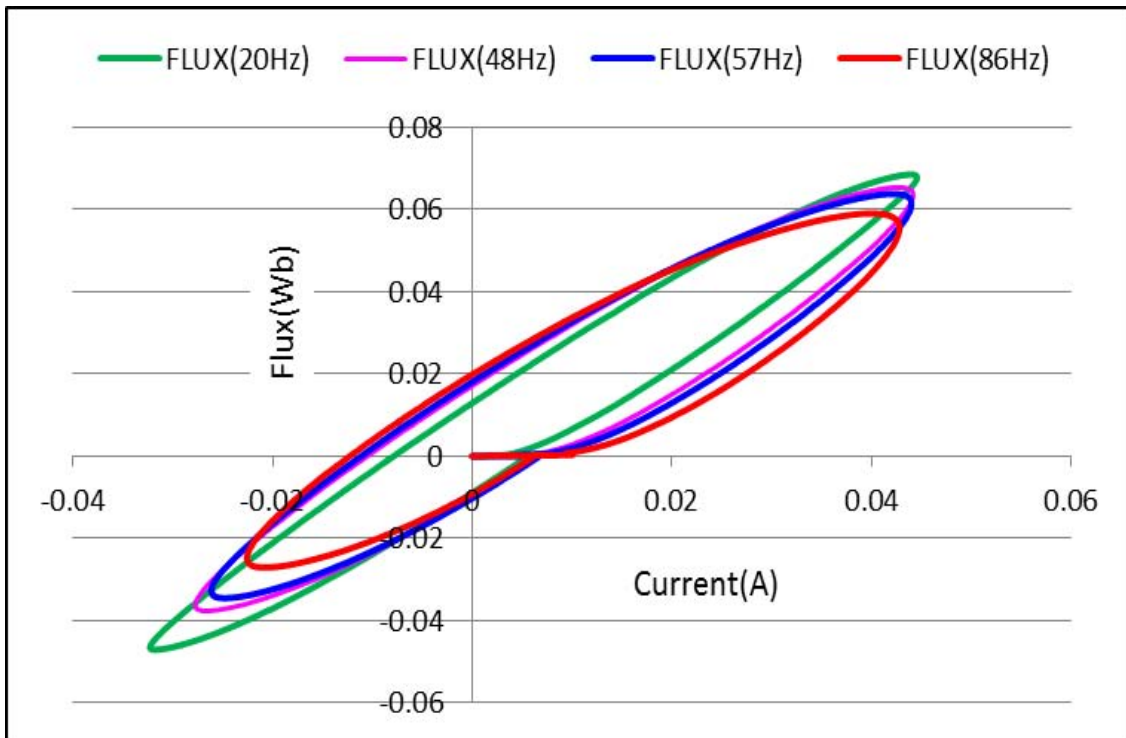


(a)

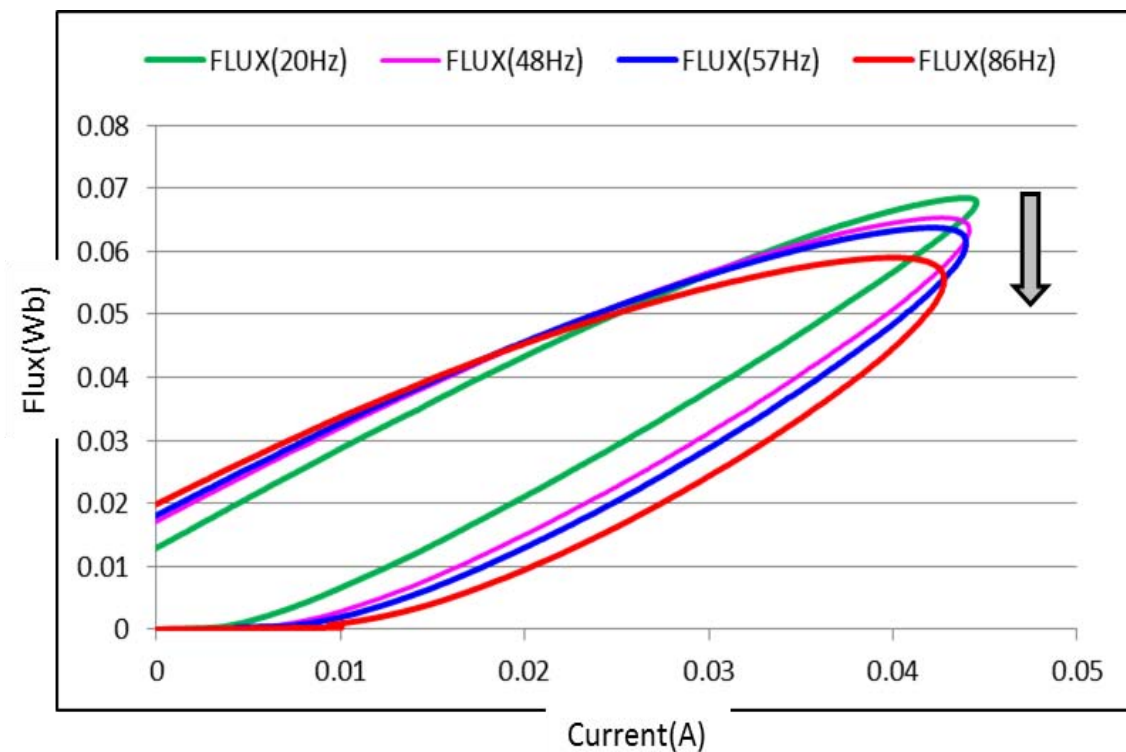


(b)

Fig. 5.11 The ϕ - I curves of 4 kVA transformer while injected current is fixed



(a)



(b)

Fig. 5.12 The ϕ - I curves of 1 kVA transformer while injected current is fixed

Table 5.8. The ϕ - I values of 4 kVA transformer (current is fixed)

No.	Capacitor (μ F)	Frequency (Hz)	Applied Voltage (V)	Current (mA)	Flux (Wb)	ϕ / I
1	42.7	34	9	78.86	0.0360	0.456
2	9	85	20.4	78.64	0.0354	0.45
3	6	106	25.2	78.52	0.0353	0.45
4	3	159	35.8	78.78	0.0341	0.433

Table 5.9. The ϕ - I values of 1 kVA transformer (current is fixed)

No.	Capacitor (μ F)	Frequency (Hz)	Applied Voltage (V)	Current(peak) (mA)	Flux(peak) (Wb)	ϕ / I
1	42.7	20	9.4	40.49	0.06848	1.6913
2	9	48	21.3	40.5	0.06535	1.6136
3	6	57	26.2	40.66	0.06377	1.5685
4	3	86	36.1	40.64	0.05903	1.4524

5.4 Current Injection Experiment with Power Amplifier

5.4.1 Experiment Setup

Current injection using a power amplifier is done to obtain the voltage and current in kHz order waveforms for ϕ - I study. Figure 5.13 is the experiment setup. First, signal voltage from function generator (FG-300) is applied to power amplifier. This signal is amplified up to require frequency by using amplifier (NF-4502) and it is injected to the secondary side of test transformer. The oscilloscope (OSC1) is used to check the signal voltage and the output of amplifier. Voltage and current were measured at secondary side while primary side is opened condition by using OSC2. Frequencies of 1 kHz, 2 kHz, 5 kHz, 7 kHz, 10 kHz, and 15 kHz waveforms are measured. In this study, 4 kVA, 200/40V low voltage transformers is used. Figures 5.14 are the photographs of experiment equipment.

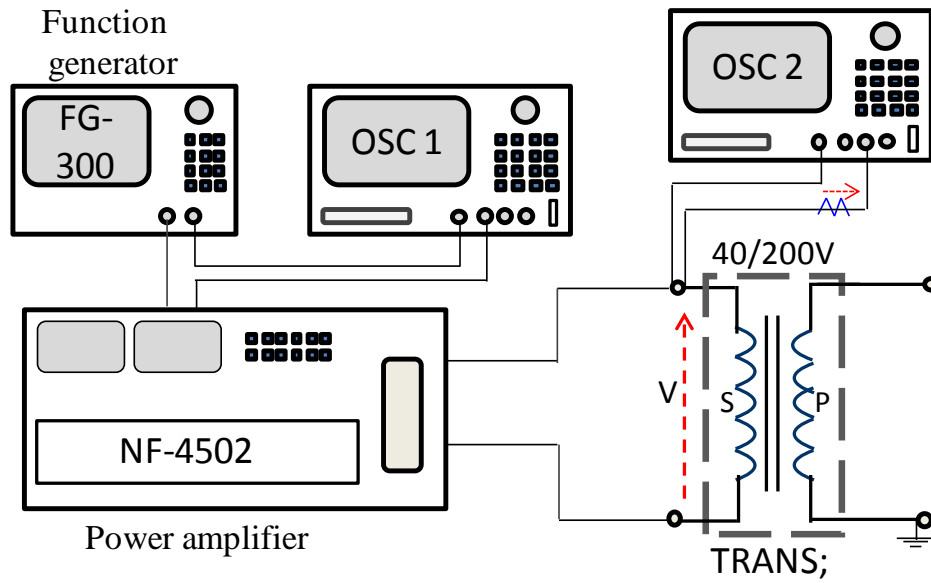


Fig. 5.13 Experiment setup of current injection with power amplifier



(a) Function generator(FG-300)



(b) Oscilloscope(TDS-3034)



(c) Oscilloscope(DPO-4054)



(d) Power amplifier (NF-4502)

Fig. 5.14 Photographs of experiment equipment

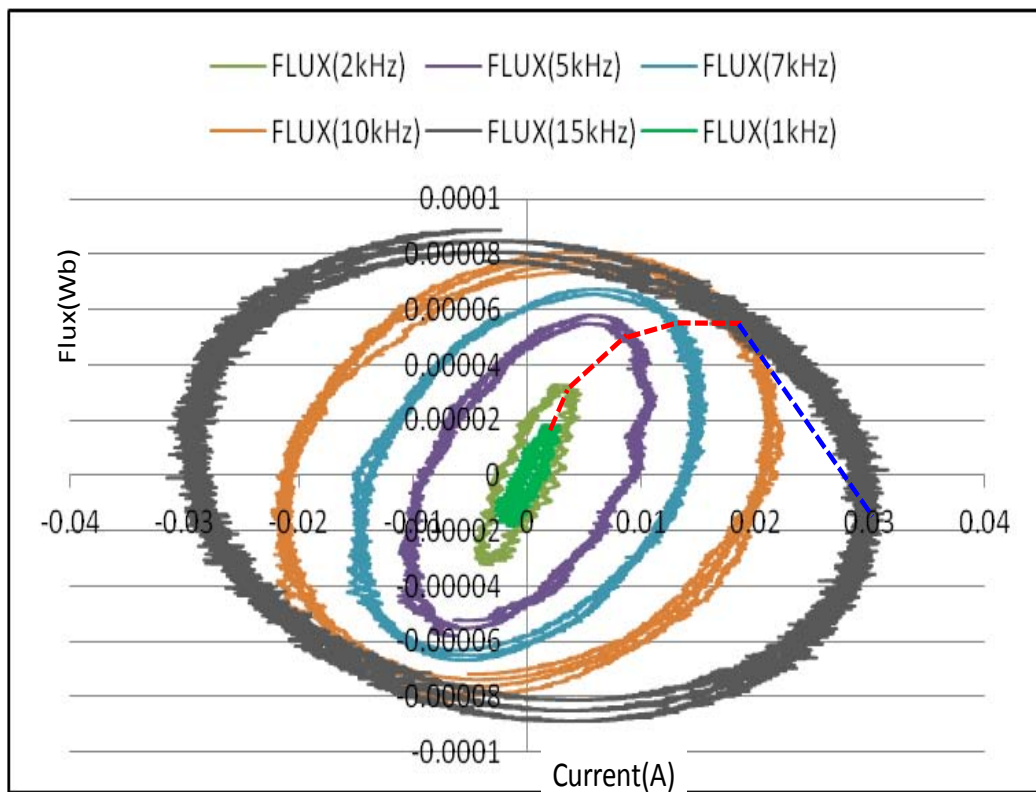


Fig. 5.15 The ϕ - I curves of 4 kVA transformer in different frequencies

Table 5.10. The $\phi - I$ comparison of 4 kVA Transformer in different frequencies

No.	Frequency (kHz)	Current (mA)	Flux (mWb)	ϕ / I
1	1	2.2	18.5	8.409
2	2	4	27.5	6.875
3	5	11	59	5.364
4	7	15	68.5	4.567
5	10	21.5	80	3.721
6	15	30.5	81	2.656

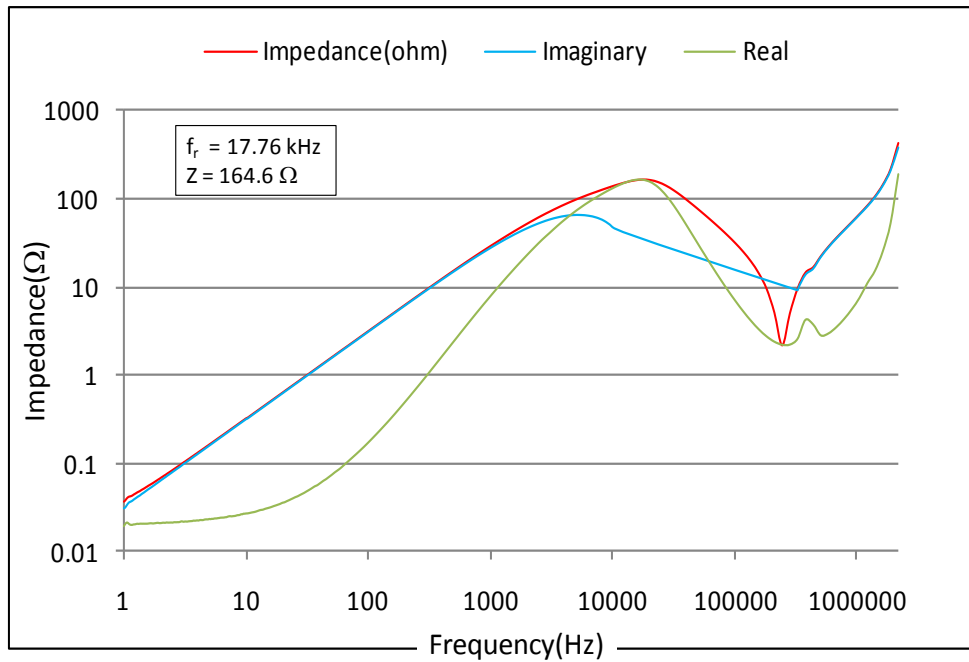


Fig. 5.16 Frequency response of 4 kVA transformer at secondary side while primary side is opened condition

5.4.2 Experiment Results

The $\phi - I$ curves of 4 kVA transformer in kHz order frequency is plotted in figure 5.15. The measured values and $\phi - I$ ratio is summarized in Table 5.10. The experiment result shows $\phi - I$ ratio decreases along with the frequency. The slope of ϕ / I decreases when frequency is increased. The slope of ϕ / I curve becomes negative near the resonance frequency. Figure 5.16 is the self-impedance of tested 4 kVA transformer which is measured by frequency response analyzer (FRA). The resonance frequency is 17.76 kHz. It can be considered that when capacitance effect occurs, the magnetic flux distribution becomes difficult. The experiment results show, $\phi - I$ curve areas become large when frequency is increased. It is considered that hysteresis loss is dependent on frequency.

5.5 Discussion

The experiment results of current ratio measurement and ϕ - I study are presented in above sections 5.2, 5.3 and 5.4. In general iron core loss consists of two parts:-

- (i) Hysteresis loss in low frequency region, and
- (ii) Eddy-current and other frequency dependent losses in high frequency region

Figure 5.17 shows an example of the flux density distribution inside silicon steel, which is used as a material for the cores of transformers, calculated while frequency is changed [4 and 6]. The thickness of the steel plate is 1 mm and the center is set to 0 in the graph. The relative permeability was constant at 7000 and the flux density distribution on the surface of the steel is set to 1. The graph reveals that the flux reaches the center of the steel plate at 50Hz when a certain magnetic field is provided on the surface. It is also found that the flux penetrates the steel plate with difficulty as frequency increases, and the flux only reaches the steel surface at 50 kHz.

Figure 5.18 shows the calculated frequency response of the relative permeability presented in complex notation [4, 7 and 8]. The thickness of the steel plate is set to 0.5mm. In the commercial frequency domain, the real part of the relative permeability is constant and the magnitude of the real part is dominant in comparison with the imaginary part. This means that the flux density keeps pace with the magnetic field and changes as the magnetic field changes. The imaginary part gradually increases along with the frequency rise and the real part and the imaginary part agree at and above a certain frequency level. This means that the change of flux density is delayed compared to the change of magnetic field. In figure 5.18, the relative permeability diminishes linearly at frequencies of more than several hundred Hz. For example, at the frequency of 1MHz, the complex relative permeability becomes approximately one hundredth (1/100) that of the commercial frequency. It is, therefore, found that the relative permeability of the iron core is frequency dependent.

Based on the conducted experiments and example calculation results it is considered that frequency dependency of transformer impedance is concerning with the following factors:-

- (a) Increase of eddy current inside the iron core, (b) reduction of flux inside the core due to the skin effect, and (c) frequency dependency of relative permeability.

However, influence of each factor and effective particular frequency region is necessary to understand clearly. Further study is needed.

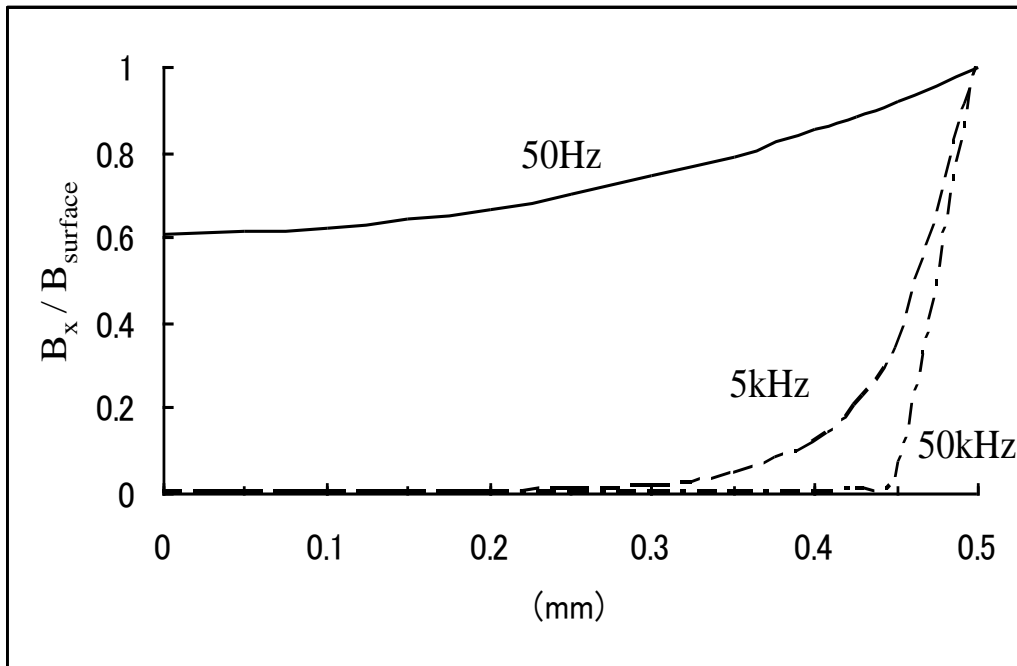


Fig. 5.17. Example of flux density distribution in iron core

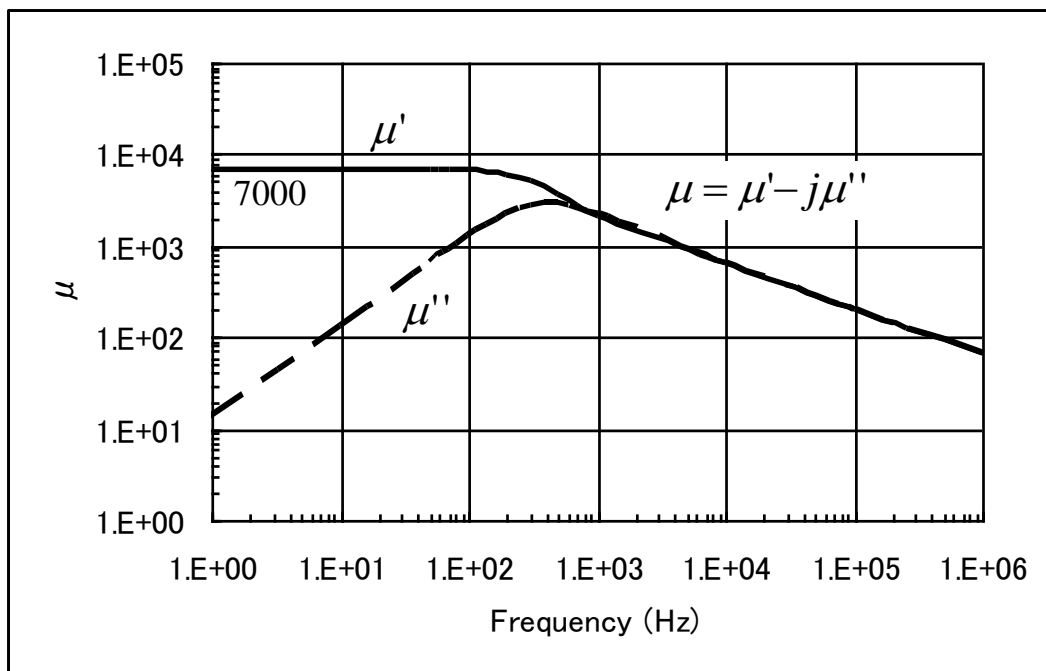


Fig. 5.18. Frequency response of complex permeability

5.6 Conclusion

From this study it is concluded:-

(1) Current ratio measurement was done to understand the relation between primary and secondary current of transformer depending on the frequency. Two transformers, 1 kVA and 4 kVA are used. The results showed secondary current decreasing is slightly larger than the primary current and current ratio (I_s/I_p) decreases along with the frequency. It is considered that eddy current loss occurs when frequency becomes high and effect on current ratio.

(2) The $\phi - I$ study results show, when frequency becomes high ϕ/I ratio decreases. It is confirmed ϕ/I ratio decreasing is do not depend on applied voltage and injected current.

References

1. M. Thein, H. Ikeda, K. Harada, S. Ohtsuka, M. Hikita, E. Haginomori and T. Koshizuka, "Investigation of Transformer Model for TRV Calculation by EMTP," IEEJ Transactions on Power and Energy, Vol.129, No.10, pp 1174-1180, Oct 2009.
2. M. Thein, H. Toda, M. Hikita, H. Ikeda, E. Haginomori and T. Koshizuka, "Frequency Dependent Transformer Model for TRV Calculation at the Transformer Limited Fault Condition by EMTP," The Seventh International Workshop on High Voltage Engineering 2010 (IWHV 2010), Kitakyushu, Kitakyushu International Conference Center, Kitakyushu, Japan, ED-10-75, SP-10-42, HV-10-37, pp 77-81, November 12-13, 2010.
3. M. Thein, H. Toda, M. Hikita, H. Ikeda, E. Haginomori and T. Koshizuka, "Investigation of Transformer Model for TRV Calculation by using Frequency Dependent Inductance Model," Journal of international Council on Electrical Engineering, Vol.1, No.2, pp 188-193, April 2011.
4. T. Koshizuka, T. Nakamoto, E. Haginomori, M. Thein, H. Toda, M. Hikita and H. Ikeda, "TRV under Transformer Limited Fault Condition and Frequency-Dependent Transformer Model," 2011 IEEE PES General Meeting, Detroit, Michigan, USA, 2011GM0415, July 26-29, 2011.
5. M. Thein, H. Toda, M. Hikita, H. Ikeda, E. Haginomori, T. Koshizuka, "Transformer Current Ratio Measurement at a High Frequency Region," The 2012 annual meeting of institute of electrical engineering of Japan, Hiroshima Institute of Technology, Japan, vol.5, paper5 -134, p.205, March 21-23, 2012.
6. Markus Zahn, "Electromagnetic Field Theory : a problem solving approach," John Wiley & Sons 1979.
7. J.Gyselinck, P.Dular, "A Time-Domain Homogenization Technique for Laminated Iron Cores in 3-D Finite-Element Models," IEEE Trans. Magnetics, Vol.40, No.2 2004.
8. N.Abeywickrama, Y.V.Serdyuk, A. M. Gubanski, "High- Frequency Modeling of Power Transformers for Use in Frequency Response Analysis (FRA)," IEEE Trans. Power Delivery, Vol.23, No.4, 2008.

Chapter 6

Conclusion

The transformer model for transient recovery voltage (TRV) at the transformer limited fault (TLF) current interruption condition was investigated. In the investigation processes current injection (CIJ) measurement method and capacitor current injection with a diode as an interruption device were used to measure the inherent TRV waveforms. There are many kinds of transformers were used which have difference capacities and different insulation medium. The experiment results show the amplitude factors (AF) of TLF-TRV are 1.4 for 4 kVA and 300 kVA transformers, 1.3 for 50 MVA transformer. It is smaller than international electrotechnical commission (IEC) standard. The current IEC standard of TLF-TRV is 1.7. Moreover, measured TRV waveforms show the center of TRV oscillation is shifted.

To simulate the TLF-TRV condition electromagnetic transient program (EMTP) is used. Transformer impedance is measured by frequency response analyzer (FRA). Transformer constants for EMTP simulation such as leakage inductance, stray capacitance and resistance are calculated from FRA impedance graph. The calculation method of transformer constants for TRV study from FRA impedance measurement could be determined in this study.

Short-circuit inductance which is calculated from FRA measurement graph shows frequency dependent and to study that frequency dependent equivalent circuit is constructed by EMTP. Frequency responses are simulated by constructed frequency dependent equivalent circuit. This results show good agreement with the measured FRA frequency response in terms of frequency response, frequency at the resonance point and impedance at the resonance point.

By using the constructed frequency dependent equivalent circuit, TLF-TRV model was constructed and simulations were done. The simulated TRV waveforms show good agreement with the measured TRV results. The simulated results show the amplitude factors (AF) of TLF-TRV are 1.38 for 4 kVA transformer, 1.5 for 300 kVA transformer and 1.3 for 50 MVA transformer. The simulated TRV waveforms also show

the center of TRV oscillation is shifted. This is because the short-circuit inductance of the transformers is frequency dependent and the inductance is apparently low just after the current interruption but gradually increases thereafter. This could be confirmed by using the frequency independent equivalent circuit and simulation result shows amplitude factor becomes higher and the center of TRV oscillation is constant.

From this study it can be concluded that:-

- (1) The inherent TRV at TLF condition could be obtained by using CIJ measurement and capacitor current injection with a diode as an interruption device.
- (2) Frequency dependent equivalent circuit for TLF-TRV study could be constructed.
- (3) The values of equivalent circuit element such as winding resistance, leakage inductance and stray capacitance could be determined from FRA measurement.
- (4) The simulated results of frequency response and TRV waveform agreed well with the experiment. It shows that transformer impedance for TRV study is possible to calculate from FRA measurement.
- (5) The amplitude factor (AF) of TRV could be determined precisely up to 50MVA transformer.
- (6) The measured and simulated amplitude factors are smaller than the IEC standard.
- (7) The constructed model can represent the frequency dependent inductance characteristics and it is understood that the frequency dependent effect of inductance is influenced on the TRV at TLF condition.

To study the frequency dependency of transformer impedance, the study of current ratio measurement that is secondary side current to primary side current (I_s/I_p) of transformer in the high frequency region up to several tens kHz and magnetic flux versus current ($\phi-I$) measurement at the high frequency region are done.

The experiment results of the current ratio study show that the current ratio of the tested transformers decreases along with the frequency. The experiment results of the magnetic flux versus current show that ($\phi-I$) values decrease along with the frequency.

Based on the conducted study results it is considered that frequency dependency

of transformer impedance is concerning with the following factors:-

- (a) Increase of eddy current inside the iron core,
- (b) Reduction of flux inside the core due to the skin effect, and
- (c) Frequency dependency of relative permeability.

However, influence of each factor and effective particular frequency region is necessary to understand clearly. Further study is needed to understand the frequency dependent characters of transformer iron core.

Acknowledgement

First and foremost, the author would like to acknowledgement to his chief supervisor Dr. Masayuki Hikita, Professor of Kyushu Institute of Technology for his advice, encouragement and guidance during this research and in the completing of this dissertation.

The author would like to express his great appreciation and special thanks to research supervisors Dr. Hisatoshi Ikeda, Professor of the University of Tokyo, Dr. Eiichi Haginomori for their kindness advice, guidance, valuable discussion, great encouragement to this research work and helpful comments through this research work. The research cannot be carried out without strong support from them.

The author is greatly indebted to Dr. Hiroaki Toda, Toshiba Corporation for his encouragement, kindness advice and helpful comments through this research work.

The author would like to express his great pleasure and special thanks to Toshiba Corporation for contributing a collaboration research with Kyushu Institute of Technology by providing materials and experiment support. The author would like to give his great pleasure and great appreciation to Mr. Tadashi Koshizuka, the person in charge of Toshiba Corporation, for all of his valuable discussion, helpful comment and technical support to succeed this research.

The author would like to express his great thank to Dr. Shinji Ishibe, Professor of Kyushu Institute of Technology and Dr. Masahiro Kozako for their warmly advice and support.

The author would like to express his thank to Ministry of Education, Culture, Science and Technology of Japan (Monbukagakusho) for granting him a scholarship during his study in Japan.

I would like to express my sincere gratitude to Government of Myanmar and Ministry of Electric Power No.2 for providing a chance to study in Japan.

I owe what I have achieved to a great number of people, who teach me from the beginning (Ka gyee) and all of my life, I will not name individually.

The author is deeply grateful the staffs of Professor Hikita Laboratory for their warmly helps.

The author would like to express his great thank to the present and previous members of Professor Hikita Laboratory, for their helps, necessary support and friendship.

Last but not least, I would like to express my heartfelt thanks to my parents, my sisters for their unconditional love and confidence on me.

List of Publications

Journal

1. Investigation of Transformer Model for TRV Calculation by EMTP

IEEJ Transactions on Power and Energy, Vol.129, No.10, pp. 1174-1180, October 2009.

Authors : **M. Thein**, H. Ikeda, K. Harada, S. Ohtsuka, M. Hikita, E. Haginomori and T.Koshizuka

2. Investigation of EMTP Transformer Model for TRV Calculation after Fault Current Interrupting by Using FRA Measurement

Proceeding of the IEEE PES T&D, Paper No. 2010TD0424, pp. 1-6, New Orleans, USA, April 19-22, 2010.

Authors: **M. Thein**, H. Toda, K. Harada, M. Hikita, S. Ohtsuka, H. Ikeda, E. Haginomori and T.Koshizuka

3. Investigation of Transformer Model for TRV Calculation by using Frequency Dependent Inductance Model

Authors: **M. Thein**, H. Toda, M. Hikita, H. Ikeda, E. Haginomori and T.Koshizuka

Journal of International Council on Electrical Engineering, Vol.1, No.2, pp. 188-193, April 2011.

4. TRV under Transformer Limited Fault Condition and Frequency-Dependent Transformer Model

Authors: T. Koshizuka, T. Nakamoto, E. Haginomori, **M. Thein**, H. Toda, M. Hikita and H. Ikeda,

Proceeding of the IEEE PES General Meeting 2011, Paper No. 2011GM 0415, pp. 1-7,

Detroit, Michigan, USA, July 26-29, 2011.

International Proceedings

5. Investigation of Transformer Model for TRV Calculation after Fault Current Interrupting

Proceeding of the International Conference on Electrical Engineering 2008 (ICEE 2008), Panel discussion, Part 2, PN2-08, Okinawa Convention Center, Okinawa, Japan, July 6-10, 2008.

Authors: E. Haginomori, **M. Thein**, H. Ikeda, S. Ohtsuka, M. Hikita, and T.Koshizuka

6. Investigation of Transformer Model for TRV Calculation by EMTP

Proceeding of the Sixth International Workshop on High Voltage Engineering 2008 (IWHV 2008), ED-08-117, SP-08-32, HV-08-46, pp. 49-52, Doshisha University, Kyoto, Japan, October 24, 2008.

Authors: **M. Thein**, M. Hikita, S. Ohtsuka, H. Ikeda, K. Harada, E. Haginomori and T. Koshizuka

7. Transformer Model for TRV Calculation at the Transformer Limited Fault Condition by EMTP

Proceeding of the International Conference on Electrical Engineering 2009 (ICEE 2009), HF1-08, I9FP0196, Shenyang, China, July 6-9, 2009.

Authors: **M. Thein**, H. Ikeda, K. Harada, M. Hikita, S. Ohtsuka, E. Haginomori and T. Koshizuka

8. Investigation of Transformer Model for TRV Calculation by using Frequency Dependent Inductance Model

Proceeding of the International Conference on Electrical Engineering 2010 (ICEE 2010),

PSMSA-05, Busan, Korea, July 11-14, 2010.

Authors: **M. Thein**, H. Toda, M. Hikita, H. Ikeda, E. Haginomori and T. Koshizuka

9. Investigation of Transformer Impedance for Transformer Limited Fault Condition by using FRA Monitoring Technique

Proceeding of the International Conference on Condition Monitoring and Diagnosis 2010 (CMD 2010), paper A7-2, pp. 197-200, Shibaura Institute of Technology, Japan, September 6-11, 2010.

Authors: **M. Thein**, H. Toda, M. Hikita, H. Ikeda, E. Haginomori and T. Koshizuka

10. Frequency Dependent Transformer Model for TRV Calculation at the Transformer Limited Fault Condition by EMTP

Proceeding of the Seventh International Workshop on High Voltage Engineering 2010 (IWHV 2010), Kitakyushu, ED-10-75, SP-10-42, HV-10-37, pp. 77-81, Kitakyushu International Conference Center, Kitakyushu, Japan, November 12-13, 2010.

Authors: **M. Thein**, H. Toda, M. Hikita, H. Ikeda, E. Haginomori and T. Koshizuka

11. Study of Transformer Iron Core Characteristics at a High Frequency

Proceeding on the International Conference on Electrical Engineering 2012 (ICEE 2012), Paper-EM2-0188, Kanazawa, Japan, July 8-12, 2012.

Authors: **M. Thein**, H. Toda, M. Hikita, H. Ikeda, E. Haginomori and T. Koshizuka

National Proceedings

12. Transformer Limited Fault Clearing: Investigation of Transformer Model for EMTP Analysis

Proceeding of the 2008 annual meeting of institute of electrical engineering of Japan, vol.5, paper 5 -164, pp.242, Fukuoka Institute of Technology, Japan, March 19-21,

2008.

Authors: **M. Thein**, M. Hikita, S. Ohtsuka, H. Ikeda, E. Haginomori and T. Koshizuka

13. Investigation of Transformer Model for TRV Calculation after Fault Current Interrupting with Pole Transformer

Proceeding of the Annual Conference of Power & Energy Society, IEE of Japan, paper 38-311, pp.17-18, Hiroshima University, Japan, September 24-26, 2008.

Authors: **M. Thein**, M. Hikita, S. Ohtsuka, H. Ikeda, K. Harada, E.Haginomori and T. Koshizuka

14. EMTP Transformer Model Investigation and TRV Calculation after Fault Current Interrupting

Proceeding of the Papers of Technical Meeting on Static Apparatus, IEE Japan, SA-08-106, pp. 13-17, Tokyo, Japan, December 12, 2008. (In Japanese)

Authors: T. Koshizuka, **M. Thein**, M. Hikita, S. Ohtsuka, H. Ikeda, K. Harada and E.Haginomori

15. EMTP Transformer Model Investigation and TRV Calculation after Fault Current Interrupting with 300 kVA Two Windings Transformer

Proceeding of the 2009 annual meeting of institute of electrical engineering of Japan, vol.6, paper 6 -199, pp. 337, Hokaido University, Japan, March 17-19, 2009.

Authors: **M. Thein**, H. Ikeda, K. Harada, M. Hikita, S. Ohtsuka, E. Haginomori and T. Koshizuka

16. Investigation of TRV at Transformer Limited Fault Condition with Small Stray Capacitance of Current Injection Circuit

Proceeding of the 62nd Joint Conference of Electrical and Electronic Engineering in Kyushu, 04-2P-12, Kyushu Institute of Technology, Iizuka Campus, Sept 28-29, 2009,

Authors: **M. Thein**, H. Toda, K. Harada, M. Hikita, S. Ohtsuka, H. Ikeda, E.Haginomori and T. Koshizuka

17. Investigation of TRV at Transformer Limited Fault by using Transformer Impedance Calculated by FRA Measurement

Proceeding of the joint technical meeting on Electrical Discharges, Switching and Protection Engineering and High Voltage Engineering, IEE Japan, ED-09-167, SP-09-38, HV-09-47, pp. 77-81, Nakasaki University, Japan, November 19-20, 2009.

Authors: **M. Thein**, H. Toda, K. Harada, M. Hikita, S. Ohtsuka, H. Ikeda, E.Haginomori and T. Koshizuka

18. Transformer Model for TRV Calculation at the Transformer Limited Fault Condition by EMTP

Proceeding of the Technical Meeting on Static Apparatus, IEE Japan, 2009, SA-09-126, pp.39-43, Tokyo, Japan, December 18, 2009. (In Japanese)

Authors: T. Koshizuka, **M. Thein**, H. Toda, K. Harada, M. Hikita, S. Ohtsuka, H. Ikeda and E. Haginomori

19. Investigation of TRV at Transformer Limited Fault Condition with Diode Interruption

Proceeding of the 2010 annual meeting of institute of electrical engineering of Japan, vol.6, paper 6-226, pp. 381, Meiji University, Japan, March 17-19, 2010.

Authors: **M. Thein**, H. Toda, K. Harada, S. Ohtsuka, M. Hikita, H. Ikeda, E.Haginomori and T. Koshizuka

20. Investigation of Frequency Dependent Transformer Model for TRV Analysis at TLF Interruption

Proceeding of the Annual Conference of Power & Energy Society, IEEJ, paper 38-306,

pp. 9-10, Kyushu University, Japan, September 1-3, 2010. (In Japanese)

Authors: T. Koshizuka, **M. Thein**, H. Toda, M. Hikita, H. Ikeda and E. Haginomori

21. Transformer Model for TRV Calculation at the Transformer Limited Fault Condition

Proceeding of the Technical Meeting on Static Apparatus, IEE Japan, 2010, SA-10-115, pp. 39-44, Tokyo, Japan, December 17, 2010. (In Japanese)

Authors: T. Koshizuka, **M. Thein**, H. Toda, M. Hikita, H. Ikeda and E. Haginomori

22. EMTP Transformer Equivalent Circuit for TRV Calculation with 50MVA Short Circuit Test Transformer

Proceeding of the 2011 annual meeting of institute of electrical engineering of Japan, vol.6, paper 6-257, pp. 455, Osaka University, Japan, March 16-18, 2011.

Authors: **M. Thein**, H. Toda, M. Hikita, H. Ikeda, E.Haginomori and T. Koshizuka

23. TRV Measurement of Transformer for Short Circuit Test

Proceeding of the 2011 annual meeting of institute of electrical engineering of Japan, vol.6, paper 6-259, pp. 457-458, Osaka University, Japan, March 16-18, 2011. (In Japanese)

Authors: H. Kusuyama, T. Koshizuka, E.Haginomori, **M. Thein**, H. Toda, M. Hikita and H. Ikeda

24. Study of TRV Characteristics with Extra Capacitance Values at TLF Condition

Proceeding of the Annual Conference of Power & Energy Society, IEE of Japan, paper 33-288, pp. 3-4, Fukui University, Japan, August 30 - September 1, 2011.

Authors: **M. Thein**, H. Toda, M. Hikita, H. Ikeda, E.Haginomori and T. Koshizuka

25. Investigation of Short Circuit Inductance of Transformer at TLF Interruption

Proceeding of the Annual Conference of Power & Energy Society, IEE of Japan, paper 33-290, pp. 7-8, Fukui University, Japan, August 30 - September 1, 2011. (In Japanese)

Authors: T. Koshizuka, **M. Thein**, H. Toda, M. Hikita, E. Haginomori and H. Ikeda

26. Transformer Current Ratio Measurement at a High Frequency Region

Proceeding of the 2012 annual meeting of institute of electrical engineering of Japan, vol.5, paper 5 -134, pp. 205, Hiroshima Institute of Technology, Japan, March 21-23, 2012.

Authors: **M. Thein**, H. Toda, M. Hikita, H. Ikeda, E.Haginomori and T. Koshizuka

Book

27. Electromagnetic Transients in Transformer and Rotating Machine Windings
Chapter 7 : Transformer Model for TRV at Transformer Limited Fault Current Interruption

Published by IGI Global, 2012

Authors: M. Hikita, H. Toda, **M. Thein**, H. Ikeda, E. Haginomori and T. Koshizuka

